Enhancing Myoblast Fusion for Therapy of Muscular Dystrophies

(Article begins on next page)

Dissertation Advisor: Professor Emanuela Gussoni   Melissa P. Wu

Enhancing Myoblast Fusion for Therapy of Muscular Dystrophies

Abstract

Skeletal muscle is a major organ comprising 30-40% of the human body mass. The coordination of processes resulting in mature muscle requires many genes, and their loss can result in debilitating muscle disorders. Of the strategies being developed to cure muscle diseases, enhancement of the natural process of muscle cell fusion in existing or introduced myogenic cells has great therapeutic potential. In this work, we determined whether a drug that stimulates proliferation and fusion of myoblasts could alleviate murine Duchenne muscular dystrophy. We also studied the necessity of a gene that is upregulated in early fusing human myoblast cultures and its role in muscle disease development.

Carbamylated erythropoietin (C-EPO) is an analog of erythropoietin, which promotes myoblast proliferation and inhibits fibrosis. We treated *mdx* mice with intraperitoneal injections of C-EPO for 4 and 12 weeks, and monitored weight, serum creatine kinase levels, and changes in muscle histology. We observed moderate histological improvement at 4 weeks that did not translate into a clinically significant improvement at 12 weeks. At the dosages tested, C-EPO was not an effective long-term therapeutic for the treatment of a Duchenne muscular dystrophy.

We also studied the role of GPR56 in muscle. Loss of GPR56 causes bilateral frontoparietal polymicrogyria, which shares the brain phenotype of dystroglycanopathies but not the severe muscle defects. We found that GPR56 is transiently upregulated in

differentiating myocytes and nascent myotubes. In muscle cultures, its loss results in decreased myoblast fusion and smaller myotubes. During in vivo muscle regeneration, the expression of myogenic regulators is delayed in GPR56 knockout mice; however, there are no gross morphological changes. These mild defects likely result from decreased signaling from GPR56 to SRE and NFAT-directed pathways for myoblast differentiation. Therefore, GPR56 promotes myoblast differentiation and fusion through activation of SRE and NFAT signaling pathways, but its loss in muscle in vivo is compensated for by other complementary factors.

In summary, these studies add to the existing literature on the role of a specific gene in muscle cell fusion and disease development, and of a specific drug in augmenting myoblast fusion in the context of muscle disease.

Table of Contents

List of Figures and Tables

Acknowledgments

Thank you, first and foremost, to my PhD advisor, **Dr. Emanuela Gussoni**, for trusting me to be the first graduate student in your lab. You willingly shared everything about being a professor with me – both the highs and the lows. This project, too, had its peaks and valleys; thanks for continually motivating and supporting me, especially through the drudge times. I couldn't have become the scientist, or person, that I am today without you.

Of course, before Emanuela there was a long line of mentors whose efforts led me graduate school. **Dr. Chawnshang Chang** allowed me to work in his lab studying prostate cancer in high school, despite the fact that I didn't even know what a plasmid was. **Dr. Monto Kumagai** taught me how to work with RNA, and gave me the chance to present research at my first conference**. Dr. Michael Cooney** accepted me into his intense summer research program; I was terrified of his critiques but that experience was invaluable for teaching me how to effectively present my research in any format – papers, proposals, resumes, and presentations. And lastly, **Dr. James Sherley** and **Dr. Ting Wu** showed me true passion in science. They led me through making my own hypotheses and gave me the responsibility and excitement of developing my own experiments. It was with them that I first realized the stimulating challenge of doing science research.

In graduate school, I met so many talented and accomplished scientists. **Dr. Ramesh Shivdasani** and **Dr. Michael Choi** mentored me through my first rotation, and I will never forget the effort they spent teaching me about intestinal development and how painstaking

Chapter 1

Introduction

Descriptions of skeletal muscle disorders first entered the Western research literature in the 1830s.[1,2] The patients described suffered from wasted muscles and progressive muscle debility. Since then, different diseases of the muscle have been defined both clinically and genetically.[rev in 3–5] In many of them, debilitating muscle failure eventually results in premature death. The fields of research have made enormous advances in understanding the pathology and causes of these muscle diseases; yet, cures for these diseases still elude us. Our work concerns understanding muscle cell fusion to aid in the development of autologous and heterologous cell-based therapies for these diseases.

Skeletal Muscle

Skeletal Muscle Development

Skeletal muscle is a major organ of the human body, comprising around 30 – 40% of its mass. Its function is to allow the human body to move. Several processes must be coordinated for mature, functioning muscle to develop from undifferentiated cells. During muscle development, muscle progenitor cells originating from the somites migrate out into the limb bud,[6] where they proliferate and undergo commitment towards myogenic differentiation. Following precursor cell migration into the limb bud, the development of muscle myofibers occurs in two waves.[7–9] In the first wave of myogenesis, called primary myogenesis, the myoblasts differentiate and fuse into multinucleated primary myofibers. A second wave of myogenesis then occurs when more myofibers develop around the initial primary myofibers. Further hypertrophic growth of these myofibers leads to mature skeletal muscle formation.

Several discrete steps are required for the formation of myofibers. After myogenic

precursor cell specification in the limb bud, myoblasts must acquire fusion competence and

undergo cell-cell recognition, cell adhesion and alignment, and finally, membrane fusion.[10–

13] After the initial fusion of myoblast to myoblast, other factors regulate the process of

myoblast-myotube and myotube-myotube fusion.[rev in 14]

These steps of myogenic specification in the somite through myoblast fusion into

myofibers are regulated by the coordination of many factors. Of these, a special group of

"master" transcription factors of the basic helix-loop-helix (bHLH) family direct these

processes in a sequential manner.[rev in 15] Precursor cells in the somites are specified to the

myogenic lineage through the expression of the bHLH factor, myogenic factor 5 (Myf5).[16]

Another master transcription factor, myogenic differentiation 1 (MyoD), is expressed

shortly after and also specifies myogenic precursor cells.[17] Although expressed in different

cells,[17,18] Myf5 and MyoD can compensate for each other's loss.[19,20] After migration to the

limb buds and exit from the cell cycle, the expression of myogenin induces myoblasts to

differentiate.[21] Myogenin promotes the expression of factors that lead to adherence and

fusion, resulting in the formation of multinucleated myofibers.

Some of the cell-surface effectors of muscle cell differentiation and fusion have also

been identified. Cell-cell adhesion molecules such as NCAM, N-cadherin, M-cadherin,

ADAM12, and VCAM-1/VLA-4 are involved in cell-cell adhesion of muscle cells.[rev in 22] Other

proteins have also been implicated as important for fusion, but their specific roles remain

unclear. These proteins include the transmembrane proteins CD81 and CD9.[23] Part of the

difficulty in identifying cell surface proteins and their roles is that many of them act

cooperatively and in parallel, thus complementing each other's function.[24] A complete

understanding of the molecular regulation of muscle development awaits further characterization of these molecules and the identification of other unknown factors that are involved.

Skeletal Muscle Structure

The final product of muscle development is a mature skeletal muscle consisting of many bundles of multinucleated myofibers (Figure 1.1A). The myofiber contains many specialized organelles that are important for muscle function. The cytoplasm of the myofiber, called the sarcoplasm, is densely packed with regularly aligned sarcomeres that form the functional contractile units for the muscle (Figure 1.1B). A modified endoplasmic reticulum, the sarcoplasmic reticulum, serves as a storage location for calcium ions.[25,26] These ions serve as important mediators of signaling for many calcium-sensitive proteins in the muscle, notably those within the sarcomere.[27, rev in 28] The transverse (T)-tubules connect the sarcolemma to the sarcoplasmic reticulum for transference of action potential signals.[29,30] The T-tubule system together with the sarcoplasmic reticulum form the excitation-contraction coupling unit that transforms the nerve cell stimuli into mechanical contractions (Figure 1.1B).[25]

The muscle fiber is sheathed by a specialized plasma membrane called the sarcolemma, which in addition to the lipid bilayer also contains an extracellular layer of polysaccharides such as collagen. Outside of the sarcolemma is a layer of extracellular matrix, or basement membrane, composed of an inner basal lamina and outer fibrillar reticular lamina.[31,32]

Figure 1.1. *Mouse skeletal muscle structure*

A. H&E staining of gastrocnemius muscle shows cross-sectional area, with tightly packed myofibers. Hematoxylin staining (blue) shows peripherally located nuclei. Eosin staining (pink) stains sarcoplasm. Scale bar, 50 μm. Methods for muscle preparation and slide staining are detailed in the Chapter 2 Methods section. **B**. Electron microscopy image of soleus muscle shows dense sarcoplasm with aligned sarcomeres (SAR), mitochondria (m), sarcoplasmic reticulum (SR), and T-tubule system (TT). Scale bar, 500 nm. Methods for muscle preparation and electron microscope are detailed in the Appendix 1 Methods section.
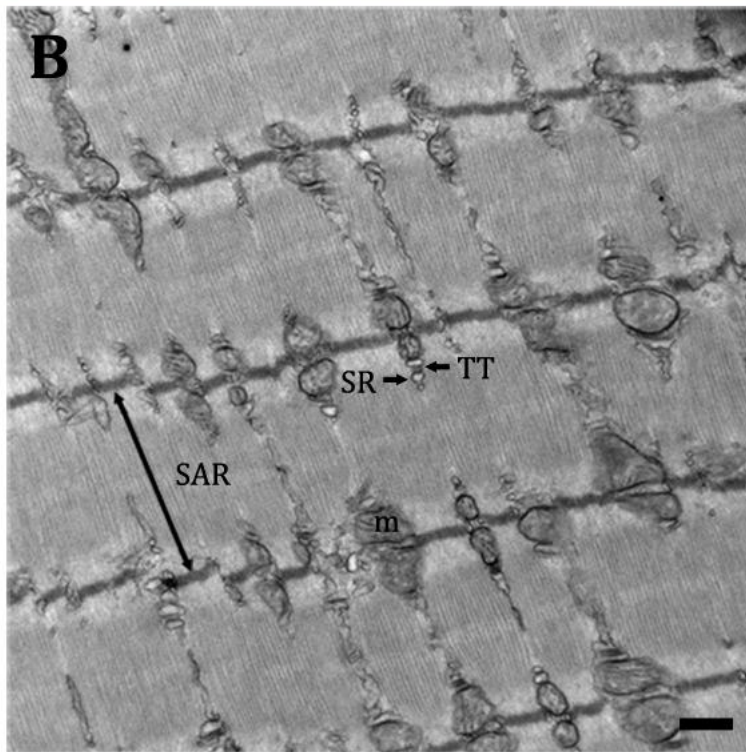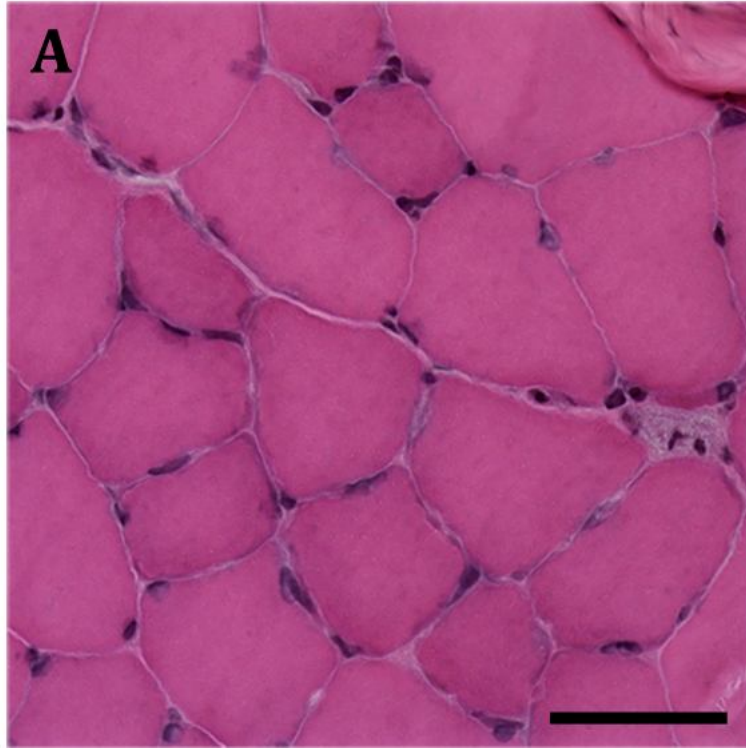
Figure 1.1 (Continued)

Besides the multinucleated myofibers, skeletal muscle also contains many mononuclear cells. The "satellite" stem cells are the major stem cells of the muscle, located at the periphery of the muscle fibers between the outer side of the sarcolemma and the basal lamina.[33] Muscle is constantly taxed by myofiber contraction, but it has an inherent capacity for repair through the activation of these satellite stem cells to proliferate and fuse into damaged myofibers.[34,35] In addition to satellite cells, the muscle contains several other mononuclear cell populations. These include cells that have demonstrated some ability to contribute to muscle cell regeneration, such as myoendothelial cells,[36] muscle side population (SP) cells,[37-41] CD133+ cells,[42] and endothelial-cell associated pericytes.[43] The exact locations within the muscle of some of these cells remain unknown, but the myoendothelial and SP cells have been shown to be located in the interstitium[36,44] and the pericytes associated with blood vessels in the muscle.[43] Additionally, the interstitial spaces of muscle include other non-myogenic cells such as fibroblasts, hematopoietic cells, endothelial cells, and adipogenic precursor cells.[45,46]

Genetic Disorders of Skeletal Muscle

In the cases of many genetically inherited muscle diseases, mutations in genes involved in the development or function of mature muscle render them non-functional and thus result in muscle disorders. The majority of genetic muscle disorders can be broadly categorized into two types: congenital myopathies and dystrophies. Congenital myopathies are characterized by having different degrees of muscle weakness and hypotonia along with certain distinct morphological changes in the muscle myofiber.[5] In patients, the congenital muscle weakness can be mild with a few muscles impaired at birth,[47] or severe

enough to have their muscle tone and body described as "floppy."[48] Typically the weakness

is non-progressive.[49] The morphological changes that characterize and have been used to

classify the myopathies include protein accumulation, the presence of cores, central nuclei,

fiber size variation, and the presence of vacuoles.[5] Distinguishing one myopathy from

another based on these manifestations alone has been difficult;[49] the development of

animal models and the association of specific genes with different myopathies has made

understanding and classification of their different pathologies easier.[3] An emerging theme

in the congenital myopathies is that they result from problems in excitation-contraction

coupling and the functional units that contribute to it.[3]

The other major group of muscle diseases is the dystrophies. These diseases are

characterized by degeneration or necrosis of the muscle fibers accompanied by some

regeneration. The inability to fully regenerate the muscle fibers often results in the

replacement of muscle by fibrotic and fat tissue.[50] These problems are often compounded

by an influx of inflammatory cells into the muscle. As with the myopathies, a major

symptom of the dystrophies is skeletal muscle weakness; in the case of the dystrophies, the

weakness is often progressive. Clinically, the muscle weakness can lead to loss of skeletal

muscle action; the failure of the diaphragm to power respiration is one cause of premature

death.[51] Traditionally, the various muscular dystrophies were grouped on the basis of their

clinical phenotypes such as the time of onset, the muscles affected, and the mode of

inheritance.[50] Over the past two decades, however, over 30 causative genes for the

muscular dystrophies have been identified; it has been proposed to re-classify the diseases

based not only on the clinical data but also on the shared defects in biochemistry and

genetics.[50,52,53] Five classes of proteins have been proposed to categorize these diseases:

sarcolemma and extracellular matrix proteins, glycosylation enzymes of α-dystroglycan, endoplasmic reticulum proteins, nuclear envelope proteins, and mitochondrial proteins.[50,52,53] Etiologically, the loss of these proteins often results in structural instability in the sarcolemma of the myofiber or its connection to the extracellular matrix. This instability in turn leads to the inability of the fibers to withstand normal muscle contraction, leading to their degeneration.

Our studies of myoblast fusion were framed in the context of two types of muscular dystrophies: Duchenne muscular dystrophy (DMD) and the dystroglycanopathies. These diseases are caused by mutations in genes that encode proteins whose functions affect the dystrophin-associated protein complex (DAPC, Figure 1.2). The DAPC, also known as the dystrophin-glycoprotein complex (DGC), spans the sarcolemma to link the extracellular matrix to actin inside the sarcoplasm.[54–56] It serves to stabilize the membrane during muscle contraction.[54,56] Protein members of the DAPC include dystrophin, the glycoproteins α/β-dystroglycan and the sarcoglycans, and other proteins such as sarcospan, syntrophin, and dystrobrevin.[56–64] These proteins can be subdivided by localization to three complexes: the extracellular/sarcolemmal dystroglycan complex, the sarcolemmal sarcoglycan complex, and the sarcoplasmic dystrophin-containing complex.[65] Given the structural and signaling importance of the DAPC, it is perhaps not surprising that mutations in the different members of the DAPC have been shown to be the primary cause of many different dystrophies.[4,50,65]

The first breakthrough in identifying a genetic cause of these dystrophies came through the efforts of the research groups of Louis Kunkel and Ron Worton in the late
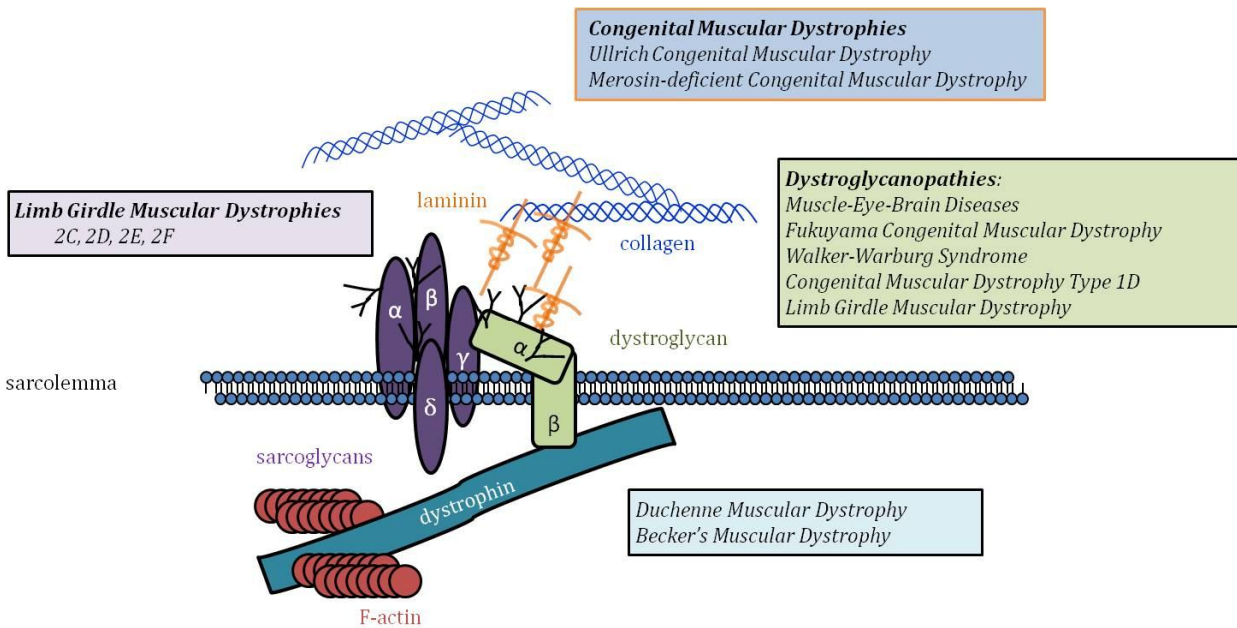
Figure 1.2

Figure 1.2. *Schematic diagram of major components of the dystrophin-associated glycoprotein complex*

Mutations in the indicated components result in muscular dystrophies (outlined). Note that mutations in enzymes that affect α-dystroglycan result in the diseases indicated for α-dystroglycan.

1980s. They identified the DMD causative gene, dystrophin, and characterized the consequences of its absence in the skeletal muscle of patients with DMD.[66–71] These patients have progressive muscle weakness in their limb muscles.[1,72] The instability in the muscle sarcolemma that results from the loss of dystrophin allows high levels of creatine kinase to leak into the bloodstream; the extremely high serum creatine kinase levels that result are used as diagnostic criteria for DMD.[72–74] Muscle biopsies show muscle fiber degeneration that is removed by an influx of inflammatory cells and replaced by adipose

and fibrotic tissue, often resulting in a phenotype of calf pseudohypertrophy.[72,75] Although

there is some regeneration, at later stages of the disease the capacity of the endogenous

muscle stem cells to replicate and repair the damaged muscle tissue is lost.[76] Ultimately,

patients with DMD live a shortened life span due to cardiac or respiratory failure.[77]

Improvements over the past few decades in patient care have extended life span such that

the majority of patients live through their twenties.[77]

In the years following, other members of the DAPC were quickly found to be

associated with other muscular dystrophies. Several groups found that dystrophin was part

of a complex that included glycoproteins, some of which were identified as the α-, β-,γ-, and

δ-sarcoglycans.[55,57–60,78] Together they form a subunit of the DAPC that spans the

sarcolemma. It was discovered that mutations in any of these sarcoglycans lead to the

development of muscular dystrophies such as severe childhood autosomal recessive

muscular dystrophy and the limb-girdle muscular dystrophies (LGMD).[79–83, rev in 84,85] In

these diseases, patients also have elevated serum creatine kinase levels, and the muscular

dystrophy is progressive.[85] They vary in onset from congenital to adult, and also in severity

of the disease. To differentiate these dystrophies from similar dystrophies caused by

mutations in other genes, the ones caused by mutations in sarcoglycans have been called

sarcoglycanopathies.[84]

A separate group of muscular dystrophies are caused by mutations affecting the

extracellular component of the DAPC. α-Dystroglycan links the DAPC to the extracellular

matrix by binding several extracellular matrix proteins,[55,78,86–88] and its glycosylation is

integral for this binding ability.[89–91] The glycosylation of α-dystroglycan is a complex

process requiring the sequential action of several enzymes.[92] Perturbations in the

glycosylation of α-dystroglycan result in the dystroglycanopathies.[92] Mutations in the genes

of six glycosylation enzymes, as well as in α-dystroglycan itself, have been found

responsible for these dystrophies.[rev in 92] The clinical manifestations of these mutations are

Walker-Warburg syndrome, Muscle-Eye-Brain disease, congenital muscular dystrophy

with or without mental retardation, congenital muscular dystrophy types 1C and 1D, and

limb girdle muscular dystrophy.[93] Patients with these diseases suffer muscle weakness in

their proximal limbs muscles and increased serum creatine kinase levels.[92] Although the

genes mutated in these diseases all participate in the same biochemical pathway, the extent

of muscle impairment between these diseases can vary from mild with late onset to severe

in the congenital muscular dystrophies.[93] Interestingly, a majority of the

dystroglycanopathies are associated with neuronal migration defects[94] resulting in a

particular brain phenotype called cobblestone malformation.[95] These associated central

nervous system defects demonstrate a role for α-dystroglycan and the DAPC in mediating

cell-extracellular matrix interactions in the brain. It also suggests that patients diagnosed

with these brain abnormalities may also exhibit defects in skeletal muscle, due to the

mutation of proteins that have a primary role in both tissues.

Therapies for Duchenne Muscular Dystrophy

Although Duchenne muscular dystrophy has been studied for nearly two centuries,

efforts to find a viable therapy are still ongoing. One of the earliest therapies, the

administration of corticosteroids, began in the 1970s with a study of prednisone as a

palliative treatment.[96] To date, corticosteroids remain one of the most effective evidence-

based treatments for DMD.[97] Although they slow the disease progression and extend

muscle function,[98–102] the use of corticosteroids only delays the effects of the disease for a few years. Efforts by a number of groups are being made to develop better palliative therapies and cures;[97,103–107] these approaches include therapies that address outcomes of dystrophin loss as well as gene and cell-based therapies that aim to replace dystrophin.

Many drugs and protein biologics are used as alleviatory therapies that address the symptoms of Duchenne muscle dystrophy. One class of drugs, the phosphodiesterase (PDE) inhibitors, has shown efficacy in preclinical trials of zebrafish[108] and mice[109,110] and are being tested in clinical trials.[97] These inhibitors combat the loss of nitric oxide signaling seen in DMD patients by preventing the inactivation of a cofactor of nitric oxide, cyclic guanosine monophosphate,[111] and promote neo-vascularization in the ischemic dystrophic model.[108,110,111] In preclinical trials, these drugs have been shown to restore muscle morphology as well as lower serum creatine kinase levels, indicating a repair of the sarcolemmal membrane.[108,110,111] Other proposed therapies that have shown efficacy in mouse models are biologics that alter the extracellular matrix. Laminin-111 that is systemically administered to the mdx mouse model of Duchenne muscular dystrophy has been shown to stabilize the sarcolemma through the promotion of α_7-integrin expression.[112] A fibrinogen-blocking peptide was used by another group to reduce deposition of fibrin and the associated inflammation.[113] A third family of drugs promotes muscle fiber growth by activating the activin IIB receptor that regulates myofiber size, or by inhibiting its antagonist, myostatin.[114] The myofiber hypertrophy results in clear improvements in histology and serum creatine kinase levels in mice[115–117] and dogs;[118] yet, clinical trials using this strategy for various dystrophies have so far been unsuccessful.[119]

More targeted therapies that modify RNA or DNA have been developed in the last decade. The dystrophin gene is one of the largest genes in the human genome, comprising 79 exons. Frameshift mutations in dystrophin lead to loss of the protein and cause DMD. Some mutations in dystrophin, however, lead to in-frame splicing that results in shortened dystrophin transcripts being translated.[120–123] Patients with these mutations have a much milder form of dystrophy, Becker's muscular dystrophy.[120] Many therapies are taking advantage of this finding by using different agents to alternatively splice out the mutation-containing exons to produce a truncated protein product in Duchenne patients. These agents are targeted antisense oligonucleotide molecules.[124–126] Proof-of-principle experiments have been successful, and a host of different chemistries that hope to overcome the delivery barrier are being tested.[127] Current clinical trials are testing two forms of antisense oligomers – phosphorodiamidate morpholino oligomers[126] and 2'O-methylphosphorothioate-modified oligoribonucleotides.[127–129] Another type of mutation that some DMD patients have are nonsense mutations resulting in premature stop codons.[120–123] Aminoglycosides that promote the read-through of mRNA transcripts by suppressing stop codons have shown some promise in mice and human patients with these mutations in dystrophin.[130–132] A synthetic drug, ataluren, that induces the read-through of only premature, and not native, stop codons was also tested in clinical trials and showed a promising outcome.[133]

One drawback of the previously described approaches to therapy is they do not fully replace the lost dystrophin gene product, or in the case of stop codon read-through therapies, can only do so for a minority of patients. Gene-therapy approaches to Duchenne have overcome the technical difficulties of immune system reactions that all gene-therapy

14

approaches faced in the past, as well as the problem that the full-length dystrophin transcript does not fit into viral vectors. The current solution undergoing trial is to use a shortened form of dystrophin (minidystrophin) that contains the functional N-terminal and C-terminal domains in an adeno-associated viral vector.[134]

One approach likely to be able to replace the full dystrophin gene is cell-based therapy. In the early 1990s, several groups used these isolated myoblasts for human therapy,[135-140] but despite evidence of dystrophin transcripts being made in recipient muscle after transplantation, the overall efficiency was too low to be clinically significant. Later analyses showed that the therapy was ineffective partially due to engrafted cells dying shortly after transplantation or not fusing with the muscle.[141-143] The collective experience of these attempts highlighted the caveats associated with the need to expand myogenic cells in vitro to obtain enough cells for clinical therapy, as well as the issues surrounding efficacious delivery.[144] Subsequent studies using isolated satellite cells showed that these cells did have a great capacity to engraft and fuse into skeletal muscle, but the in vitro culture of these cells needs to be optimized to maintain their myogenicity.[145,146] Since then, efforts to improve the purification of satellite cells to find the most engraftable population have been underway. The marker-based prospective isolation of satellite cells has demonstrated that they are a heterogenous population, and subsets with greater potential for myoblast engraftment exist.[147] However, donor cell expansion *in vitro*,[148-150] efficient delivery of cells to all muscles,[151,152] and improving cell survivability after injection[150,153-156] still remain issues to be solved. Advances in induced pluripotent stem cell technology in conjunction with gene therapy correction have the promise of providing an easily expandable source of stem cells for autologous cell replacement, which

would sidestep immune rejection.[157–161] Nevertheless, the prospect of cell-based therapy as a cure is still some years away. In the meantime, the development of other therapeutics is necessary for treating the current Duchenne muscular dystrophy patients.

Hypothesis and Overview of Dissertation

As noted earlier, the enhancement of muscle cell fusion can be used as a strategy to either activate endogenous cells to repair damaged muscle or to improve the efficacy of heterologous donor cell fusion following transplantation. The development of translational approaches to increase muscle cell fusion can be achieved through the testing of drugs and the identification of key proteins that promote myoblast cell fusion. To better understand the process of muscle cell fusion for clinical use, this work includes studies exploring both of these strategies.

In the first approach, I examined the utility of a drug that would promote the proliferation and fusion of endogenous satellite cells in the context of a mouse model of Duchenne muscular dystrophy. If the use of this drug resulted in significant changes in muscle function, then it would serve as a pre-clinical candidate for the ameliorative therapy of Duchenne muscular dystrophy patients. In addition, it could be tested for use in increasing the efficacy of fusion of transplanted cells. The use of the hormone erythropoietin, which has shown the ability to stimulate the proliferation of satellite cells[162] and growth of muscle fibers,[163] had been proposed as a therapeutic drug for muscular dystrophy.[164] It had also showed the ability to limit the development of fibrosis in many injury models.[165] Synthetic analogs of erythropoietin were created that endeavored to preferentially activate erythropoietin signaling independent of the erythropoietin

receptor,[165] thus avoiding overstimulation of hematopoiesis.[165] In Chapter 2, I detail our work on testing the ability of one of these analogs, carbamylated erythropoietin, to alleviate the signs of muscular dystrophy in the mdx mouse.

Our second approach was to characterize a potential cell-surface candidate gene that is important for muscle cell fusion and could promote the fusion of myogenic cells following transplantation. Our laboratory identified G-protein coupled receptor 56 (GPR56) as one of the cell-surface receptors upregulated during the in vitro differentiation of human myoblasts.[166] At the same time, mutations in the G-protein coupled receptor 56 (GPR56) were found to cause the disease bilateral frontoparietal polymicrogyria (BFPP),[167] which shares the brain phenotype seen in the dystroglycanopathies.[95,168] Whether loss of GPR56 affects the muscle in this disease, however, remains unclear. As such, establishing its role in muscle cell differentiation and fusion would be important for both understanding these processes as well as for understanding the relationship between the muscle pathology of BFPP and the dystroglycanopathies. I studied the muscle phenotype and fusion competence of myoblasts from GPR56 knockout mice. These studies were followed with the delineation of how GPR56 signaling promoted myoblast differentiation, and the findings were related to the clinical findings of muscle phenotypes in BFPP patients. Chapter 3 describes these studies. Peripheral findings of tubular aggregates in GPR56 knockout mouse muscle are also detailed in Appendix 1.

In Chapter 4, I discuss the overall impact of these findings and future directions for this work.

References

1. Duchenne, G.-B. *Selections from the clinical works of Dr. Duchenne (De Boulogne)*. (The New Syndenham Society: 1883).at <http://books.google.com/books/reader?id=MygJAAAAIAAJ>

2. Gardner-Thorpe, C. Charles Bell (1774–1842) and an early case of muscular dystrophy The Third Meryon Society Lecture read at Worcester College, Oxford on 28 July, 2000. *Neuromuscular Disorders* **12**, 318–321 (2002).

3. Nance, J. R., Dowling, J. J., Gibbs, E. M. & Bönnemann, C. G. Congenital myopathies: an update. *Curr Neurol Neurosci Rep* **12**, 165–74 (2012).

4. Brown, R. H. Dystrophin-associated proteins and the muscular dystrophies. *Annu Rev Med* **48**, 457–66 (1997).

5. North, K. What's new in congenital myopathies? *Neuromuscul Disord* **18**, 433–42 (2008).

6. Chevallier, A., Kieny, M. & Mauger, A. Limb-somite relationship: origin of the limb musculature. *J Embryol Exp Morphol* **41**, 245–58 (1977).

7. Kelly, A. M. & Zacks, S. I. The histogenesis of rat intercostal muscle. *J Cell Biol* **42**, 135–53 (1969).

8. Rubinstein, N. A. & Kelly, A. M. Development of Muscle Fiber Specialization in the Rat Hindlimb. *Journal of Cell Biology* **90**, 50–52 (1981).

9. Fredette, B. & Landmesser, L. Relationship of primary and secondary myogenesis to fiber type development in embryonic chick muscle. *Dev Biol* **18**, 1–18 (1991).

10. Knudsen, K. A. & Horwitz, A. F. Tandem events in myoblast fusion. *Developmental Biology* **58**, 328–338 (1977).

11. Wakelam, M. J. The fusion of myoblasts. *Biochem J* **228**, 1–12 (1985).

12. Robertson, T. A., Grounds, M., Mitchell, C. A. & Papadimitriou, J. M. Fusion between myogenic cells in Vivo: An ultrastructural study in regenerating murine skeletal muscle. *Journal of Structural Biology* **105**, 170–182 (1990).

13. Doberstein, S. K., Fetter, R. D., Mehta, A. Y. & Goodman, C. S. Genetic Analysis of Myoblast Fusion: blown fuse Is Required for Progression Beyond the Prefusion Complex. *The Journal of Cell Biology* **136**, 1249–1261 (1997).

14. Pavlath, G. K. Spatial and functional restriction of regulatory molecules during mammalian myoblast fusion. *Exp Cell Res* **316**, 3067–72 (2010).

15. Lassar, A., Skapek, S. & Novitch, B. Regulatory mechanisms that coordinate skeletal muscle differentiation and cell cycle withdrawal. *Curr Opin Cell Biol* **6**, 788–94 (1994).

16. Ott, M. O., Bober, E., Lyons, G., Arnold, H. & Buckingham, M. Early expression of the myogenic regulatory gene, myf-5, in precursor cells of skeletal muscle in the mouse embryo. *Development* **111**, 1097–107 (1991).

17. Braun, T. & Arnold, H. Myf-5 and myoD genes are activated in distinct mesenchymal stem cells and determine different skeletal muscle cell lineages. *EMBO J* **15**, 310–318 (1996).

18. Kablar, B. *et al.* MyoD and Myf-5 differentially regulate the development of limb versus trunk skeletal muscle. *Development* **124**, 4729–38 (1997).

19. Rudnicki, M. *et al.* MyoD or Myf-5 is required for the formation of skeletal muscle. *Cell* **75**, 1351–9 (1993).

20. Rudnicki, M., Braun, T., Hinuma, S. & Jaenisch, R. Inactivation of MyoD in mice leads to up-regulation of the myogenic HLH gene Myf-5 and results in apparently normal muscle development. *Cell* **71**, 383–90 (1992).

21. Wright, W., Sassoon, D. & Lin, V. Myogenin, a factor regulating myogenesis, has a domain homologous to MyoD. *Cell* **56**, 607–17 (1989).

22. Abmayr, S. M. & Pavlath, G. K. Myoblast fusion: lessons from flies and mice. *Development* **139**, 641–56 (2012).

23. Tachibana, I. & Hemler, M. Role of transmembrane 4 superfamily (TM4SF) proteins CD9 and CD81 in muscle cell fusion and myotube maintenance. *J Cell Biol* **146**, 893–904 (1999).

24. Krauss, R. S. Regulation of promyogenic signal transduction by cell-cell contact and adhesion. *Exp Cell Res* **316**, 3042–9 (2010).

25. Ebashi, S. & Endo, M. Calcium and muscle contraction. *Progress in Biophysics and Molecular Biology* **18**, 123–183 (1968).

26. Endo, M., Tanaka, M. & Ogawa, Y. Calcium induced release of calcium from the sarcoplasmic reticulum of skinned skeletal muscle fibres. *Nature* **228**, 34–6 (1970).

27. Winegrad, S. The Intracellular Site of Calcium Activation of Contraction in Frog Skeletal Muscle. *The Journal of General Physiology* **55**, 77–88 (1970).

28. Berchtold, M. W., Brinkmeier, H. & Muntener, M. Calcium Ion in Skeletal Muscle: Its Crucial Role for Muscle Function, Plasticity, and Disease. *Physiol Rev* **80**, 1215–1265 (2000).

29. Block, B. A., Imagawa, T., Campbell, K. P. & Franzini-Armstrong, C. Structural evidence for direct interaction between the molecular components of the transverse tubule/sarcoplasmic reticulum junction in skeletal muscle. *J Cell Biol* **107**, 2587–600 (1988).

30. Huxley, A. & Taylor, R. Local activation of striated muscle fibres. *J Physiol* **144**, 426–41 (1958).

31. Mauro, A. & Adams, W. R. The structure of the sarcolemma of the frog skeletal muscle fiber. *J Biophys Biochem Cytol* **10**, 177–85 (1961).

32. Sanes, J. R. The basement membrane/basal lamina of skeletal muscle. *J Biol Chem* **278**, 12601–4 (2003).

33. Mauro, A. Satellite cell of skeletal muscle fibers. *J Biophys Biochem Cytol* **9**, 493–5 (1961).

34. Le Gros Clark, W. E. An experimental study of the regeneration of mammalian striped muscle. *J Anat* **80**, 24–36 (1946).

35. Bischoff, R. Regeneration of single skeletal muscle fibers in vitro. *Anat Rec* **182**, 215–35 (1975).

36. Tamaki, T. *et al.* Identification of myogenic-endothelial progenitor cells in the interstitial spaces of skeletal muscle. *J Cell Biol* **157**, 571–7 (2002).

37. Asakura, A., Seale, P., Girgis-Gabardo, A. & Rudnicki, M. A. Myogenic specification of side population cells in skeletal muscle. *J Cell Biol* **159**, 123–34 (2002).

38. Meeson, A. P. *et al.* Cellular and molecular regulation of skeletal muscle side population cells. *Stem Cells* **22**, 1305–20 (2004).

39. Muskiewicz, K. R., Frank, N. Y., Flint, A. F. & Gussoni, E. Myogenic potential of muscle side and main population cells after intravenous injection into sub-lethally irradiated mdx mice. *J Histochem Cytochem* **53**, 861–73 (2005).

40. Schienda, J. *et al.* Somitic origin of limb muscle satellite and side population cells. *Proc Natl Acad Sci U S A* **103**, 945–50 (2006).

41. Motohashi, N. *et al.* Muscle CD31(-) CD45(-) side population cells promote muscle regeneration by stimulating proliferation and migration of myoblasts. *Am J Pathol* **173**, 781–91 (2008).

42. Negroni, E. *et al.* In vivo myogenic potential of human CD133+ muscle-derived stem cells: a quantitative study. *Mol Ther* **17**, 1771–8 (2009).

43. Dellavalle, A. *et al.* Pericytes of human skeletal muscle are myogenic precursors distinct from satellite cells. *Nat Cell Biol* **9**, 255–67 (2007).

44. Frank, N. Y. *et al.* Regulation of myogenic progenitor proliferation in human fetal skeletal muscle by BMP4 and its antagonist Gremlin. *J Cell Biol* **175**, 99–110 (2006).

45. Schulz, T. J. *et al.* Identification of inducible brown adipocyte progenitors residing in skeletal muscle and white fat. *Proc Natl Acad Sci U S A* **108**, 143–8 (2011).

46. McKinney-Freeman, S. L. *et al.* Muscle-derived hematopoietic stem cells are hematopoietic in origin. *Proc Natl Acad Sci U S A* **99**, 1341–6 (2002).

47. Batten, F. E. Three Cases of Myopathy, infantile type. *Proceedings of the Neurological Society of the United Kingdom* 147–8 (1903).

48. Greenfield, J. G., Cornman, T. & Shy, G. M. The prognostic value of the muscle biopsy in the floppy infant. *Brain* **81**, 461–84 (1958).

49. Laing, N. G., Sewry, C. A. & Lamont, P. Congenital myopathies. *Handbook of clinical neurology* **86**, 1–33 (2007).

50. Amato, A. A. & Griggs, R. C. Overview of the muscular dystrophies. *Handbook of clinical neurology* **101**, 1–9 (2011).

51. Davies, K. E. & Nowak, K. J. Molecular mechanisms of muscular dystrophies: old and new players. *Nat Rev Mol Cell Biol* **7**, 762–73 (2006).

52. Muntoni, F. & Voit, T. The congenital muscular dystrophies in 2004: a century of exciting progress. *Neuromuscul Disord* **14**, 635–49 (2004).

53. Mercuri, E. & Muntoni, F. The ever-expanding spectrum of congenital muscular dystrophies. *Ann Neurol* **72**, 9–17 (2012).

54. Rybakova, I. N., Patel, J. R. & Ervasti, J. M. The dystrophin complex forms a mechanically strong link between the sarcolemma and costameric actin. *Journal of Cell Biology* **150**, 1209–14 (2000).

55. Ervasti, J. M. & Campbell, K. P. A role for the dystrophin-glycoprotein complex as a transmembrane linker between laminin and actin. *The Journal of Cell Biology* **122**, 809–823 (1993).

56. Ervasti, J. & Sonnemann, K. Biology of the Striated Muscle Dystrophin-Glycoprotein Complex. *Int Rev Cytol* **265**, 191–225 (2008).

57. Campbell, K. & Kahl, S. Association of dystrophin and an integral membrane glycoprotein. *Nature* **338**, 259–262 (1989).

58. Yoshida, M. & Ozawa, E. Glycoprotein complex anchoring dystrophin to sarcolemma. *J Biochem* **108**, 748–52 (1990).

59. Ervasti, J. M., Ohlendieck, K., Kahl, S. D., Gaver, M. G. & Campbell, K. P. Deficiency of a glycoprotein component of the dystrophin complex in dystrophic muscle. *Nature* **345**, 315–9 (1990).

60. Ervasti, J. & Campbell, K. Membrane organization of the dystrophin-glycoprotein complex. *Cell* **66**, 1121–31 (1991).

61. Suzuki, A. *et al.* Molecular organization at the glycoprotein-complex-binding site of dystrophin. Three dystrophin-associated proteins bind directly to the carboxy-terminal portion of dystrophin. *Eur J Biochem* **220**, 283–92 (1994).

62. Crosbie, R. H., Heighway, J., Venzke, D. P., Lee, J. C. & Campbell, K. P. Sarcospan, the 25-kDa transmembrane component of the dystrophin-glycoprotein complex. *J Biol Chem* **272**, 31221–4 (1997).

63. Peters, M. F. *et al.* B-Dystrobrevin , a New Member of the Dystrophin Family. *Journal oF Biological Chemistry* **272**, 31561–31569 (1997).

64. Johnson, E. A new model for the dystrophin associated protein complex in striated muscles. (2012).

65. Blake, D. J., Weir, A., Newey, S. E. & Davies, K. E. Function and genetics of dystrophin and dystrophin-related proteins in muscle. *Physiol Rev* **82**, 291–329 (2002).

66. Monaco, A. *et al.* Detection of deletions spanning the Duchenne muscular dystrophy locus using a tightly linked DNA segment. *Nature* **316**, 842–5 (1985).

67. Koenig, M. *et al.* Complete cloning of the Duchenne muscular dystrophy (DMD) cDNA and preliminary genomic organization of the DMD gene in normal and affected individuals. *Cell* **50**, 509–17 (1987).

68. Hoffman, E. P., Brown, R. H. & Kunkel, L. M. Dystrophin: the protein product of the Duchenne muscular dystrophy locus. *Cell* **51**, 919–28 (1987).

69. Ray, P. N. *et al.* Cloning of the breakpoint of an X;21 translocation associated with Duchenne muscular dystrophy. *Nature* **318**, 672–675 (1985).

70. Burghes, A. H. M. *et al.* A cDNA clone from the Duchenne/Becker muscular dystrophy gene. **328**, 434–437 (1987).

71.   Zubrzycka-Gaarn, E. E. *et al.* The Duchenne muscular dystrophy gene product is localized in sarcolemma of human skeletal muscle. *Nature* **333**, 466–9 (1988).

72.   Jennekens, F. G. I., Ten Kate, L. P., De Visser, M. & Wintzen, A. R. Diagnostic criteria for Duchenne and Becker muscular dystrophy and myotonic dystrophy. *Neuromuscular Disorders* **I**, 389–391 (1991).

73.   Pearce, J. Serum enzyme studies in muscle disease: Part II Serum creatine kinase activity in muscular dystrophy and in other myopathic and neuropathic disorders. *Journal of Neurology, Neurosurgery, and Psychiatry* **27**, 96–99 (1964).

74.   Nichol, C. Serum creatine phosphokinase measurements in muscular dystrophy studies. *Clinica Chimica Acta* **11**, 404–407 (1965).

75.   Cros, D., Harnden, P., Pellissier, J. & Serratrice, G. Muscle hypertrophy in Duchenne muscular dystrophy. *J Neurol* **236**, 43–47 (1989).

76.   Blau, H. M., Webster, C. & Pavlath, G. K. Defective myoblasts identified in Duchenne muscular dystrophy. *Proc Natl Acad Sci U S A* **80**, 4856–60 (1983).

77.   Passamano, L. *et al.* Improvement of survival in Duchenne Muscular Dystrophy: retrospective analysis of 835 patients. *Acta Myol* **31**, 121–5 (2012).

78.   Ibraghimov-Beskrovnaya, O. *et al.* Primary structure of dystrophin-associated glycoproteins linking dystrophin to the extracellular matrix. *Nature* **355**, 696–702 (1992).

79.   Mizuno, Y. *et al.* Selective Defect of Sarcoglycan Complex in Severe Childhood Autosomal Recessive Muscular Dystrophy Muscle. *Biochemical and Biophysical Research Communications* **203**, 979–983 (1994).

80.   Lim, L. E. *et al.* Beta-sarcoglycan: characterization and role in limb-girdle muscular dystrophy linked to 4q12. *Nat Genet* **11**, 257–65 (1995).

81.   Bönnemann, C. G. *et al.* Beta-sarcoglycan (A3b) mutations cause autosomal recessive muscular dystrophy with loss of the sarcoglycan complex. *Nat Genet* **11**, 266–73 (1995).

82.   Noguchi, S. *et al.* Mutations in the Dystrophin-Associated Protein gamma-Sarcoglycan in Chromosome 13 Muscular Dystrophy. *Science (80-)* **270**, 819–822 (1995).

83.   Nigro, V. *et al.* Autosomal recessive limb-girdle muscular dystrophy, LGMD2F, is caused by a mutation in the delta-sarcoglycan gene. *Nat Genet* **14**, 195–8 (1996).

84.   Hack, A. A., Groh, M. E. & McNally, E. M. Sarcoglycans in muscular dystrophy. *Microsc Res Tech* **48**, 167–80 (2000).

85.   Mathews, K. D. & Moore, S. A. Limb-girdle muscular dystrophy. *Curr Neurol Neurosci Rep* **3**, 78–85 (2003).

86.   Gee, S. H., Montanaro, F., Lindenbaum, M. H. & Carbonetto, S. Dystroglycan-α, a dystrophin-associated glycoprotein, is a functional agrin receptor. *Cell* **77**, 675–686 (1994).

87.   Pall, E. A., Bolton, K. M. & Ervasti, J. M. Differential Heparin Inhibition of Skeletal Muscle alpha-Dystroglycan Binding to Laminins. *Journal of Biological Chemistry* **271**, 3817–3821 (1996).

88.   Talts, J. F., Andac, Z., Göhring, W., Brancaccio, A. & Timpl, R. Binding of the G domains of laminin alpha1 and alpha2 chains and perlecan to heparin, sulfatides, alpha-dystroglycan and several extracellular matrix proteins. *EMBO J* **18**, 863–70 (1999).

89.   Kim, D.-S. *et al.* POMT1 mutation results in defective glycosylation and loss of laminin-binding activity in a-DG. *Neurology* **62**, 1009–1011 (2004).

90.   Saito, F. *et al.* Aberrant glycosylation of alpha-dystroglycan causes defective binding of laminin in the muscle of chicken muscular dystrophy. *FEBS Lett* **579**, 2359–63 (2005).

91.   Jimenez-Mallebrera, C. *et al.* A comparative study of alpha-dystroglycan glycosylation in dystroglycanopathies suggests that the hypoglycosylation of alpha-dystroglycan does not consistently correlate with clinical severity. *Brain pathology* **19**, 596–611 (2009).

92.   Muntoni, F., Torelli, S., Wells, D. J. & Brown, S. C. Muscular dystrophies due to glycosylation defects: diagnosis and therapeutic strategies. *Curr Opin Neurol* **24**, 437–42 (2011).

93.   Moore, C. J. & Hewitt, J. E. Dystroglycan glycosylation and muscular dystrophy. *Glycoconj J* **26**, 349–57 (2009).

94.   Michele, D. E. *et al.* Post-translational disruption of dystroglycan-ligand interactions in congenital muscular dystrophies. *Nature* **418**, 417–22 (2002).

95.   Barkovich, Aj., Millen, K. J. & Dobyns, W. B. A developmental and genetic classification for midbrain-hindbrain malformations. *Brain* **132**, 3199–230 (2009).

96.   Drachman, D., Toyka, K. & Myer, E. Prednisone in Duchenne muscular dystrophy. *The Lancet* 1409–1412 (1974).

97.   Scully, M. A., Pandya, S. & Moxley, R. T. Review of Phase II and Phase III clinical trials for Duchenne muscular dystrophy. *Expert Opinion on Orphan Drugs* **1**, 33–46 (2013).

98. Fenichel, G. M. *et al.* Long-term benefit from prednisone therapy in Duchenne muscular dystrophy. *Neurology* **41**, 1874–1874 (1991).

99. Balaban, B., Matthews, D. J., Clayton, G. H. & Carry, T. Corticosteroid Treatment and Functional Improvement in Duchenne Muscular Dystrophy. *American Journal of Physical Medicine & Rehabilitation* **84**, 843–850 (2005).

100. Biggar, W. D., Harris, V. A., Eliasoph, L. & Alman, B. Long-term benefits of deflazacort treatment for boys with Duchenne muscular dystrophy in their second decade. *Neuromuscul Disord* **16**, 249–55 (2006).

101. Moxley, R. T., Pandya, S., Ciafaloni, E., Fox, D. J. & Campbell, K. Change in natural history of Duchenne muscular dystrophy with long-term corticosteroid treatment: implications for management. *J Child Neurol* **25**, 1116–29 (2010).

102. McAdam, L. C., Mayo, A. L., Alman, B. A. & Biggar, W. D. The Canadian experience with long-term deflazacort treatment in Duchenne muscular dystrophy. *Acta Myol* **31**, 16–20 (2012).

103. Perkins, K. J. & Davies, K. E. Recent advances in Duchenne muscular dystrophy. *Degenerative Neurological and Neuromuscular Disease* **2**, 141–64 (2012).

104. Konieczny, P., Swiderski, K. & Chamberlain, J. S. Gene and cell-mediated therapies for muscular dystrophy. *Muscle & Nerve* **1**, Accepted Article (2012).

105. Meregalli, M. *et al.* Perspectives of Stem Cell Therapy in Duchenne Muscular Dystrophy. *FEBS J* (2012).doi:10.1111/febs.12083

106. Farini, A., Razini, P., Erratico, S., Torrente, Y. & Meregalli, M. Cell based therapy for Duchenne muscular dystrophy. *J Cell Physiol* **221**, 526–34 (2009).

107. Péault, B. *et al.* Stem and progenitor cells in skeletal muscle development, maintenance, and therapy. *Mol Ther* **15**, 867–77 (2007).

108. Kawahara, G. *et al.* Drug screening in a zebrafish model of Duchenne muscular dystrophy. *Proc Natl Acad Sci U S A* **108**, 5331–6 (2011).

109. Khairallah, M. *et al.* Sildenafil and cardiomyocyte-specific cGMP signaling prevent cardiomyopathic changes associated with dystrophin deficiency. *Proc Natl Acad Sci U S A* **105**, 7028–33 (2008).

110. Adamo, C. M. *et al.* Sildenafil reverses cardiac dysfunction in the mdx mouse model of Duchenne muscular dystrophy. *Proc Natl Acad Sci U S A* **107**, 19079–83 (2010).

111. Kass, D. A., Takimoto, E., Nagayama, T. & Champion, H. C. Phosphodiesterase regulation of nitric oxide signaling. *Cardiovasc Res* **75**, 303–14 (2007).

112. Rooney, J. E., Gurpur, P. B. & Burkin, D. J. Laminin-111 protein therapy prevents muscle disease in the mdx mouse model for Duchenne muscular dystrophy. *Proc Natl Acad Sci U S A* **106**, 7991–6 (2009).

113. Vidal, B. *et al.* Amelioration of Duchenne muscular dystrophy in mdx mice by elimination of matrix-associated fibrin-driven inflammation coupled to the αMβ2 leukocyte integrin receptor. *Hum Mol Genet* **21**, 1989–2004 (2012).

114. McPherron, A. C., Lawler, A. M. & Lee, S. J. Regulation of skeletal muscle mass in mice by a new TGF-beta superfamily member. *Nature* **387**, 83–90 (1997).

115. Lee, S.-J. Quadrupling muscle mass in mice by targeting TGF-beta signaling pathways. *PLoS One* **2**, e789 (2007).

116. Haidet, A. M. *et al.* Long-term enhancement of skeletal muscle mass and strength by single gene administration of myostatin inhibitors. *Proc Natl Acad Sci U S A* **105**, 4318–22 (2008).

117. Nakatani, M. *et al.* Transgenic expression of a myostatin inhibitor derived from follistatin increases skeletal muscle mass and ameliorates dystrophic pathology in mdx mice. *FASEB* **22**, 477–87 (2008).

118. Bish, L. T. *et al.* Long-term systemic myostatin inhibition via liver-targeted gene transfer in golden retriever muscular dystrophy. *Hum Gene Ther* **22**, 1499–509 (2011).

119. Wagner, K. R. *et al.* A phase I/II trial of MYO-029 in adult subjects with muscular dystrophy. *Ann Neurol* **63**, 561–71 (2008).

120. Beggs, A. H. *et al.* Exploring the molecular basis for variability among patients with Becker muscular dystrophy: dystrophin gene and protein studies. *Am J Hum Genet* **49**, 54–67 (1991).

121. Koenig, M. *et al.* The molecular basis for Duchenne versus Becker muscular dystrophy: correlation of severity with type of deletion. *Am J Hum Genet* **45**, 498–506 (1989).

122. Monaco, A. P., Bertelson, C. J., Liechti-Gallati, S., Moser, H. & Kunkel, L. M. An explanation for the phenotypic differences between patients bearing partial deletions of the DMD locus. *Genomics* **2**, 90–95 (1988).

123. Ahn, A. & Kunkel, L. The structural and functional diversity of dystrophin. *Nat Genet* **3**, 283–91 (1993).

124. Incitti, T. *et al.* Exon skipping and duchenne muscular dystrophy therapy: selection of the most active U1 snRNA antisense able to induce dystrophin exon 51 skipping. *Mol Ther* **18**, 1675–82 (2010).

125. Lu, Q. L. *et al.* Functional amounts of dystrophin produced by skipping the mutated exon in the mdx dystrophic mouse. *Nat Med* **9**, 1009–14 (2003).

126. Cirak, S. *et al.* Restoration of the dystrophin-associated glycoprotein complex after exon skipping therapy in Duchenne muscular dystrophy. *Mol Ther* **20**, 462–7 (2012).

127. Lu, Q.-L. *et al.* The status of exon skipping as a therapeutic approach to Duchenne muscular dystrophy. *Mol Ther* **19**, 9–15 (2011).

128. Goemans, N. *et al.* Systemic Administration of PRO051 in Duchenne's Muscular Dystrophy. *New England Journal of Medicine* **364**, 1513–1522 (2011).

129. Van Deutekom, J. C. *et al.* Local dystrophin restoration with antisense oligonucleotide PRO051. *N Engl J Med* **357**, 2677–86 (2007).

130. Barton-Davis, E. R., Cordier, L., Shoturma, D. I., Leland, S. E. & Sweeney, H. L. Aminoglycoside antibiotics restore dystrophin function to skeletal muscles of mdx mice. *J Clin Invest* **104**, 375–81 (1999).

131. Wagner, K. R. *et al.* Gentamicin treatment of Duchenne and Becker muscular dystrophy due to nonsense mutations. *Annals of Neurology* **49**, 706–711 (2001).

132. Malik, V. *et al.* Gentamicin-induced readthrough of stop codons in Duchenne muscular dystrophy. *Ann Neurol* **67**, 771–80 (2010).

133. Finkel, R. *et al.* P3.51 Results of a Phase 2b, dose-ranging study of ataluren (PTC124®) in nonsense mutation Duchenne/Becker muscular dystrophy (nmDBMD). *Neuromuscular Disorders* **20**, 656–657 (2010).

134. Bowles, D. E. *et al.* Phase 1 gene therapy for Duchenne muscular dystrophy using a translational optimized AAV vector. *Mol Ther* **20**, 443–55 (2012).

135. Law, P. K. *et al.* Dystrophin production induced by myoblast transfer therapy in Duchenne muscular dystrophy. *Lancet* **336**, 114–5 (1990).

136. Gussoni, E. *et al.* Normal dystrophin transcripts detected in Duchenne muscular dystrophy patients after myoblast transplantation. *Nature* **356**, 435–8 (1992).

137. Law, P. K. *et al.* Feasibility, safety, and efficacy of myoblast transfer therapy on Duchenne muscular dystrophy boys. *Cell Transplant* **1**, 235–44 (1992).

138. Karpati, G. *et al.* Myoblast transfer in Duchenne muscular dystrophy. *Ann Neurol* **34**, 8–17 (1993).

139. Tremblay, J. P. *et al.* Results of a triple blind clinical study of myoblast transplantations without immunosuppressive treatment in young boys with Duchenne muscular dystrophy. *Cell Transplant* **2**, 99–112 (1993).

140. Mendell, J. R. *et al.* Myoblast transfer in the treatment of Duchenne's muscular dystrophy. *N Engl J Med* **333**, 832–8 (1995).

141. Gussoni, E., Blau, H. M. & Kunkel, L. M. The fate of individual myoblasts after transplantation into muscles of DMD patients. *Nat Med* **3**, 970–7 (1997).

142. Huard, J., Verreault, S., Roy, R., Tremblay, M. & Tremblay, J. P. High efficiency of muscle regeneration after human myoblast clone transplantation in SCID mice. *J Clin Invest* **93**, 586–99 (1994).

143. Beauchamp, J. R. Dynamics of Myoblast Transplantation Reveal a Discrete Minority of Precursors with Stem Cell-like Properties as the Myogenic Source. *The Journal of Cell Biology* **144**, 1113–1122 (1999).

144. Huard, J., Acsadi, G., Jani, A., Massie, B. & Karpati, G. Gene transfer into skeletal muscles by isogenic myoblasts. *Hum Gene Ther* **5**, 949–58 (1994).

145. Montarras, D. *et al.* Direct isolation of satellite cells for skeletal muscle regeneration. *Science* **309**, 2064–7 (2005).

146. Sacco, A., Doyonnas, R., Kraft, P., Vitorovic, S. & Blau, H. M. Self-renewal and expansion of single transplanted muscle stem cells. *Nature* **456**, 502–6 (2008).

147. Cerletti, M. *et al.* Highly efficient, functional engraftment of skeletal muscle stem cells in dystrophic muscles. *Cell* **134**, 37–47 (2008).

148. Malerba, A. *et al.* Macrophage-secreted factors enhance the in vitro expansion of DMD muscle precursor cells while preserving their myogenic potential. *Neurological Research* **32**, 8 (2010).

149. Lapan, A. D., Rozkalne, A. & Gussoni, E. Human fetal skeletal muscle contains a myogenic side population that expresses the melanoma cell-adhesion molecule. *Hum Mol Genet* **21**, 3668–80 (2012).

150. Gérard, C., Dufour, C., Goudenege, S., Skuk, D. & Tremblay, J. P. AG490 improves the survival of human myoblasts in vitro and in vivo. *Cell Transplant* **21**, 2665–76 (2012).

151. Skuk, D., Goulet, M. & Tremblay, J. P. Transplanted myoblasts can migrate several millimeters to fuse with damaged myofibers in nonhuman primate skeletal muscle. *J Neuropathol Exp Neurol* **70**, 770–8 (2011).

152. Borselli, C., Cezar, C. a, Shvartsman, D., Vandenburgh, H. H. & Mooney, D. J. The role of multifunctional delivery scaffold in the ability of cultured myoblasts to promote muscle regeneration. *Biomaterials* **32**, 8905–14 (2011).

153. Laumonier, T., Pradier, A., Hoffmeyer, P., Kindler, V. & Menetrey, J. Low molecular weight dextran sulfate binds to human myoblasts and improves their survival after transplantation in mice. *Cell Transplant* (2012).doi:10.3727/096368912X657224

154. Liu, W. *et al.* Hypoxia promotes satellite cell self-renewal and enhances the efficiency of myoblast transplantation. *Development* **139**, 2857–65 (2012).

155. Pellegrini, K. L. & Beilharz, M. W. The survival of myoblasts after intramuscular transplantation is improved when fewer cells are injected. *Transplantation* **91**, 522–6 (2011).

156. Fan, Y., Maley, M., Beilharz, M. & Grounds, M. Rapid death of injected myoblasts in myoblast transfer therapy. *Muscle Nerve* **19**, 853–60 (1996).

157. Kazuki, Y. *et al.* Complete genetic correction of iPS cells from Duchenne muscular dystrophy. *Mol Ther* **18**, 386–93 (2010).

158. Darabi, R. *et al.* Functional myogenic engraftment from mouse iPS cells. *Stem Cell Rev* **7**, 948–57 (2011).

159. Darabi, R. *et al.* Human ES- and iPS-derived myogenic progenitors restore DYSTROPHIN and improve contractility upon transplantation in dystrophic mice. *Cell Stem Cell* **10**, 610–9 (2012).

160. Goudenege, S. *et al.* Myoblasts Derived From Normal hESCs and Dystrophic hiPSCs Efficiently Fuse With Existing Muscle Fibers Following Transplantation. *Mol Ther* **20**, 2153–2167 (2012).

161. Trokovic, R. *et al.* Small Molecule Inhibitors Promote Efficient Generation of Induced Pluripotent Stem Cells From Human Skeletal Myoblasts. *Stem Cells Dev* **ePub**, ahead of print (2012).

162. Ogilvie, M. *et al.* Erythropoietin stimulates proliferation and interferes with differentiation of myoblasts. *J Biol Chem* **275**, 39754–61 (2000).

163. Davenport, A., King, R. F., Ironside, J. W., Will, E. J. & Davison, A. M. The effect of treatment with recombinant human erythropoietin on the histological appearance

and glycogen content of skeletal muscle in patients with chronic renal failure treated by regular hospital haemodialysis. *Nephron* **64**, 89–94 (1993).

164. Scoppetta, C. & Grassi, F. Erythropoietin: a new tool for muscle disorders? *Med Hypotheses* **63**, 73–5 (2004).

165. Leist, M. *et al.* Derivatives of erythropoietin that are tissue protective but not erythropoietic. *Science* **305**, 239–42 (2004).

166. Cerletti, M. *et al.* Melanoma cell adhesion molecule is a novel marker for human fetal myogenic cells and affects myoblast fusion. *J Cell Sci* **119**, 3117–27 (2006).

167. Piao, X. *et al.* Genotype-phenotype analysis of human frontoparietal polymicrogyria syndromes. *Ann Neurol* **58**, 680–7 (2005).

168. Piao, X. *et al.* G protein-coupled receptor-dependent development of human frontal cortex. *Science* **303**, 2033–6 (2004).

Chapter 2

Carbamylated erythropoietin does not alleviate signs of dystrophy in *mdx* mice

The data from this chapter were published in Muscle and Nerve on January 2011. The article was coauthored by Melissa P. Wu and Emanuela Gussoni.

Attribution of Collaborator Contributions

Abstract

INTRODUCTION: Erythropoietin promotes myoblast proliferation and inhibits fibrosis, thus it could impede the pathogenesis of muscle degenerative diseases. However, its stimulation of erythropoiesis limits its use as a therapeutic. An erythropoietin analog, carbamylated erythropoietin (C-EPO), retains these protective actions yet does not interact with the erythropoietin receptor. METHODS: To determine whether treatment with C-EPO alleviates the signs of muscular dystrophy in an animal model of Duchenne muscular dystrophy, we treated *mdx* mice with intraperitoneal injections of 50 μg/kg and 100 μg/kg C-EPO for 4 and 12 weeks, and we monitored weight, serum creatine kinase levels, and changes in muscle histology. RESULTS: We observed moderate histological improvement at 4 weeks which did not translate into a significantly decreased level of serum creatine kinase. DISCUSSION: At the dosages tested, C-EPO is not an effective therapeutic for the treatment of a mouse model of Duchenne muscular dystrophy.

Introduction

Muscular dystrophies are a group of diseases characterized by muscle weakness and wasting. One of the most common forms of muscular dystrophies is Duchenne muscular dystrophy (DMD), a disease caused by mutations in the dystrophin gene.[1] This disease is often modeled using *mdx* mice,[2] which carry a point mutation in the dystrophin gene that results in premature termination of the protein product.[3-6] By three weeks of age, *mdx* mice exhibit DMD-like histological changes in limb muscles, including variation in myofiber size, an increase in inflammatory cells, and regenerating myofibers which can be distinguished by the presence of centrally located nuclei.[7-10] The histological changes in the diaphragm

33

muscle of *mdx* mice at three weeks of age are similar to those of the limb muscles, but there is progressive muscle degeneration after this age that is accompanied by greater connective tissue infiltration. Functionally, the diaphragm muscle in *mdx* mice becomes the most severely affected,[9,10] and it parallels the degeneration observed in the human disease.[11] In both *mdx* mice and humans with DMD, reduced muscle membrane integrity leads to leakage of muscle proteins, usually measured as creatine kinase (CK), into the bloodstream. Measurement of serum CK levels is an accepted test for supporting a diagnosis of DMD.[12-15]

Thus far, no effective specific therapy is available for DMD. Many types of interventions are undergoing testing in both animal studies and human clinical trials, and these include approaches aimed at slowing the disease progression via correction of dystrophin expression in the myofibers,[16-20] or by alteration of activity of pathways known to promote myofiber growth or inhibit myofiber loss and fibrosis.[21,22]

In the hematopoietic system, the cytokine erythropoietin (EPO) prevents apoptosis of late erythroid progenitors, and it also supports the proliferation of progenitor cells by signaling through the EPO receptor. EPO can act through other receptors, such as the GM-CSF and IL-3 receptors.[23,24] Several studies have highlighted EPO's protective biological effects in organs other than the hematopoietic system,[25] and it is hypothesized that these effects occur through EPO binding to the common beta receptor, a subunit of GM-CSF, IL3 and IL5 receptors.[26] In particular, EPO has shown an anti-apoptotic effect in both the heart and the central nervous system following ischemic- or trauma-induced injury.[26,27]

EPO has several effects that could aid in repair of skeletal muscle injury and prevention of fibrosis. In vitro, EPO promotes proliferation of C2C12 and primary mouse

myoblasts, suggesting that it can stimulate the progenitor cell population during muscle repair.[28] In vivo, EPO administration for treatment of chronic renal failure increased muscle fiber diameter.[29] It promoted angiogenesis[30] and increased capillary density in the muscle of a mouse injury model of sepsis.[31]

One side effect of therapeutic EPO administration is a potentially harmful rise in hemoglobin concentration.[32,33] Overexpression of EPO in mice causes excessive erythrocytosis that leads to multiple organ degeneration, including skeletal muscle degeneration.[34] To avoid the hematopoietic effects of EPO and target its other protective biological effects, EPO analogs have been developed, such as carbamylated EPO (C-EPO). These analogs do not bind to the EPO receptor and lack erythropoietic activity.[35] Proof-of-principle experiments demonstrated that they retain anti-apoptotic, neuroprotective and regenerative activity in tissues other than the hematopoietic system by binding to the common ⬚-receptor.[26] C-EPO has been effective in preventing tissue degeneration in a number of disease models, including protecting against motor neuron death in a mouse model of amyotrophic lateral sclerosis.[36] C-EPO also reduces the inflammatory response in cortical[37] and cerebral infarcts,[35] as well as in experimental autoimmune encephalomyelitis,[38] and it has been indicated to reduce fibrosis in renal damage caused by ureteral obstruction.[39]

In a proof-of-principle experiment for the treatment of DMD, we tested whether administration of C-EPO to *mdx* mice could ameliorate dystrophic signs in muscle. *mdx* mice were injected intraperitoneally 3 times/week with 50 µg/kg or 100 µg/kg C-EPO for 4 and 12 weeks. Following treatment, serum CK levels were assessed, and histological evaluations of myofiber size, percentage of regenerating myofibers and presence of fibrotic

35

tissue were performed in the diaphragm, gastrocnemius, tibialis anterior and quadriceps muscles of treated and control *mdx* mice. Our studies demonstrated that, although moderate histological improvement was observed 4 weeks following C-EPO treatment in some muscles, lowered serum creatine kinase levels did not accompany these changes.

Materials and Methods

Animals

C57BL/10ScSn-*Mdx*/J mice (*mdx*) were purchased from the Jackson Laboratory (Bar Harbor, ME). The mice werea cohort of 5-8 week old females that were homozygous for the *mdx* mutation (a nonsense mutation in exon 23 of the dystrophin gene).[4] Doses of 0 μg/kg (control), 50 μg/kg or 100 μg/kg weight of carbamylated-erythropoietin (C-EPO) in 0.2% bovine serum albumin in phosphate-buffered saline were administered 3 times weekly via intraperitoneal (IP) injection, for 4 or 12 weeks. C-EPO was provided by Shire Human Genetic Therapies. Previous studies found beneficial effects at these dosages in the central and peripheral nervous systems and in the myocardium.[35,38,40,41] The total volume of each IP injection did not exceed 100 μL. Animals were weighed once a week for the duration of the study. Prior to euthanasia, blood was collected from the tail vein to measure serum CK. Animals were euthanized via CO_2 asphyxiation, and the diaphragm, gastrocnemius, quadriceps, and tibialis anterior muscles were collected from each animal and snap frozen in Optimal Cutting Temperature (OCT) for histological analysis. Animal groups consisted of 5-7 mice. All animals were handled in accordance with protocols approved by the Institutional Animal Care and Use Committee at Boston Children's Hospital.

Histological analyses of muscle tissue sections

For each muscle collected, 10 μm thick tissue sections were stained with hematoxylin and eosin. Measurements were made from 3 to 4 representative fields per muscle. Individual myofiber size was determined by measuring the shortest diameter of the fiber (n = 200 to 600 myofibers per muscle). Measurement of shortest diameter was chosen over measurement of cross-sectional area to reduce the bias in size due to obliquely cut fibers. To determine the fraction of regenerating muscle fibers, the number of myofibers with centrally located nuclei was counted and divided by the total number of myofibers in a field (n = 50 to 200 per field, n = 150 to 600 per muscle). The presence of fibrotic tissue was assessed by determining the area of extracellular spacing between muscle fibers using the NIH ImageJ software and dividing it by the total area of the muscle tissue within each section. The use of interstitial area as a measure for fibrotic area was validated by staining some sections for the intermediate filament protein, vimentin. The area of extracellular spacing between fibers calculated from H&E-stained tissue corresponded to the area expressing vimentin (data not shown).

Evaluation of CK levels in serum

One day prior to euthanasia, 200 μL of blood was collected via tail vein nick into BD Microtainer serum separator tubes from at least 5 mice per group. Blood was allowed to coagulate for 1 hour at room temperature and then centrifuged. Five to 25 μL of plasma serum were used in the Stanbio CK-NAC (UV-Rate) CK test to determine serum CK levels. For each blood sample, two measurements were taken and averaged.

Data are presented as mean values; error bars denote standard error of measurement. For all tests, one-way ANOVA with alpha = 0.05 was calculated using the ANOVA: Single Factor analysis tool in Excel. If significance was found ($p < 0.05$), pair wise comparisons were made using Student's t-test. The resulting t-test p-value is reported.

Results

To test the effectiveness of C-EPO in reducing the signs of muscular dystrophy, 5-8 week old *mdx* female mice were injected IP with vehicle only, 50 μg/kg, or 100 μg/kg C-EPO. Throughout the study, the weight of the animals was monitored to determine whether treatment promoted muscle growth and concurrent gains in muscle weight. Administration of C-EPO did not significantly change the weight of the animals compared to vehicle-only controls (Figure 2.1). Due to the sacrifice of some of the mice for the 4 week time point, the relative weights between treatment groups at 5 weeks changed. Outside of this imbalance, the weights of treated mice did not change significantly over time compared to control mice.

After 4 weeks, H&E-stained muscle sections were examined for improvements in muscle histology (Figure 2.2, A-F). The percentage of regenerating fibers and percent area of fibrosis were measured in the diaphragm, gastrocnemius, quadriceps, and tibialis anterior muscles of each animal. The myofiber diameter was measured in the diaphragm only. The percentage of myofibers with centrally located nuclei was significantly higher in the diaphragm of both the 50 μg/kg and 100 μg/kg treatment groups, as compared to the
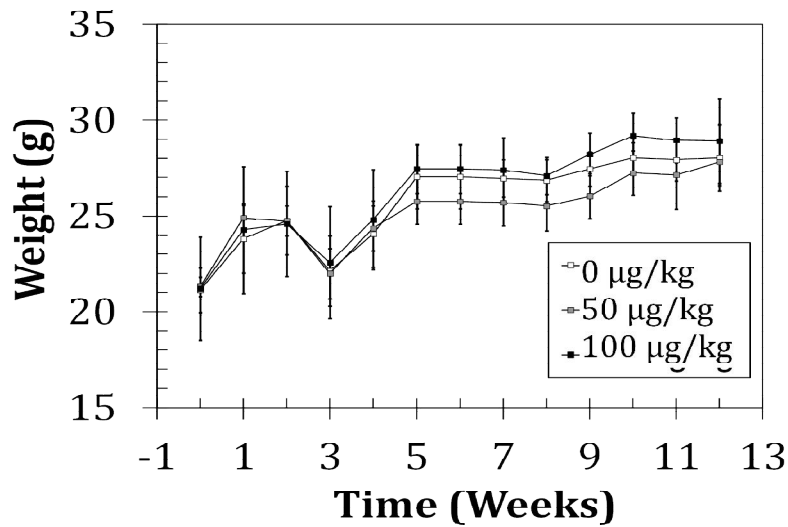
Figure 2.1

Figure 2.1. *Gross weight of female* mdx *mice treated with C-EPO*

Black squares: 0 µg/kg. Gray squares: 50 µg/kg. White squares: 100 µg/kg C-EPO.

control group (48%, 43%, and 34%, respectively; p < 0.05; Fig 2.2G). The average diameter

size of the myofibers in the diaphragm was not changed in the 50 µg/kg group compared to

control, while in the 100 µg/kg group it was decreased (p<0.05; Fig 2.2H). The distribution

of myofiber diameters in the diaphragm demonstrates that the smaller average size is due

to an overall shift towards all myofibers being smaller (Figure 2.2I). In the gastrocnemius

muscle, the percentage of centrally located nuclei was also slightly increased with

administration of 50 µg/kg C-EPO (80% vs 65%, p = 0.039; Figure 2.2G). However, no

differences were seen in the tibialis anterior or quadriceps muscles. Evaluation of the

percent area of interstitial connective tissue in the diaphragms showed a statistically

significant increase in the group administered 100 µg/kg C-EPO (p = 0.007; Figure 2.2J).

However, no changes were found in any other muscles analyzed.

Figure 2.2. *Muscle histology of mdx mice treated with C-EPO for 4 weeks*

A-C: H&E stained diaphragm, scale bar = 50 μm. **D-F:** H&E stained gastrocnemius, scale bar = 100 μm. **A, D:** 0 μg/kg treatment. **B, E:** 50 μg/kg treatment. **C, F:** 100 μg/kg treatment. **G:** Percentage of centrally located nuclei in the diaphragm (Dia), tibialis anterior (TA), quadriceps (Quad), and gastrocnemius (GA) muscles. **H**: Average myofiber diameter in the diaphragm. **I:** Distribution of fiber diameters in the diaphragm. **J.** Percentage of interstitial area in digraph, tibialis anterior, quadriceps, and gastrocnemius muscles. **G-J**: Black squares: 0 μg/kg. Gray squares: 50 μg/kg. White squares: 100 μg/kg C-EOP. '*' denotes statistically significant difference versus control (p<0.05).

Figure 2.2 (Continued)

After 12 weeks of treatment, each group underwent similar histological analyses (Figure 2.3). Unlike what was seen at 4 weeks, there was no significant difference in the percentages of regenerating myofibers in treated versus vehicle-treated mice (Figure 2.3G). There was also no significant difference in the average myofiber diameter (Figure 2.3H) or in the distribution of myofiber diameters (Figure 2.3I). An apparent increase in area of the interstitial tissue was observed in the diaphragms of treated mice compared to untreated mice, although this difference was not statistically significant (Figure 2.3J).

Previous studies using *mdx* mice have shown that a growth in the number of regenerating fibers can be accompanied by a gain in muscle function and a decrease in the levels of serum CK.[42] To test whether C-EPO administration led to such changes, serum CK levels were assayed (Figure 2.4). At neither 4 nor 12 weeks was there a significant decrease in the levels of serum CK in C-EPO-treated compared to untreated *mdx* animals.

Discussion

Because of its known neuroprotective effects, as well as indications from several studies that erythropoietin had a stimulatory effect on processes that could promote muscle regeneration and repair, it was proposed that erythropoietin could be a useful therapeutic for muscular disorders.[43] To harness the neuroprotective effects of EPO, nonhematopoietic derivatives were created, including C-EPO.[35] C-EPO has shown effectiveness in preventing damage in numerous injury models, including experimental myocardial infarction,[41] and brain and spinal cord injuries.[44] In the myocardium after ischemia, C-EPO stimulates PI3-kinase and Akt ,[45] genes that are also involved in skeletal muscle growth.[46,47]

Figure 2.3. *Muscle histology of* mdx *mice treated with C-EPO for 12 weeks*

A-C: H&E stained diaphragm, scale bar = 50 μm. **D-F:** H&E stained gastrocnemius, scale bar = 100 μm. **A, D:** 0 μg/kg treatment. **B, E:** 50 μg/kg treatment. **C, F:** 100 μg/kg treatment. **G:** Percentage of centrally located nuclei in the diaphragm (Dia), tibialis anterior (TA), quadriceps (Quad), and gastrocnemius (GA) muscles. **H:** Average myofiber diameter in the diaphragm. **I:** Distribution of fiber diameters in the diaphragm. **J.** Percentage of interstitial area in digraph, tibialis anterior, quadriceps, and gastrocnemius muscles. **G-J:** Black squares: 0 μg/kg. Gray squares: 50 μg/kg. White squares: 100 μg/kg C-EOP. '*' denotes statistically significant difference versus control (p<0.05).

Figure 2.3 (Continued)
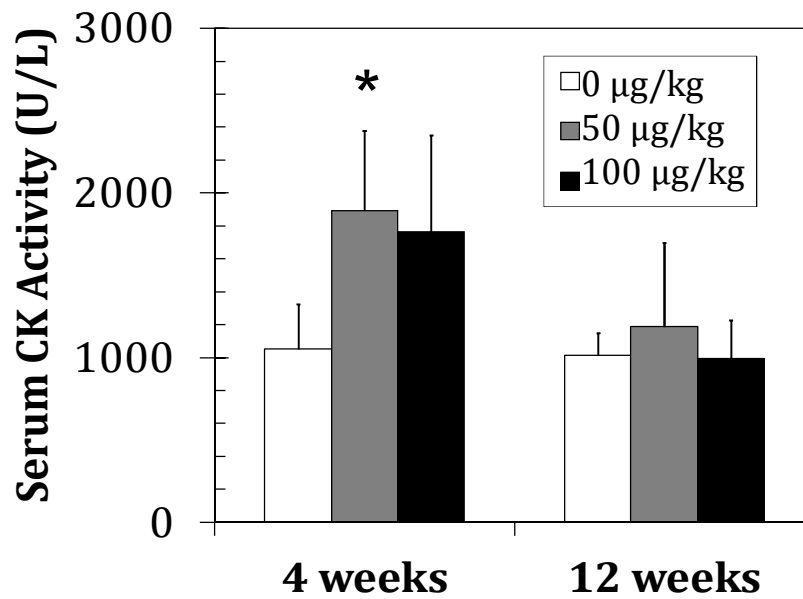
Figure 2.4

Figure 2.4. *Serum creatine kinase activity in* mdx *mice treated with C-EPO for 4 and 12 weeks*

Serum creatine kinase levels significantly increased in the 50 µg/kg-treated group at 4 weeks (p=0.02) but returned to levels in untreated mice by 12 weeks. '*' denotes a statistically significance difference versus control.

We hypothesized that administration of C-EPO would alleviate the pathology of disease in the *mdx* mouse model of Duchenne muscular dystrophy by promoting progenitor cell proliferation *in vivo.*[28] The increased pool of cells would fuse into existing myofibers, thus increasing myofiber size, or it would form new (regenerating) myofibers. In addition, it was thought that C-EPO could deter the development of fibrosis in muscular dystrophy. Two dosages of C-EPO were selected based on studies by others that had demonstrated efficacy in central and peripheral nervous system injuries.[35,38,40,41]

We found that 50 µg/kg of C-EPO stimulated a significant increase in muscle regeneration following 4 weeks of administration, however this effect did not persist at 12 weeks. The observed short-term increase in regenerating myofibers in the diaphragm and gastrocnemius muscles was not accompanied by a significant increase in myofiber diameter. Surprisingly, the average myofiber diameter of the diaphragm in the 100 µg/kg group was decreased. This finding could indicate that, in the presence of C-EPO, activated muscle progenitors formed new, small myofibers rather than fusing into and increasing the size of existing muscle fibers. However, the distribution of fiber sizes indicates a slight shift towards all existing fibers being smaller rather than induction of new small regenerating fibers.

Overall, C-EPO administration did not significantly reduce the amount of interstitial (fibrotic) tissue in the muscles of treated *mdx* mice compared to controls. Unexpectedly, at the highest dosage the amount of fibrosis compared to untreated mice increased significantly in the diaphragm muscle 4 weeks following C-EPO treatment. This increase compared to untreated mice was not observed in any other muscle analyzed at this time point, nor in any of the muscles analyzed from animals that received 12 weeks of C-EPO treatment.

The serum CK levels at both time points did not decrease in treated versus untreated animals. This finding supports the conclusion that despite an increase in the number of regenerating myofibers in some of the muscles of the C-EPO-treated *mdx* mice, the overall muscle integrity did not significantly improve. Therefore, we conclude that, although C-EPO has been effective in preventing damage in other disease conditions, it did not effectively alleviate the pathogenesis of muscular dystrophy in *mdx* mice. It is unclear

46

as to why C-EPO-treatment did not result in the intended effect. Other studies using either erythropoietin or C-EPO for prolonged therapy in mice have noted development of anemia.[38] In the case of erythropoietin, it has been speculated that anemia might have arisen from development of neutralizing antibodies that recognize endogenous proteins.[48] In our study, possible signs of anemia, characterized by whiteness in the paws and a lack of blood flow in the tail, were noted at 12 weeks following treatment (data not shown). These effects seemed worse with the 100 μg/kg treatment group. It is thus possible that the development of anemia might have contributed to the lack of efficacy at 12 weeks.

While similar treatment regimens have proven beneficial in decreasing fibrosis and improving repair in other injury/disease models, we noted only nominal effects 4 weeks following treatment of *mdx* mice with C-EPO. It remains possible that lower dosages of C-EPO may result in beneficial effects in *mdx* skeletal muscle while reducing the chance of developing anemia. Future investigations may consider lower dosages to achieve long-term improvement in muscle diseases.

Acknowledgements

References

1.   Monaco, A. P. & Kunkel, L. M. Cloning of the Duchenne/Becker muscular dystrophy locus. *Adv Hum Genet* **17**, 61–98 (1988).

2.   Bulfield, G., Siller, W. G., Wight, P. A. & Moore, K. J. X chromosome-linked muscular dystrophy (mdx) in the mouse. *Proc Natl Acad Sci U S A* **81**, 1189–92 (1984).

3.   Hoffman, E. P., Brown, R. H. & Kunkel, L. M. Dystrophin: the protein product of the Duchenne muscular dystrophy locus. *Cell* **51**, 919–28 (1987).

4.   Sicinski, P. *et al.* The molecular basis of muscular dystrophy in the mdx mouse: a point mutation. *Science* **244**, 1578–80 (1989).

5.   Ryder-Cook, A. S. *et al.* Localization of the mdx mutation within the mouse dystrophin gene. *EMBO J* **7**, 3017–21 (1988).

6.   Cavanna, J. S. *et al.* Molecular and genetic mapping of the mouse mdx locus. *Genomics* **3**, 337–41 (1988).

7.   Spencer, M. J., Montecino-Rodriguez, E., Dorshkind, K. & Tidball, J. G. Helper (CD4(+)) and cytotoxic (CD8(+)) T cells promote the pathology of dystrophin-deficient muscle. *Clin Immunol* **98**, 235–43 (2001).

8.   Spencer, M. J. & Tidball, J. G. Do immune cells promote the pathology of dystrophin-deficient myopathies? *Neuromuscular Disorders* **11**, 556–564 (2001).

9.   Karpati, G., Carpenter, S. & Prescott, S. Small-caliber skeletal muscle fibers do not suffer necrosis in mdx mouse dystrophy. *Muscle Nerve* **11**, 795–803 (1988).

10.   Tanabe, Y., Esaki, K. & Nomura, T. Skeletal muscle pathology in X chromosome-linked muscular dystrophy (mdx) mouse. *Acta Neuropathol* **69**, 91–5 (1986).

11.   Stedman, H. H. *et al.* The mdx mouse diaphragm reproduces the degenerative changes of Duchenne muscular dystrophy. *Nature* **352**, 536–9 (1991).

12.   Nichol, C. Serum creatine phosphokinase measurements in muscular dystrophy studies. *Clinica Chimica Acta* **11**, 404–407 (1965).

13.   Pearce, J., RJ, P. & JN, W. Serum enzyme studies in muscle disease: Part II Serum creatine kinase activity in muscular dystrophy and in other myopathic and neuropathic disorders. *Journal of Neurology, Neurosurgery, and Psychiatry* **27**, 96–99 (1964).

14.   Fowler, W. M. Diagnostic and Prognostic Significance of Serum Enzymes. I. Muscular Dystrophy. *Arch Phys Med Rehabil* **45**, 117–24 (1964).

15.	Swaiman, K. F. & Sandler, B. The Use of Serum Creatine Phosphokinase and Other Serum Enzymes in the Diagnosis of Progressive Muscular Dystrophy. *J Pediatr* **63**, 1116–9 (1963).

16.	Nelson, S. F., Crosbie, R. H., Miceli, M. C. & Spencer, M. J. Emerging genetic therapies to treat Duchenne muscular dystrophy. *Curr Opin Neurol* **22**, 532–8 (2009).

17.	Muir, L. A. & Chamberlain, J. S. Emerging strategies for cell and gene therapy of the muscular dystrophies. *Expert Rev Mol Med* **11**, e18 (2009).

18.	Péault, B. *et al.* Stem and progenitor cells in skeletal muscle development, maintenance, and therapy. *Mol Ther* **15**, 867–77 (2007).

19.	Heemskerk, H., De Winter, C. L., Van Ommen, G.-J. B., Van Deutekom, J. C. T. & Aartsma-Rus, A. Development of antisense-mediated exon skipping as a treatment for duchenne muscular dystrophy. *Ann N Y Acad Sci* **1175**, 71–9 (2009).

20.	Wood, M. J. A., Gait, M. J. & Yin, H. RNA-targeted splice-correction therapy for neuromuscular disease. *Brain* **133**, 957–72 (2010).

21.	Patel, K., Macharia, R. & Amthor, H. Molecular mechanisms involving IGF-1 and myostatin to induce muscle hypertrophy as a therapeutic strategy for Duchenne muscular dystrophy. *Acta Myol* **24**, 230–41 (2005).

22.	Khurana, T. S. & Davies, K. E. Pharmacological strategies for muscular dystrophy. *Nat Rev Drug Discov* **2**, 379–90 (2003).

23.	Hanazono, Y., Sasaki, K., Nitta, H., Yazaki, Y. & Hirai, H. Erythropoietin induces tyrosine phosphorylation of the beta chain of the GM-CSF receptor. *Biochem Biophys Res Commun* **208**, 1060–6 (1995).

24.	Jubinsky, P. T., Krijanovski, O. I., Nathan, D. G., Tavernier, J. & Sieff, C. A. The beta chain of the interleukin-3 receptor functionally associates with the erythropoietin receptor. *Blood* **90**, 1867–73 (1997).

25.	Ghezzi, P. & Brines, M. Erythropoietin as an antiapoptotic, tissue-protective cytokine. *Cell Death Differ* **11 Suppl 1**, S37–44 (2004).

26.	Brines, M. *et al.* Erythropoietin mediates tissue protection through an erythropoietin and common beta-subunit heteroreceptor. *Proc Natl Acad Sci U S A* **101**, 14907–12 (2004).

27.	Joyeux-Faure, M., Godin-Ribuot, D. & Ribuot, C. Erythropoietin and myocardial protection: what's new? *Fundam Clin Pharmacol* **19**, 439–46 (2005).

28.	Ogilvie, M. *et al.* Erythropoietin stimulates proliferation and interferes with differentiation of myoblasts. *J Biol Chem* **275**, 39754–61 (2000).

29.   Davenport, A., King, R. F., Ironside, J. W., Will, E. J. & Davison, A. M. The effect of treatment with recombinant human erythropoietin on the histological appearance and glycogen content of skeletal muscle in patients with chronic renal failure treated by regular hospital haemodialysis. *Nephron* **64**, 89–94 (1993).

30.   Vaziri, N. D. Cardiovascular effects of erythropoietin and anemia correction. *Curr Opin Nephrol Hypertens* **10**, 633–7 (2001).

31.   Kao, R. *et al.* Erythropoietin improves skeletal muscle microcirculation and tissue bioenergetics in a mouse sepsis model. *Crit Care* **11**, R58 (2007).

32.   Fishbane, S. & Besarab, A. Mechanism of increased mortality risk with erythropoietin treatment to higher hemoglobin targets. *Clin J Am Soc Nephrol* **2**, 1274–82 (2007).

33.   Rosner, M. H. & Bolton, W. K. The mortality risk associated with higher hemoglobin: is the therapy to blame? *Kidney Int* **74**, 695–7 (2008).

34.   Heinicke, K. *et al.* Excessive erythrocytosis in adult mice overexpressing erythropoietin leads to hepatic, renal, neuronal, and muscular degeneration. *Am J Physiol Regul Integr Comp Physiol* **291**, R947–56 (2006).

35.   Leist, M. *et al.* Derivatives of erythropoietin that are tissue protective but not erythropoietic. *Science* **305**, 239–42 (2004).

36.   Mennini, T. *et al.* Nonhematopoietic erythropoietin derivatives prevent motoneuron degeneration in vitro and in vivo. *Molecular medicine* **12**, 153–60 (2006).

37.   Villa, P. *et al.* Reduced functional deficits, neuroinflammation, and secondary tissue damage after treatment of stroke by nonerythropoietic erythropoietin derivatives. *J Cereb Blood Flow Metab* **27**, 552–63 (2007).

38.   Savino, C. *et al.* Delayed administration of erythropoietin and its non-erythropoietic derivatives ameliorates chronic murine autoimmune encephalomyelitis. *J Neuroimmunol* **172**, 27–37 (2006).

39.   Srisawat, N. *et al.* Erythropoietin and its non-erythropoietic derivative: do they ameliorate renal tubulointerstitial injury in ureteral obstruction? *Int J Urol* **15**, 1011–7 (2008).

40.   Bianchi, R. *et al.* Protective effect of erythropoietin and its carbamylated derivative in experimental Cisplatin peripheral neurotoxicity. *Clin Cancer Res* **12**, 2607–12 (2006).

41.   Fiordaliso, F. *et al.* A nonerythropoietic derivative of erythropoietin protects the myocardium from ischemia-reperfusion injury. *Proc Natl Acad Sci U S A* **102**, 2046–51 (2005).

42.	Bogdanovich, S. *et al.* Functional improvement of dystrophic muscle by myostatin blockade. *Nature* **420**, 418–21 (2002).

43.	Scoppetta, C. & Grassi, F. Erythropoietin: a new tool for muscle disorders? *Med Hypotheses* **63**, 73–5 (2004).

44.	Lapchak, P. A. Carbamylated erythropoietin to treat neuronal injury: new development strategies. *Expert Opin Investig Drugs* **17**, 1175–86 (2008).

45.	Xu, X. *et al.* Carbamylated erythropoietin protects the myocardium from acute ischemia/reperfusion injury through a PI3K/Akt-dependent mechanism. *Surgery* **146**, 506–14 (2009).

46.	Glass, D. J. Molecular mechanisms modulating muscle mass. *Trends Mol Med* **9**, 344–50 (2003).

47.	Lai, K.-M. V *et al.* Conditional activation of akt in adult skeletal muscle induces rapid hypertrophy. *Mol Cell Biol* **24**, 9295–304 (2004).

48.	Casadevall, N. *et al.* Pure red-cell aplasia and antierythropoietin antibodies in patients treated with recombinant erythropoietin. *N Engl J Med* **346**, 469–75 (2002).

Chapter 3

Establishing a role for GPR56 in the muscle:
Investigating the difference in phenotypes between bilateral frontoparietal
polymicrogyria and the dystroglycanopathies

Attribution of Collaborator Contributions

Abstract

Mammalian muscle cell differentiation is a complex process of multiple steps for which many of the factors involved have not yet been defined. In a screen to identify the cell-surface regulators of myogenic cell fusion, we found that the G-protein coupled receptor 56 (GPR56) was upregulated during the early fusion of human myoblasts and downregulated during late differentiation. At the same time, this gene was identified to be the causative gene for the disease bilateral frontoparietal polymicrogyria (BFPP). The defects in brain development in BFPP are nearly indistinguishable from brain defects in patients with the dystroglycanopathy form of muscular dystrophies. Yet, BFPP patients do not seem to share the muscle phenotype. Using GPR56 knockout mice, we investigated the role of GPR56 in the muscle. We found that GPR56 knockout mice had slight but statistically significant increases in serum creatine kinase. GPR56 is transiently upregulated in myocytes and nascent myotubes following the induction of MyoD expression. Loss of GPR56 resulted in decreased overall myoblast fusion and smaller myotube sizes in culture. Decreased signaling through SRE and NFAT signaling pathways likely resulted in these phenotypes. Despite delays in the expression of MyoD, myogenin, and NFATc2 during regeneration, no overt differences in morphological phenotype were seen in the muscle of GPR56 knockout mice compared to wildtype. Because of its transient expression and it likely being one of many factors promoting differentiation, complementation of its function by other factors results in its loss not being accompanied by clinically significant defects in muscle development or function.

Introduction

The development of muscle from undifferentiated cells is a highly complex, multistep process. Genetic defects that result in the loss of any of the proteins involved in these processes have the potential to cause muscle disorders such as myopathies or dystrophies.[1,2] Hence, a clear understanding of the proteins involved in muscle development is necessary to understanding how to treat these diseases. Only then can new strategies for the treatment of different muscle diseases be unveiled.

During muscle development, muscle progenitor cells in the somites, migrate out to the limb buds and undergo two waves of myogenesis to form mature muscle.[3–5, rev in 6] Several steps in this process of differentiation include progenitor cell proliferation and migration, the commitment to differentiation, myoblast-myoblast adhesion, and the fusion of cells to form syncytial myofibers.[rev in 7] These steps are largely recapitulated during adult muscle regeneration in vivo. During muscle regeneration, satellite cells, the adult stem cells of skeletal muscle, are activated to proliferate; then they differentiate and fuse to create new myofibers or repair damaged myofibers. To study the process of muscle cell differentiation, satellite cells can be isolated and cultured in vitro. Isolated satellite cells turn into activated myoblasts, which proliferate and can be induced to differentiate and fuse upon serum withdrawal.[8]

Transcription Factor Regulation of Myogenic Differentiation

Both in vitro and in vivo, the process of differentiation and fusion is enacted through the activation of myogenic transcription factors, as well as the extracellular, transmembrane, and cytosolic proteins that control the various steps of migration through

fusion. Several "master" basic helix-loop helix (bHLH) transcription factors, named for their ability to induce myogenicity in non-myogenic cells,[9–12] are critical for this regulation.[rev in 13] Myf5, which specifies myogenic cells in the somites,[14] supports the proliferation of isolated myoblasts in culture, as well as in satellite cells and their progeny during in vivo regeneration.[15] MyoD is also expressed in proliferating myoblasts and activated satellite cells,[16] but its upregulation is associated with exit from the cell cycle.[17] After exit from the cell cycle, the expression of myogenin induces myoblasts to differentiate.[18] The marter regulator mrf4 is normally expressed after myogenin and maintained in adult muscle,[19–21]

Although the master transcription factors are the major directors of muscle differentiation, other transcription factors also support the various phases of myogenesis. The serum response factor (SRF) has a large role in regulating cell cycle exit and commitment to differentiation[22–27] by inducing and maintaining MyoD expression.[22–24] Like MyoD, SRF can activate a sets of genes that either promote a proliferation program or a differentiation program.[22,26] This switch is controlled by phosphorylation of the SRF.[26] In either case of proliferation or differentiation, the induction of SRF-directed transcription has been tightly tied to the activation of the GTPase RhoA.[23,27,28] Later in muscle development, SRF signaling pathways are re-used to promote skeletal fiber hypertrophy.[29,30]

Another important family of transcription factors is the NFAT family, which plays multiple roles in the muscle during all stages of development from myogenic determination through fiber type specification.[31] To date, five family members have been identified: NFATc1/NFAT2/NFATc, NFATc2/NFAT1/NFATp, NFATc3/NFAT4/NFATx, NFATc4/NFAT3, and NFAT5. As the muscle field predominantly uses the "c" nomenclature,

56

this nomenclature will be used throughout. As with the bHLH family members, the activation of the various NFAT family members, by translocation into the nucleus, largely overlaps sequentially during myoblast differentiation.[32] Immunohistochemical studies in differentiating human myoblasts showed NFATc3 translocation in mononuclear myoblasts.[32] NFATc3 has been shown to cooperate with MyoD to induce the transcription of myogenin.[33] NFATc2 is active in nascent myotubes[32] and promotes further growth of the nascent myotubes into mature myotubes.[34] NFATc1 translocation to the nucleus is seen in both nascent and mature myotubes.[32] As expected from this expression pattern, NFATc1 promotes both early and late fusion of myotubes.[35] However, there is also evidence that it has a role in promoting Myf5 expression in myogenic reserve cells[36] (i.e., cells that remain uncommitted in differentiation cultures). In addition to their roles during myoblast differentiation, the NFATs are also involved in fiber type specification in mature myofibers.[37,38, rev in 39–41]

Cell-surface Receptor Regulation of Myogenic Differentiation

While the transcription factor regulation of myoblast differentiation and fusion is well understood, identification of the cell-surface receptors that are important for these processes has been more difficult. Much of our understanding of the molecular regulation of muscle development comes from work in *Drosophila*,[rev in 7] a genetically tractable model. Several, but not all, of the genes involved in fly myoblast cell fusion have yielded vertebrate homologs.[42–46] Furthermore, increased redundancy in vertebrate systems has made it difficult to definitively identify molecules as necessary, sufficient, or important for the fusion process.[47] Thus, the specific roles for the cell surface molecules are often left unclear.

Finally, the process of fusion itself is also more complicated in mammalian cells than in fly cells. The acquisition of myoblast fusion competence is achieved not only by the expression of molecules necessary for adhesion and fusion, but also by changes that increase membrane "fluidity" in preparation for membrane fusion between the cells[48, 49, rev in 7] After the initial fusion of a myoblast to another myoblast, different molecules are often required for myoblast to myotube and myotube to myotube fusion.[rev in 50]

Nevertheless, the identification of some of the mammalian cell-surface effectors of muscle cell differentiation and fusion has been made. The cell-surface molecules NCAM, N-cadherin, M-cadherin, ADAM12, and VCAM-1/VLA-4 are involved in cell-cell adhesion of muscle cells.[rev in 7] Other proteins have also been implicated as important for fusion, but their specific roles in fusion remain unclear. The transmembrane proteins CD81 and CD9 promote the fusion of myoblasts through an unknown mechanism,[51] while nephrin promotes secondary fusion.[44] Part of the difficulty in identifying cell surface proteins and their roles is that many of them act cooperatively and in parallel, thus complementing each other's function.[47]

Identification of Novel Regulators of Myogenesis

While some strides have been made in understanding the molecular basis of muscle development, it is clear that gaps remain. Uncovering the proteins involved is important for basic biology and can lead to insights for cell-based therapy of muscle diseases. To identify candidate factors that are involved in mammalian myoblast differentiation and fusion, our lab used microarray profiling to study the gene expression in proliferating mononuclear myoblasts, early differentiating myotubes (2-5 nuclei), and late differentiating myotubes

(>15 nuclei) derived from human fetal myoblast cultures.[52] Several genes changed in

expression during one or both of the stages of fusion when compared to proliferating

mononuclear myoblasts and subsequent studies in our lab have elucidated the roles of two

genes in myogenesis identified in this screen, MCAM[52,53] and C6ORF32.[54] In the current

study, we focused on genes whose expression were transiently upregulated in early

differentiating cultures to find candidates that were more likely to be involved in the early

stage of fusion. In particular, we were interested in cell surface molecules that could

possibly lend themselves to protein therapeutics for the enhancement of myoblast fusion in

vivo. One family of interest was the G-protein coupled receptors (GPCRs) family. They

comprise the largest protein family targeted for therapeutics,[55] yet many remain

uncharacterized. Of the genes identified that were upregulated specifically during early

myoblast differentiation, GPR56 was one of the GPCRs of interest for it being the causative

gene of a disease with delays in motor development and suggestions in the litereature that

suggested it played a role in muscle cell differentiation.

The G-protein Coupled Receptor 56 May Play a Role in Myogenesis

GPR56 belongs to the adhesion subfamily of G-protein coupled receptors (aGPCRs).

To date, this family contains 33 members, the majority of which have unknown ligands and

thus are categorized as orphans.[56] These aGPCRs are uniquely characterized by their

extracellular N-terminal structure, which is relatively large for GPCRs and contains a GPCR

proteolytic site (GPS) domain.[57] The GPS site is auto-catalytically cleaved during protein

translation through the action of a recently identified GAIN (GPCR-autoproteolysis

inducing) domain that encompasses both the GPS domain and regions N-terminal to the

GPS domain.[58] The resulting extracellular N-terminal fragment (NTF) and membrane-bound C-terminal fragment (CTF) then re-associate with each other non-covalently at the cell surface.[59–61]

How aGPRCRs activate G-protein signaling is under debate. Several studies have shown that their activation is controlled by the association and disassociation of the NTF and CTF,[62,63] suggesting that the NTF acts as an inhibitor of the CTF and that agonist binding to the NTF frees the CTF for signaling.[61] There is complementary evidence that the NTF and CTF fragments from different aGPCRs can associate with each other; for example GPR56 has been pulled down with the NTF of latrophilin in the brain.[64] An alternative view, however, has emerged disputing the necessity of GPS cleavage for aGPCR signaling.[65]

The cleavage products of GPR56 have been detected in metastatic melanoma,[66] pancreatic cancer cells,[67] neural progenitor cells,[68] kidney tissue,[61] and Sertoli gonadal cells.[69] However, there is also evidence for the expression of an uncleaved form in human glioma cell lines[70] and adult mouse heart, lung, liver, skeletal muscle, and adipose tissue.[68] Despite evidence that uncleaved GPR56 is endogenously expressed, there is increasing evidence that the association of the GPR56 NTF with the CTF inhibits signaling, and removal of the NTF from the CTF allows the CTF to activate G-proteins and downstream second messengers.[61,68] Paavola et al demonstrated that the expression of the GPR56 CTF increased various signs of receptor activity, including RhoA activation, ubiquitination, association with β-arrestins, and internalization.[61] Their truncated mutant included the GPS domain, however, which would normally not be included in the CTF as cleavage occurs after the GPS domain. Given that they did not include the putative N-terminal GAIN domain which would recognize and cleave off the GPS domain,[58] it remains possible that signaling

occurred via interactions between the remaining GPS sequence and the CTF, as Promel et al demonstrated was the case with the C. elegans latrophilin protein.[65]

There are several studies that support the hypothesis that GPR56 is involved in myoblast differentiation. In addition to our and other studies that showed GPR56 mRNA upregulation during early differentiation,[52,71] GPR56 has been shown to associate with factors that are involved in myoblast fusion.[51,72] Pull-down assays demonstrated that GPR56 localized to a tetraspanin microdomain specified by the tetraspanins CD81 and CD9, which were associated with the $G\alpha_{q/11}$ subunit.[72] CD81 and CD9 have been implicated as partners that promote the fusion of myoblasts.[51] GPR56 expression has been associated with the migration and adhesion of neural progenitor cells, gliomas, and melanoma cells,[68,70,73,74] processes that are also important for myoblasts.

Most notably, mutations in GPR56 have been identified as the cause of the disease bilateral frontoparietal polymicrogyria (BFPP),[75,76] which largely affects the development of the brain. This disease is characterized by mental retardation, motor developmental delay, seizures, and defects in the brainstem and cerebellum.[76] The defects in the brainstem and cerebellum present as the development of polymicrogyria, which are aberrantly small convolutions on the brain surface.[77] Loss of GPR56 in BFPP patients leads to breaks in the surface of the pial basement membrane, decreased adherence of glial cells, and the overmigration of neurons.[78,79] Interestingly, this initial diagnosis of patients with BFPP is often congenital myopathy, due to muscle atrophy.[80] Furthermore, the brain phenotype seen in BFPP is indistinguishable from the phenotype seen in many dystroglycanopathies, especially Muscle-Eye-Brain disease and Walker-Warburg Syndrome.[77,81] These diseases are caused by defects in the glycosylation of the protein α-dystroglycan[1] and result in the

decreased integrity of the pial basement membrane, loss of adherence of glial cells, and overmigration of neurons that are seen in BFPP.[77] However, the loss of α-dystroglycan glycosylation also results in the development of a severe muscular dystrophy, which is not seen in BFPP patients.[1,77] Patients with BFPP do show early muscle weakness and developmental delays. [76] Given the similar etiologies of disease in the brain, there has been speculation for what role GPR56 plays in the muscle.

These lines of evidence suggest that GPR56 has a role in muscle and given its relevance to BFPP, it is important to determine what effects its loss has on muscle development. Using knockout GPR56 mice, shRNA in C2C12 cells, and luciferase assays to determine signaling, we studied the role of GPR56 in muscle. We found that GPR56 is transiently upregulated in myocytes (differentiated myoblasts that have not yet fused) and nascent myotubes following the induction of MyoD expression and concurrent with myogenin expression. Loss of GPR56 resulted in decreased overall myoblast fusion and smaller myotube sizes in culture. Decreased signaling through SRE and NFAT signaling pathways likely resulted in these phenotypes. Despite delays in the expression of MyoD, myogenin, and NFATc2 during muscle regeneration, no overt differences in morphological phenotype were observed in the muscle of GPR56 knockout mice compared to wildtype littermate controls. Additionally, although defects in fusion due to decreased SRE and NFAT signaling were seen, no differences in the later stages of myofiber hypertrophy or fiber type specification were seen. Thus, GPR56 is involved in promoting myoblast differentiation through SRE and NFAT signaling, but not myofiber hypertrophy or fiber type specification. Because of its transient expression and it being one of many factors promoting

differentiation, complementation of its function by other factors results in its loss not being accompanied by clinically significant defects in muscle development or function.

Methods

Animals

GPR56 knockout mice (B6N.129S5-*Gpr56^{tm1Lex}*/Mmcd) were generated by Genentech/Lexicon Genetics; these mice have exon 2 (which contains the start codon) and exon 3 deleted by homologous recombination. The absence of GPR56 protein in these knockout mice was previously verified,[78] and also confirmed in our studies by mRNA and protein expression in the muscle. Animals were euthanized by CO_2 asphyxiation and the appropriate muscles dissected out. Unless otherwise stated, tissue was collected from one-month-old animals. Skeletal muscle was processed for myoblast isolation as described below. For tissue section analyses, tissue was snap-frozen by embedding in OCT (Tissue-Tek #4583) in liquid nitrogen-cooled isopentane and stored at -80°C. For mRNA and protein analyses, tissue was placed into a cryotube, snap-frozen in liquid nitrogen, and stored at -80°C. All assays were performed using male animals. All animals were handled in accordance with protocols approved by the Institutional Animal Care and Use Committee at Boston Children's Hospital.

Hematoxylin and Eosin (H&E) staining and determination of myofiber diameter

Ten micron sections of TA muscle tissue were sectioned onto charged glass slides. For uninjured muscle, sections were taken from the approximate belly of the muscle. For cardiotoxin-injured muscle, sections were taken from areas of high injury. Tissue sections

were fixed for 3 min in 70% ethanol/3% formalin/5% glacial acetic acid, and then rinsed in water. Slides were then dipped in hematoxylin (Harleco #638) for at least 5 min, rinsed in tap water, and differentiated in acid alcohol (0.3% HCl, 70% ethanol). Hematoxylin was then allowed to blue in Scott's Tap Water (0.2% $NaHCO_3$ w/v, 2% $MgSO_4 \cdot 7H_2O$ w/v) for 1 hr to overnight and rinsed in tap water. Slides were then stained in Eosin Y alcoholic (Sigma #HT110116) for 2 minutes, dehydrated in an ethanol series (50%, 70%, 80%, 90%, 100%, 100%), cleared in Histoclear-II (Electron Microscopy Sciences #64111-01), and mounted in Cytoseal. (Richard-Allan #8310-16). Tissue sections were imaged using a Nikon E1000 microscope with a SPOT Insight Color 3.2.0 camera using SPOT 4.5.9.9 software (Diagnostic Instruments).

Fiber diameter was measured using ImageJ 1.4r (NIH) and the plug-in "Measure and Label.java." For regenerating fibers, only fibers that contained centrally-located nuclei were measured. For each field, all fibers were measured. For each mouse, the results were an average of the fiber diameter measurements within 2-3 fields. Approximately 140 fibers were counted per field, totaling 280-420 fibers per mouse. Each data point represents the measurements of 3-5 mice. Error bars represent the standard deviation between the measurements for the mice. Significance was determined using an unpaired Student's t-test.

Myoblast isolation and purification

Limb skeletal muscles were dissected from one-month-old WT and GPR56 KO mice and then weighed. Tissue was finely minced with scalpels. Up to 3.5 mL collagenase D (Roche #11088882001, stock 10 mg/mL in 5 mM $CaCl_2$ in Hanks' Buffered Saline Solution

(HBSS)) and 3.5 mL dispase II (Roche #04942078001, stock 10 mg/mL in Hepes-buffered saline) per gram of tissue was added to the minced tissue. Tissue was incubated up to an hour at 37°C, and periodically triturated with 25 mL pipettes. Following dissociation, myoblast growth media (30% fetal bovine serum (FBS) and 1x penicillin/streptomycin/glutamine (PSG) in 1:1 F10/high-glucose DMEM) was added to the cells, and the mix was filtered through a 100 µm filter. Cells were pelleted and resuspended with 1 mL growth media and 7 mL Red Blood Cell Lysis Buffer (Qiagen #158904) and then filtered through a 40 µm filter. Cells were again pelleted and resuspended at 1 x 10^7 cells/mL in warm 0.5% bovine serum albumin (BSA) in HBSS. The samples were incubated for 1 hour on ice at 0.5 µg antibody/1x10^6 cells in 0.5% BSA/HBSS with the following antibodies: FITC rat anti-mouse Sca-1 (BD Biosciences #553335), APC rat anti-mouse PDGF-α (Biolegend #135908), and PE rat anti-mouse CD45 (BD Biosciences #553081). After incubation, the cells were washed with cold 0.5% BSA in HBSS, filtered with a 40 µm filter, spun down and resuspended in 0.3 mL 0.5% BSA in HBSS with 1 µL propidium iodide. Cells were FACS sorted for live PI-/CD45-/Sca-1-/PDGFa- cells[82] to remove dead cells and debris (PI+), hematopoietic (CD45+), endothelial (Sca-1+), and fibroblast (PDGF+) cells. They were then plated on 6 cm plastic plates coated with 5 µg/cm^2 collagen type I (BD Biosciences #354236) in myoblast growth media supplemented with 10 ng/mL bFGF (Atlanta Biologicals #X07995). Flow cytometry was performed on a BD FACSAria (488 nm laser) by Marie Torres in the Stem Cell Core Facility, Boston Children's Hospital, which is supported by NIH-P30-HD1865, or on a BD FACSAria II SORP by Suzan Lazo-Kallanian at the Hematologic Neoplasia Core facility, Dana Farber Cancer Institute.

Immunocytochemistry

Myoblasts were plated on 0.15% gelatin-coated (gel-coated) 4-well Permanox chamber slides and differentiated (see fusion assays for protocol). Cells were fixed with 4% paraformaldehyde (PFA) in phosphate buffered saline (PBS) for 15 min and permeabilized with 1% Triton X-100/PBS for 3 min. After washing with PBS, cells were blocked with blocking buffer (10% FBS/0.1% Triton X-100 in PBS) for 1 hour at RT. Cells were then treated with 1% SDS for 1 min and rinsed 3 times for 5 min in PBS. Cells were then incubated with the primary antibody in blocking buffer overnight at 4^oC. The primary antibodies used were: rabbit anti-V5 (1:200, Sigma #V8137), mouse anti-GPR56 (1:100, Sigma #SAB1400340), and rabbit anti-caveolin-1 (1:200, Cell Signaling #3238). After washing 3 times with PBS, cells were incubated with the secondary antibody (Dylight 488 anti-mouse IgG or Dylight 594 anti-rabbit IgG, Jackson Immunoresearch #715-486-150, #711-516-152, respectively) in blocking buffer for 1 hour at RT. After incubation, cells were washed 3 times with PBS, and mounted with DAPI Vectashield (Vector Labs #H-1200). Cells were imaged with an Orca-ER camera (#C4742-95-12ER) mounted on a Nikon E1000 microscope with Openlab 5.5.0 software (Improvision).

For C2C12 cells, cells were fixed and stained as above, without 1% SDS treatment. The primary antibody used was mouse anti-myosin (1:100, Developmental Studies Hybridoma Bank (DSHB) #MF-20, developed by D.A. Fischman).

Silencing of GPR56 in C2C12 cells

Short hairpin oligos were designed against mouse GPR56 mRNA (accession # NM_018882) and annealed into the BD RNAi-Ready pSiren-RetroQ viral vector (#631526).

The following sequences were used: 5'-TCACGTGACTACACCATCA-3', and 5'-CGTTGGTGGATGTGAATAA-3'. For virus generation, 293GP cells were plated at a 1:3 split onto a 15 cm plate in 10% FBS/1x PSG in DMEM and transfected the next day with 8 μg VSV-G plasmid and 8 μg silencing or control vector, using a standard calcium phosphate protocol for transfection. Twelve to 16 hours after transfection, the media was replaced with fresh media. After 65-72 hours, the media (containing virus) was collected and filtered through a 0.45 μm PES low-protein binding filter to remove cell debris. Virus was stored at 4°C for up to 4 days, or at -80°C for longer-term storage.

The viral infection followed a protocol based on Springer et al.[83] The viral suspension was supplemented with FBS to a final concentration of 20% FBS, and with polybrene to a final concentration of 8 ng/μL. The viral mix was added to C2C12s (plated the previous day on gel-coated 6-well plates at 7×10^4 cells), incubated for 15 min in a cell culture incubator (37°C, 5% CO_2), and spun on a Beckman Coulter Allegra 6R centrifuge at 1100 x g (~2000 revolutions per minute, (rpm)) for 30 minutes at 32°C. The viral mix was then removed and replaced with fresh C2C12 growth media (20% FBS, 1x PSG in high-glucose DMEM). Cells were re-infected with this protocol at 8, 16, and 24 hours after the first infection. They were then switched to differentiation media 6 hours after the last infection, and assayed for fusion and mRNA and protein profiles as described below. The Day 0 (D0) timepoint was taken just prior to switching the media to differentiation. Subsequent time points were taken at D1, D2, D3, and D5 for mRNA and protein, and D2 and D5 for the fusion assay.

The efficiency of infection was verified in parallel infections with virus carrying the pQCLIN construct, which expresses LacZ. Cells were assayed for LacZ at the D0, D2, and D5

67

time points. Cells were washed with PBS, fixed for 15 min with 4% PFA in PBS, permeabilized for 3 min with 1% Triton X-100 in PBS, and stained overnight at 4°C in the dark with LacZ staining solution (1 mg/mL X-gal, 5 mM $K_4Fe(CN)_6$, 5 mM $K_3Fe(CN)_6$, 1 mM $MgCl_2$ in 1x PBS, made fresh). Between 95 to 100% of the C2C12 cells expressed LacZ (data not shown).

Fusion assays

For myoblast fusion assays, $2x10^5$ WT and KO (littermate) myoblasts were plated on gel-coated 6-well dishes in myoblast growth media + 10 ng/mL bFGF. The next day (D0), they were switched to differentiation media (2% horse serum/1x PSG in low-glucose DMEM), which was changed daily for up to 6 days. To assess fusion, cells were fixed with 4% PFA in PBS for 15 min at RT, and washed with PBS; the nuclei were then stained with DAPI in PBS. Images of cells were taken using a Photometrics CoolSNAP *EZ* camera mounted on a Nikon Eclipse TE2000-S microscope with NIS Elements AR 2.30 SP4 software. Fusion was analyzed using the cell counter function in ImageJ 1.4r or 1.47b (Wayne Rasband, NIH). For each sample, 3 fields were taken and the results were averaged per duplicate or triplicate well. Each field contained approximately 100 to 200 nuclei, depending on the day of fusion. The fusion index was calculated as: 100 x (total number of nuclei in myotubes) / (total number of nuclei). The average myotube size was calculated as: (total number of nuclei in myotubes) / (total number of myotubes counted). For these counts, myotubes were defined as cells containing 2 or more nuclei. The final results are the averages of each experiment with 4 total experiments comprising 3 sets of littermate mouse myoblast isolations. Comparisons between WT and KO were made using a paired

Student's t-test, with significance set at p<0.05. Error bars show the standard deviation between experimental sets.

For GPR56-silenced C2C12 assays, cells were switched to differentiation media 6 hours after the last round of infection. The fusion index and myotube size were assayed as with the primary myoblasts, with the average of 10 fields taken per single well per sample per trial. The final results are the averaged results from three independent viral infections. Comparisons between GPR56-silenced samples and control samples were made using ANOVA with one-way variance from StatPlus:mac LE (Analyst Soft Inc, ver. 2009). Error bars show the standard deviation between experimental sets.

Proliferation assays

Littermate wildtype and knockout myoblasts were plated at 1×10^4 cells on collagen-coated 12-well plates. Every 2 days for up to 10 days, duplicate wells of myoblasts were trypsinized and counted using a hemacytometer. The myoblast growth media was replaced every 2 days. The total number of cells was then calculated for each sample. Comparisons between wildtype and knockout myoblasts were made using a paired Student's t-test. Error bars show the standard deviation between experimental sets. Data represents an average of 4 trials.

RNA isolation from cells and tissue

For cultured cells, cells were trypsinized and pelleted. RNA was isolated using the RNeasy Mini kit (Qiagen #74104) and was stored at -80ºC.

For tissues, RNA was isolated using the RNeasy Fibrous Tissue kit (Qiagen #74704) with a few modifications. Approximately 10 mg snap-frozen tissue was homogenized in 650 μL RLT + 1% β-mercaptoethanol (v/v) with Lysing Matrix D beads (MP Bio #6913) in a Fastprep F120 homogenizer (Thermo Electric) for two cycles of 40 sec at speed 6, with a 5 min incubation on ice in between. Homogenized tissue was then spun down at 4°C at 13.2 rpm for 4 min, and 300 μL of the supernatant containing the RNA was transferred to an eppendorf tube. Ten microliters of proteinase K solution and 590 μL RNase-free water was then added, and the sample was incubated for 10 min at 55°C. The RNA was then isolated using the RNeasy Fibrous Tissue Kit with the DNA removal step as per the manufacturer's recommendations. The RNA was eluted in 100 μL RNAse-free water and stored at -80°C.

Reverse Transcription and Quantitative Real-Time PCR

cDNA was reversed-transcribed from 0.5 to 2 μg RNA using either the Quantitect Reverse Transcription kit (Qiagen #205311), or the Superscript III Reverse Transcription kit (Invitrogen #18080-051) with a mix of random hexamers and oligodT primers. For each experimental set, the same kit was used.

For quantitative PCR, 1/40 to 1/20 volume (0.5 to 1 μL) of cDNA from the above reaction was amplified using SYBR green (Invitrogen #4364346) and quantified in a 7900HT Fast Real-Time PCR System (Applied Biosystems). Relative expression was calculated using the delta delta Ct method.[84] All primers were optimized to run at the same efficiency as control primers (β-2-microglobulin (B2M) for cell and uninjured muscle assays or GAPDH for cardiotoxin injury assays).[85] When possible, primers were designed to

Table 3.1. *RT-qPCR primer sequences and concentrations*

Gene	Forward primer (5'→3)	Final conc. (nM)	Reverse primer (5'→3')	Final conc. (nM)
B2M	ctgaccggcctgtatgctat	50	ccgttcttcagcatttggat	50
GAPDH	aactttggcattgtggaagg	50	acacattgggggtaggaaca	50
GPR56	gtgaataactacggccccatt	300	catagcgacgttgaacaggaa	200
Myf5	ggcatgcctgaatgtaacag	100	gacacggagcttttatctgc	100
MyoD	tacagtggcgactcagatgc	37.5	cggtgtcgtcgccattctg	37.5
Myogenin	cagtgaatgcaactcccaca	100	caaatgatctcctgggttgg	100
NFATc1	acatgacggggctggag	200	cataactgtagtgttctgctgcggc	400
NFATc2	atgtgagcaggaggagagga	300	tggacctcaatccgtagctc	200
NFATc3	gaaaaatgtcaaggggctca	50	gcaaagatggaactgaaggc	50
NFATc4	gccgcaagctgcgaggatga	200	tcccccagggccaaacgaca	100
FHL1-1	caacctccggggcaggcatc	200	gcctttaccaaacccgggcttc	400
Embryonic MHC	cgcagaatcgcaagtcaata	100	caggaggtcttgctcactcc	100

span exon-intron junctions and/or large introns. All assays were run with no template and minus reverse transcriptase controls. The primers used are listed in Table 3.1.

Protein isolation

Cells were lysed directly on the plate with RIPA cell lysis buffer (50 mM Tris pH 7.4, 150 mM NaCl, 1% NP-40, 1 mM EDTA) with 0.1% SDS, protease inhibitor cocktail (Roche #4693159001) and phosphatase inhibitor cocktail (Roche #4906837001). Plates were then incubated for 30 minutes at 4°C on a shaker. Lysate was collected into 1.5 mL microcentrifuge tubes with a plastic spatula and rotated for another 30 minutes at 4°C. They were then centrifuged for 25 min at 4°C, 13.2 rpm on a tabletop minicentrifuge. The supernatant was aliquoted and the protein concentration was quantified using the Bio-Rad DC Protein Assay Kit II (#500-0112). Lysates were stored at -20 or -80°C.

Tissue samples were snap-frozen as described above. They were then crushed into a powder using a liquid-nitrogen cooled ceramic mortar and pestle. An aliquot of the powder was taken and homogenized in TPER buffer (Thermo Scientific #78510) with 0.1% SDS/ protease inhibitor cocktail/phosphatase inhibitor cocktail for 1 min at 4°C, using a hand-held homogenizer and plastic pestles. Samples were then rotated at 4°C for one hour and frozen at -20°C to complete lysis. After thawing, samples were centrifuged and the supernatant aliquoted and quantified as with the cell lysates.

Western blot analyses

One to 20 μg protein per sample was prepared with NuPage LDS loading buffer (Invitrogen #NP0007) and 5% β-mercaptoethanol (v/v); samples were then denatured for 10 minutes at 65°C before loading onto 4-12% Bis-Tris gels (Invitrogen #WG1402BOX). Gels were run in MES (Invitrogen #NP0002) or MOPS buffer (Invitrogen #NP0001) at 100 V. Protein was transferred to nitrocellulose for 1 hour in transfer buffer (12.5 mM Tris-Glycine pH 8.3, 10% methanol). Blots were blocked in 5% BSA/1% milk in TBST (25 mM Tris, 3 mM KCl, 140 mM NaCl, 0.01% Tween-20) for one hour at RT and incubated in primary antibody in blocking buffer overnight at 4°C on a shaker. For detecting GPR56, blots were blocked and incubated with primary antibody in 5% BSA/2% milk/ TBST. After 3 washes with TBST, blots were incubated with the appropriate HRP-conjugated secondary antibodies (1:10,000, Jackson Immunoresearch, anti-mouse IgG #715-035-150, anti-mouse IgM #715-036-020, anti-rabbit IgG #711-035-152, anti-goat IgG # 705-035-003) in 5% milk in TBST for 40 min at RT. Bands were detected using the Western Lightning chemiluminescent detection reagent (Perkin Elmer #NEL105001EA). After detection, blots

were stripped for 25 min at 80°C in stripping buffer (0.2 M glycine pH 2.5, 0.05% Tween-20), washed for 1 hour in TBST, and re-probed for other proteins. The following primary antibodies were used: mouse anti-mouse GPR56 (1:1000, H11 clone, generous gift from Xianhua Piao, Boston Children's Hospital, Boston, MA), mouse anti-MyoD (1:1000, BD Biosciences #554130), mouse anti-myogenin (1:1000, DHSB #F5D, developed by F.W. Wright), goat anti-FHL1 (1:1000, Abcam #Ab23937), mouse anti-PCNA (1:1000, Santa Cruz #sc-56), rabbit anti-GAPDH 14C10 (1:1000, Cell Signaling #2118), rabbit anti-α/β-tubulin (1:5000, Cell Signaling #2148), and rabbit anti-RhoA (2 µg/mL, Sigma #R9404). For the analysis of primary mouse myoblasts, protein lysates from four sets of myoblasts isolated from littermate WT and KO mice were analyzed. For the analysis of silenced C2C12 cells, protein lysates were made from three sets of C2C12 cells that were independently infected.

For quantification of myosin heavy chains (MHC), separate gels were run for each MHC Western blot. The total protein on nitrocellulose blots was stained with SYPRO Ruby Protein Blot Stain (Invitrogen #S-11791). Bands were imaged using the Bio-rad Chemidoc XRS+ molecular imaging system and densitometry readings were taken using the volume rectangle tool in Quantity One 4.6.2 software. The blot was destained and then blotted for mouse anti-slow MHC (1:1000, Sigma #M8421), mouse anti-MHC Type IIA (1:1000, DSHB #SC-71, developed by S. Schiaffino), or mouse anti-MHC Type IIB (1:1000, DSHB #BF-F3, developed by S. Schiaffino). Multiple ECL readings of the MHC bands were taken using the Bio-rad Chemidoc XRS+ to ensure that measurements could be taken from an exposure that was not saturated. The densitometry measurements for MHC bands were normalized to the total protein SYPRO bands, and the results from three to five mice were averaged.

Significance was determined using the Student's t-test (unpaired) in Excel. Error bars show the standard deviation between samples.

Cardiotoxin injections

One-month-old WT and KO mice were anesthetized with isoflurane. The lower right legs were shaved over the tibialis anterior (TA) muscle and disinfected with ethanol. A total of 15 μL of 0.5 μg/mL cardiotoxin (Sigma #C9759-5MG) in PBS was injected into three different sites in the TA with a Hamilton syringe (26 G needle). Mice were sacrificed at 2, 3, 4, 6, and 18 days after cardiotoxin injury and their right and left TA muscles were dissected for IHC and RNA analyses. Left (uninjured) TA muscles were used as uninjured (D0) controls.

Determination of fiber type proportions by IHC

One-month-old WT and KO mice were sacrificed and their gastrocnemius muscle dissected out, mounted on OCT drops for freezing, and snap-frozen in liquid-nitrogen-cooled isopentane. Sequential 10 μm muscle cross-sections from the approximate center of the muscle were fixed in cold acetone for 5 min and then air-dried for 20 min. They were then washed with 1x PBS-T (0.1% Tween-20 in PBS) and blocked for 30 min in 2.5% horse serum in PBS-T. Sections were then incubated overnight at 4°C in primary antibody in PBS-T using the following myosin-type specific antibodies: mouse IgG anti-Type I (1:100, Sigma #M8421), mouse IgG anti-Type IIA (1:50, DSHB #SC-71, developed by S. Schiaffino), or mouse IgM anti-Type IIB (1:50, DSHB #BF-F3, developed by S. Schiaffino) myosin heavy chains, and co-stained with a rabbit anti-laminin antibody (1:100, Sigma #L9393) to

outline the myofibers. After three 3 min washes in PBS-T, the slides were incubated with 1:500 Alexa488 anti-mouse IgM (Invitrogen #A-21042) or IgG (Jackson Immunoresearch #715-546-150) and 1:500 Dylight594 anti-rabbit IgG (Invitrogen #A-21069) in PBS-T. After three 5 min washes in PBS-T, the slides were mounted with DAPI Vectashield.

The entire section was photographed in sequential fields using a Hamamatsu Orca-ER camera (#C4742-95-12ER) mounted on a Zeiss Axioplan 2 microscope (5x objective) using Axiovision 4.5 SP1 software. The individual fields were merged together into one photograph using Photoshop CS3. The total number of positive fibers in each section were counted digitally by Hui Meng and Alexandra Lerch-Gaggl at the Medical College of Wisconsin. Percentages were found by taking the total number of positive fibers per MHC divided by the sum of total positive fibers for each MHC per mouse, multiplied by 100. To verify the counts, select tissues were manually counted for positive and total fibers for each section using the cell counter function in ImageJ 1.4r (NIH) and compared to the positive counts obtained digitally. Digital quantification counted approximately 60% of the fibers but maintained the proportion of counts for the various fiber types (Suppl. Figure A2.1). Significance was determined using the Student's t-test (paired) in Excel with significance at $p < 0.05$. The error bars represent the standard deviation between samples.

Evaluation of serum creatine kinase (CK) levels

Mice aged between 5 and 10 months were nicked in the tail vein, and 200 μL blood was collected into BD Microtainer serum separator tubes (BD Biosciences #365956). Blood was allowed to coagulate for 1 hour at room temperature and then centrifuged at 13.2 rpm in a table-top microfuge for 1.5 min. Twenty microliters of plasma serum were used in the

CK-NAC (UV-Rate) CK test (Stanbio #0910) to determine serum CK levels. Spectrophotometric readings were taken at 340 nm over the course of 3 minutes in a Beckman DU640 spectrophotometer and used to determine enzyme activity. For each blood sample, two measurements were taken and averaged. A total of 11 WT and 12 KO animals were analyzed. Data were analyzed for statistical significance using the Student's t-test (unpaired, homoscedastic) in Excel with significance at $p < 0.05$. The error bars represent the standard deviation between samples.

Luciferase assays

The mouse GPR56 coding sequence was amplified from a V5-tagged mouse GPR56 (accession# NM_018882) construct created and kindly provided by Samir Koirala (Boston Children's Hospital, Boston, MA).[79] Constitutively active, truncated GPR56 (tGPR56) was cloned into pCMV-XL4 by amplifying the C-terminal domain of GPR56 after the GPS cleavage site. The location of GPS cleavage was determined by homology to the GPS cleavage sites in other aGPCRs.[8] The forward primers incorporated NotI restriction enzyme sites, a Kozak initiation sequence, and a methionine amino acid translational start site: full-length GPR56 (mGPR56) forward primer 5'-AAGCGGCCGCCACCATGGCTGTCCAGGTGCTG-3' and tGPR56 forward primer 5'-AAGCGGCCGCCACCATGACCTACTTTGCAGTGCTGAT-3'. The reverse primer incorporated a NotI restriction enzyme site after the stop codon and was used for both mGPR56 and tGPR56: 5'-TTGCGGCCGCTGCAGAATTGCCCTAGATGC-3'. The following luciferase reporters, which were generous gifts from Alan Kopin (Tufts Medical Center, Boston, MA), were used: SRE$_{5x}$-luc and NFAT-RE-luc.

HEK293 cells were plated at 6000 cells/96 well one day prior to transfection, or at 3000 cells/96 well two days prior to transfection, in 10% FBS/DMEM. They were transfected with Lipofectamine (Invitrogen #18324-012) with 0-8 ng mGPR56-pCMV-XL4, tGPR56-pCMV-XL4, or pCMV-XL4 empty vector control, 20 ng reporter, and 5 ng β-galactosidase (β-gal) pcDNA1.1 control (generous gift from Alan Kopin, Tufts University, Boston, MA), in serum-free DMEM. Twenty-four to 30 hours after transfection, cells were assayed for luciferase and B-gal activity. Fifty microliters Steadylite Plus luciferin substrate (1:6 dilution in water, Perkin Elmer #6016756) was added to the cells and luminescence was measured with a TopCount NXT instrument (Perkin Elmer). β-gal activity was measured by adding 80 µL Solution A (4 µL/mL β-mercaptoethanol, 60 mM Na_2HPO_4, 40 mM NaH_2PO_4, 10 mM KCl, 1 mM $MgSO_4 \cdot 7$ H_2O) and 50 µL Solution B (4 mg/mL 2-Nitrophenyl β-D-galactopyranoside (Sigma #N1127), 60 mM Na_2HPO_4, 40 mM NaH_2PO_4, 10 mM KCl, 1 mM $MgSO_4 \cdot 7$ H_2O) to cells on top of the Steadylite solution, incubating at 37°C, and measuring color development in a spectrophotometer. Relative luciferase activity was measured by dividing luminescence counts by β-gal counts. Averaged triplicate data for each experiment were normalized to the 0 ng/mL data point for mGPR56-pCMV-XL4, and the data from three separate experiments were averaged to produce the normalized relative luciferase activity. Significance was analyzed using two-way ANOVA with Bonferroni correction in GraphPad Prism 5. Error bars denote the standard deviation between experiments.

Results

GPR56-deficient muscles develop with slight defects

Patients with BFPP share similarities in the brain pathology with dystroglycanopathy patients, who also exhibit severe muscle defects.[77] Some patients with BFPP have a motor delay or early muscle hypotonia resulting in an early mis-diagnosis of congenital myopathy.[76] Studies on differentiating muscle cells reported the upregulation of GPR56 during fusion,[52,71] leaving open the possibility that GPR56 could play an important function in skeletal muscle tissue. To determine whether the absence of GPR56 results in muscle defects, we used the GPR56 knockout mouse. This mouse replicates the brain pathology seen in BFPP,[78,79] suggesting that it would serve as a good model for understanding the phenotype and etiology of any muscle defects caused by the loss of GPR56.

We did not notice any motor developmental delays or muscle hypotonia in GPR56 knockout mice (data not shown). We examined the muscle histology of 1- to 3-month old wildtype and knockout mouse gastrocnemius and tibialis anterior muscles by H&E (Figure 3.1A). In the knockout muscle, there were no signs of myopathy or dystrophy that are often seen in muscle disorders, such as fibrosis, necrosis, or increased fiber size heterogeneity. Quantification of the myofiber sizes in knockout versus wildtype mice revealed no difference in size (Figure 3.1B). However, we did note the presence of tubular aggregates in the knockout muscle that were not initially seen in wildtype muscle. However, later examinations also revealed tubular aggregates in wildtype muscle, which may have arisen due to inbreeding within the colony.[86] Therefore, we determined that this phenotype was

not a significant pathogenic phenotype that is due to the absence of GPR56 (data on tubular aggregates are detailed in Appendix A).

Another broad indicator widely used in the diagnosis of muscle disorders is an increased serum creatine kinase (CK) level,[87] an indicator of structural weakness in the muscle fiber structure that leads to the leakage of muscle proteins into the bloodstream. We found a slight but statistically significant increase in the serum CK levels of GPR56 knockout mice over the levels observed in wildtype mice (Figure 3.1C, n=11-12 mice/group). The GPR56 knockout mice exhibited increased variability in serum CK that ranged higher than the levels found in wildtype mice. This mild increase, in addition to the data showing that GPR56 is upregulated in human fetal myoblasts undergoing differentiation in vitro,[52] supported the further investigation of GPR56's role in muscle cell differentiation.

GPR56 is transiently expressed in differentiating myoblasts

To more carefully define the timing of GPR56 during differentiation, primary mouse myoblasts were isolated and induced to differentiate by serum withdrawal. mRNA and protein lysates were collected at various time points throughout differentiation (Figure 3.2A). Both GPR56 mRNA (Figure 3.2B) and protein (Figure 3.2C) are transiently induced during early fusion of primary mouse myoblasts (D1, D2), and quickly downregulated during later fusion stages. GPR56 protein expression in myoblast cultures follows the onset of MyoD expression which marks myoblast commitment and overlaps with the MyoD expression that is maintained during early differentiation (Figure 3.2C). GPR56 expression is concomitant with myogenin expression, which marks early differentiation. Thus, its

Figure 3.1. *Gross phenotypes in GPR56 knockout mice*

A. H&E staining of one-month-old gastrocnemius (top, GA) and tibialis anterior (bottom,

TA) muscles shows no difference between wildtype and knockout muscle. Scale bars = 50

μm. **B.** Myofiber diameter in TA muscle shows no difference between wildtype and

knockout. **C.** Serum CK levels in wildtype and knockout mice shows slightly elevated serum

CK levels in knockout mice. *p=0.012.

A

WT KO

GA

TA

B Average Myofiber Diameter

C Serum Creatine Kinase
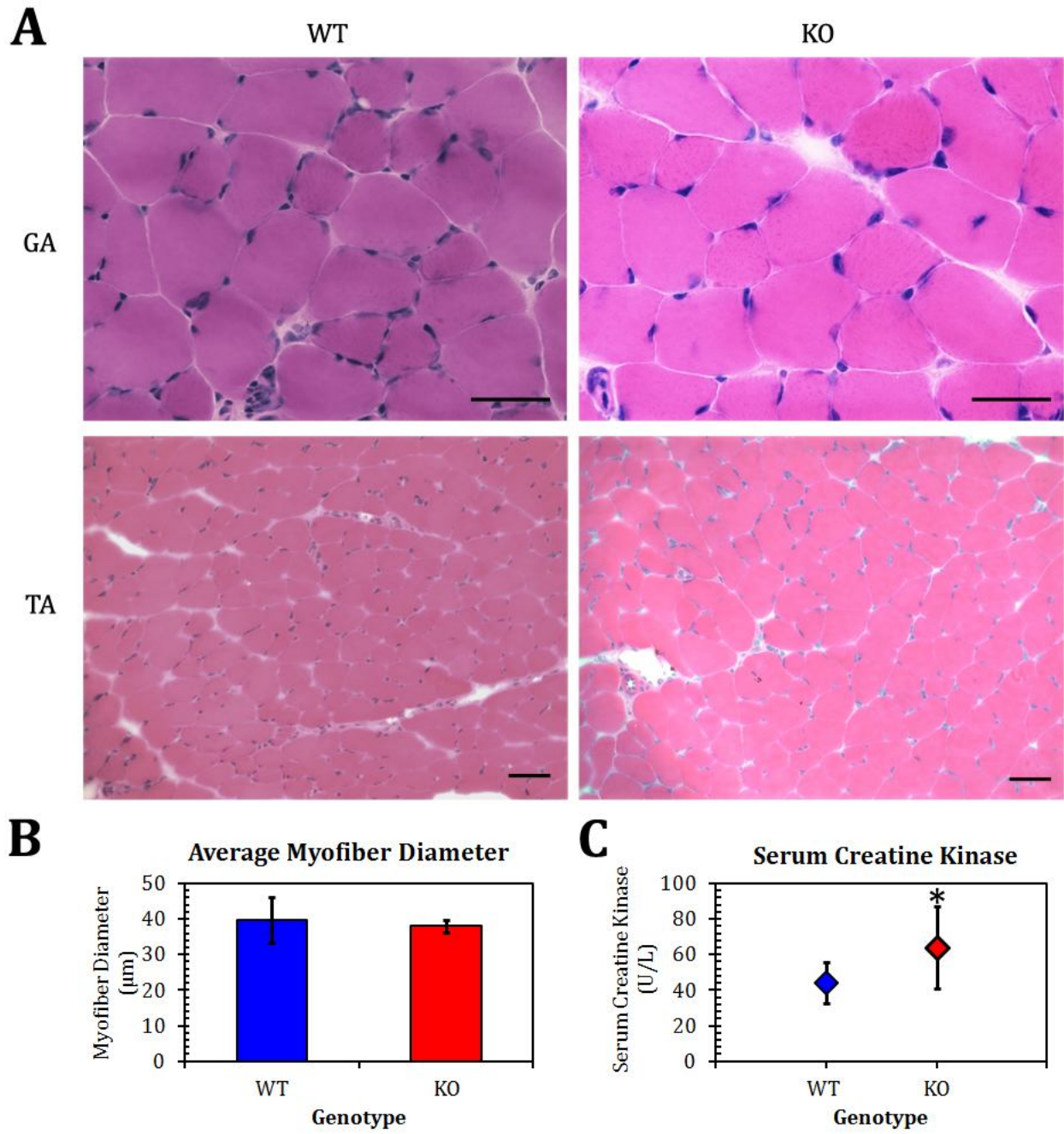
Figure 3.1 (Continued)

expression profile suggests that GPR56 is expressed in myoblasts between commitment and early fusion.

The *in vitro* myoblast cultures at D1 and D2, where GPR56 expression is the highest, contain a mixture of proliferating and quiescent myoblasts, committed myocytes, and early myotubes with few nuclei. To determine which of these cells were expressing GPR56, we performed immunocytochemistry on myoblasts at D1 (Figure 3.2D-G). We detected GPR56 expression in mononuclear cells that were not associated with myotubes, as well as mononuclear cells in close association with myotubes (Figure 3.2D). We also saw some expression in myotubes, close to nuclei. To better distinguish whether the GPR56-positive mononuclear cells were in myoblasts or myocytes, we co-stained the cultures with caveolin-1 (Figure 3.2D-G), which is expressed in proliferating and elongated myoblasts.[88] We found that GPR56 was never co-expressed in cells expressing caveolin-1, suggesting that GPR56 is only expressed in early differentiating myocytes. Thus, we narrowed the expression of GPR56 from early differentiating myocytes to early fusion and formation of small myotubes.

Loss of GPR56 results in less efficient differentiation and fusion

The pattern of expression of GPR56 prompted us to study the effect of its loss-of-function on differentiating myoblasts in vitro. We isolated three sets of myoblasts from the limb and back muscles of one-month-old littermate wildtype and GPR56 knockout mice, differentiated them for 5 days, and analyzed their fusion competence (Figure 3.3). Knockout myoblasts exhibited a decreased ability to fuse, as measured by their fusion index at days 2 and 5 in differentiation media (Figure 3.3B). Quantification of the myotube

Figure 3.2. *GPR56 is transiently expressed in the early differentiation phase of mouse myoblasts*

 A. Phase images of mouse myoblasts induced to differentiate over the course of 6 days (D0 – D6) illustrating the degree of myotube formation. **B**. GPR56 mRNA expression by qRT-PCR in primary mouse myoblasts differentiated from D0 to D6. GPR56 mRNA expression peaks at D1, then rapidly decreases. **C**. Protein expression of GPR56, MyoD, myogenin, and α/β-tubulin in myoblasts at D0 to D6, as assessed by Western blot. GPR56 protein expression peaks at D1 and rapidly decreases by D3, where little expression remains. **D-G.** GPR56 (green) and caveolin-1 (red) staining in differentiating primary mouse myoblasts at D1. DAPI (blue) was used to stain nuclei. Arrows depict GPR56+ cells that look close to fusion.
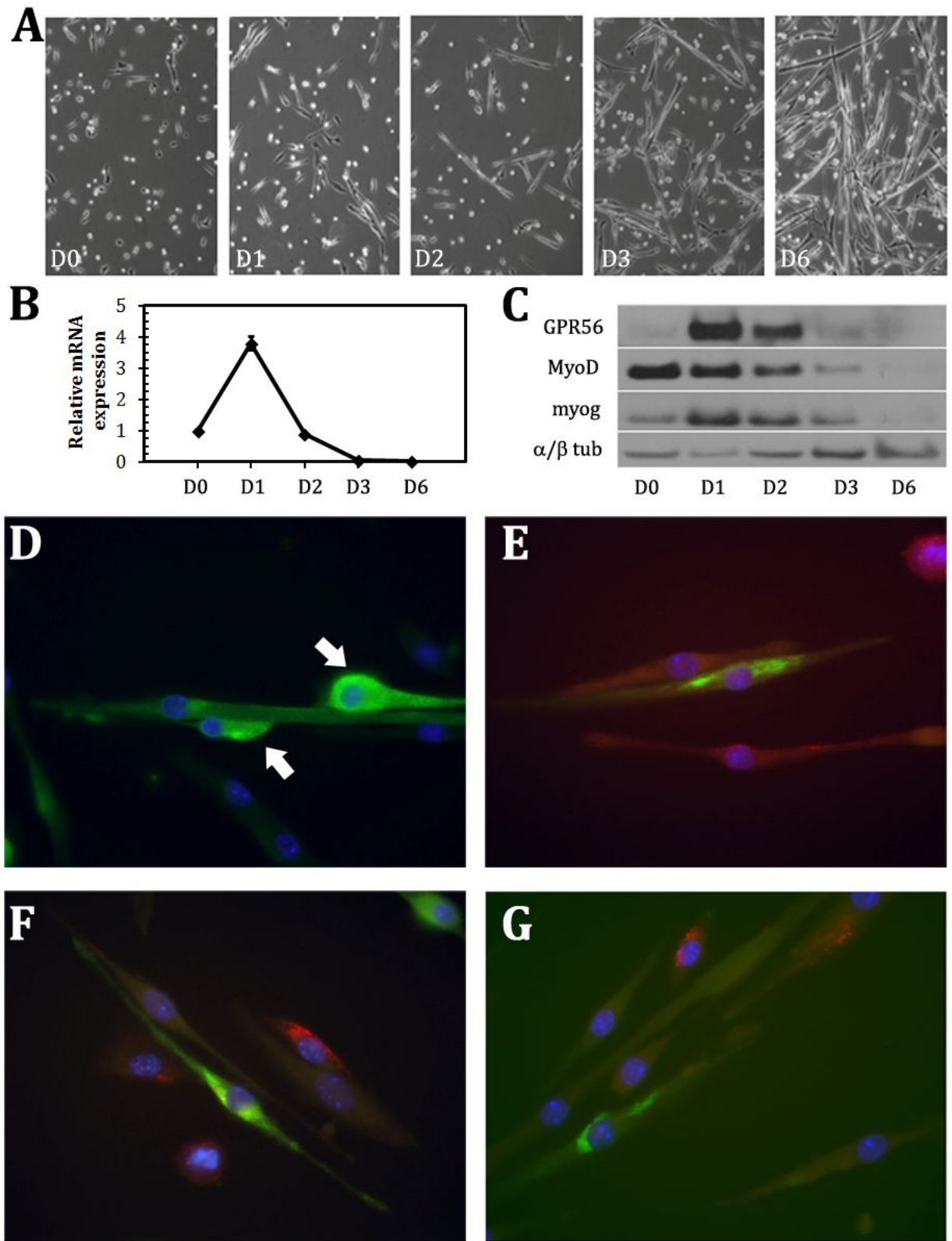
Figure 3.2 (Continued)
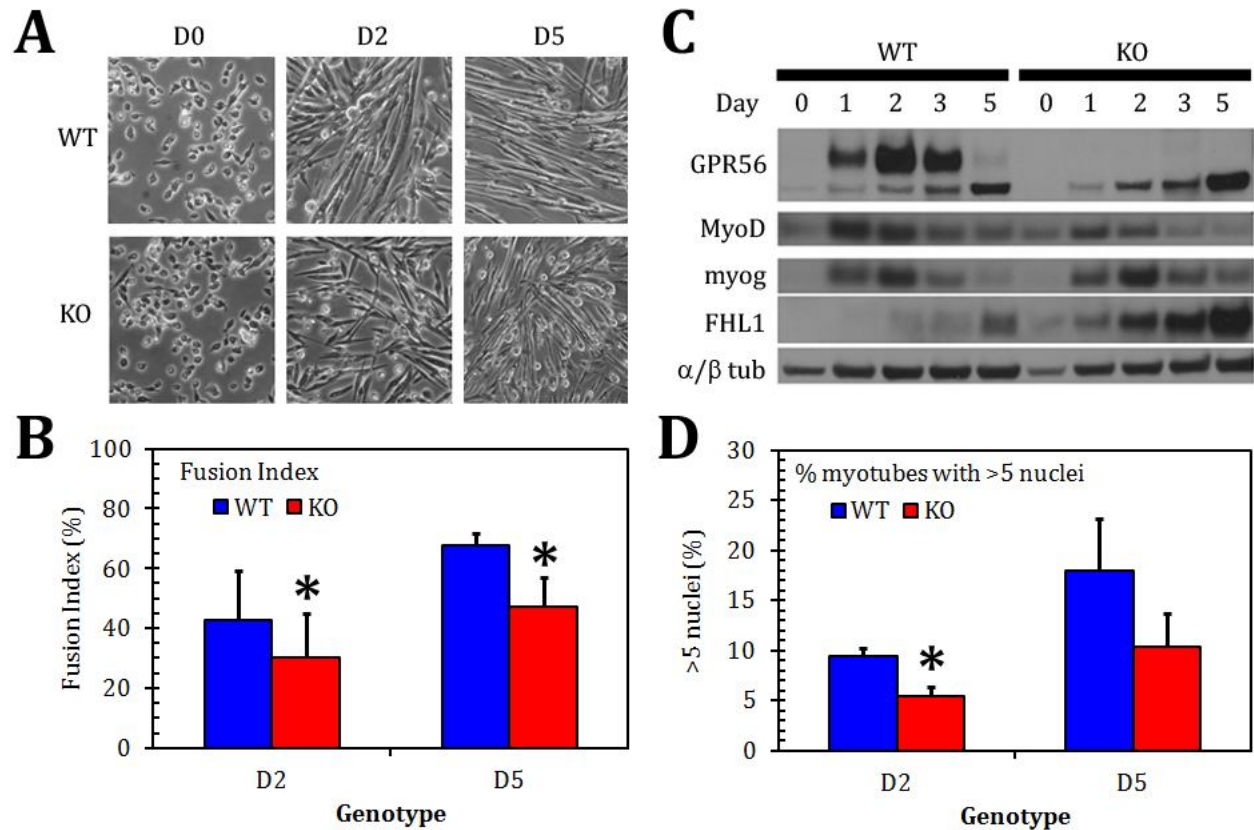
Figure 3.3

Figure 3.3. *GPR56 knockout myoblasts fuse less and have decreased MyoD expression*

A. Phase images of WT and GPR56 KO mouse myoblasts undergoing differentiation at D0,

D2, and D6. **B.** Fusion index in WT (blue) and KO (red) differentiating mouse myoblasts.

GPR56 KO myoblasts have decreased fusion at D2 and D5. * $p < 0.0.5$. **C.** Protein expression

by Western blot of GPR56, MyoD, myogenin, and α/β-tubulin in differentiating myoblasts at

D0-D5. GPR56 KO myoblasts have decreased MyoD expression. **D.** Percent of myotubes

with greater than 5 nuclei in WT (blue) and KO (red) differentiating mouse myoblasts.

GPR56 KO myoblasts have smaller tubes at D2 compared to wildtype. * $p < 0.05$.

size demonstrates that knockout cells also form smaller myotubes at D2 (Figure 3.3D), whereas by D5 the myotube size is not significantly different between knockout and wildtype cultures. The ability of the knockout myotubes to grow to sizes similar to those of wildtype myotubes by D5 suggests that GPR56 plays a role only in the early stages of myoblast fusion.

To more precisely define GPR56 function in relation to myogenic progression, we looked at the protein expression of myogenic transcription factors involved in different stages of differentiation (Fig 3.3C). We found that MyoD was decreased in the knockouts compared with wildtype myoblasts at similar time points, whereas there was no change in the early marker of differentiation, myogenin. NFATc1[89] and NFATc2[34] promote fusion and myotube growth in myoblasts and myotubes after the onset of myogenin expression. Their transcriptional activity is supported by the co-activator FHL1.[35] We found that FHL1 is highly upregulated in the knockouts.

Because MyoD is expressed prior to and during the period of peak GPR56 expression, it is somewhat surprising to see that it is downregulated in GPR56 knockout myoblasts. It is possible that this downregulation was due to the myoblasts having developed in a GPR56-deficient environment, and thus the isolated myoblasts have developed compensatory mechanisms that resulted in decreased MyoD expression. To confirm that the decrease in fusion was a direct consequence of the loss of GPR56, GPR56 was silenced using two separate shRNA constructs in the mouse myoblast C2C12 cell line (Figure 3.4A). Silencing of GPR56 allows the evaluation of its loss without interference from compensatory mechanisms that may have developed in vivo due to long-term loss of GPR56. GPR56 expression was efficiently silenced at both the mRNA (Figure 3.4B) and
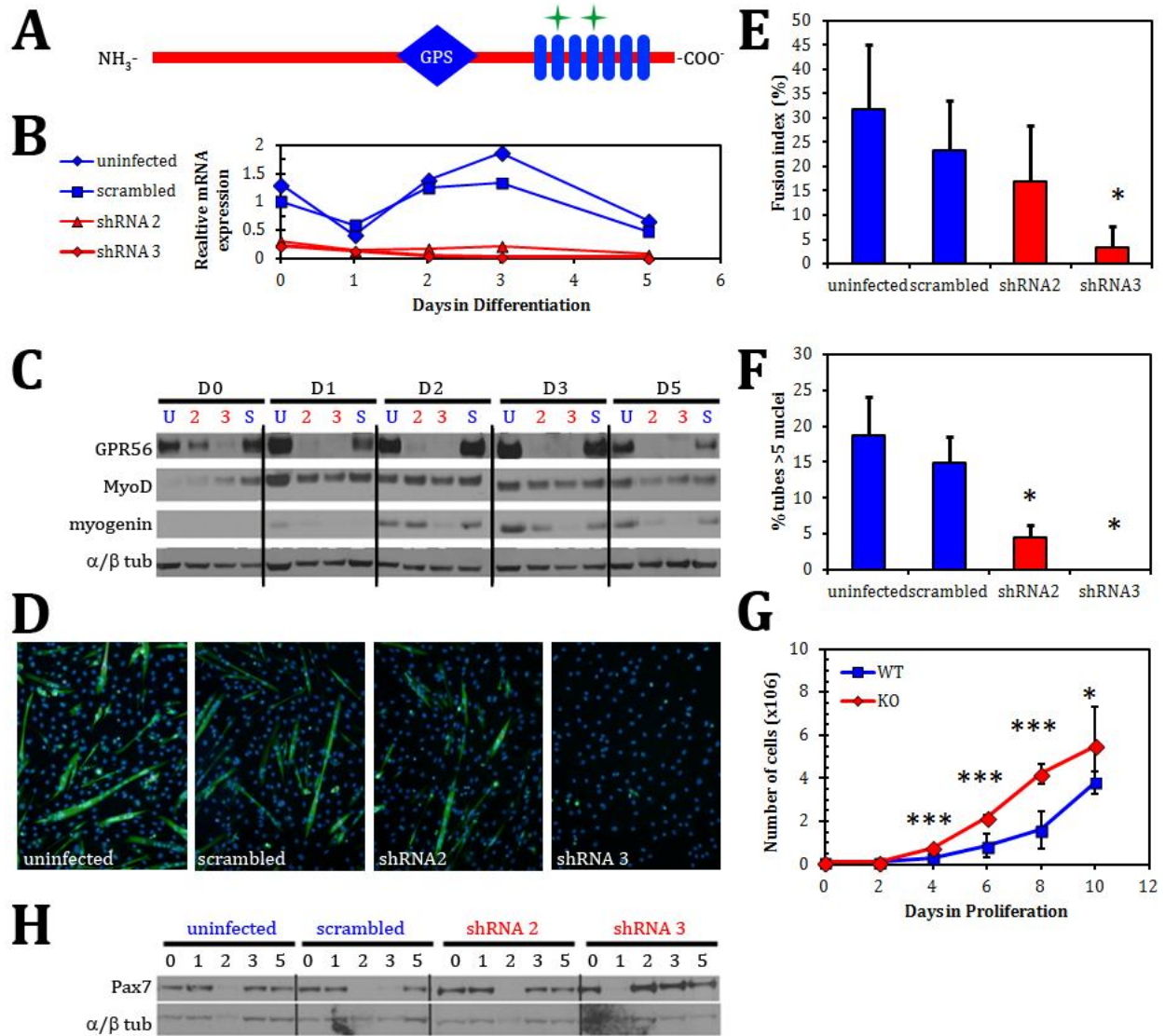
Figure 3.4

Figure 3.4. *Silencing of GPR56 in C2C12 cells results in less efficient fusion and differentiation*

A. Schematic diagram showing the location of GPR56 shRNA constructs (green stars) against GPR56 transmembrane domains (rectangles) 2 and 4. GPS = G-proteolytic site. **B.** GPR56 mRNA expression by RT-qPCR in silenced C2C12s. Both shRNA 2 and 3 yielded a significant decrease in the expression of GPR56. **C.** Protein expression by Western blot of GPR56-silenced cultures at D0 through D5. U=uninfected; 2, 3 = GPR56 shRNA;

Figure 3.4 (Continued). S = scrambled. There is a consistent decrease in GPR56 and myogenin protein expression with shRNA 2 and 3. **D**. Myosin Heavy Chain staining in GPR56-silenced cultures shows decreased myotube formation in GPR56 shRNA2 and 3 silenced cells. **E**. Fusion is decreased in GPR56-silenced cells. * p < 0.01. **F.** Myotube size is decreased in GPR56-silenced cells. *p < 0.01. **G.** GPR56 KO myoblasts proliferate more than WT myoblasts (* p<0.05, *** p<0.001, n=4 trials). **H**. Pax7 expression is increased in GPR56-silenced C2C12 cells (shRNA 2 and 3) compared to uninfected and scrambled C2C12s in differentiation for 0 to 5 days.

protein level (Figure 3.4C). As had been seen with the knockout myoblasts, both fusion and myotube size was decreased in the silenced C2C12 cells (Figure 3.4D, E, F). Unlike in the knockout myoblasts, MyoD expression was unchanged, whereas myogenin expression was decreased, particularly with the shRNA 3 construct (Figure 3.4C). This difference from the data generated using the primary myoblasts suggests that GPR56 might not directly affect MyoD expression, but that the downstream effects of GPR56 signaling lead to a decrease in MyoD expression in the knockout myoblasts. Unlike in the GPR56-knockout myoblasts, there was no upregulation in FHL1 expression. The decrease in myogenin expression suggests that GPR56 is upstream of myogenin, and that loss of GPR56 results in the inefficient activation of factors promoting the commitment to differentiation.

If the loss of GPR56 contributed to a decreased ability to commit to differentiation, then knockout myoblast cultures might display signs of increased or persistent proliferation. Indeed, Pax7 expression was maintained in silenced, differentiating cell cultures to a greater degree than in the control cells (Figure 3.4H). We also noticed that

88

knockout myoblasts tended to expand in culture to a greater degree than wildtype myoblasts. To quantify this phenotype, we plated equal numbers of littermate wildtype and knockout myoblasts and counted the number of cells produced over the course of 10 days. We found significantly increased proliferation in the knockout myoblasts (Figure 3.4G). Taken together with the data from the fusion assays, this suggests that GPR56 promotes the commitment of myoblasts that leads to differentiation and then fusion.

The fusion defects seen in vitro are not replicated in vivo

The proliferation and differentiation of myoblasts in vitro mirrors the process of myofiber formation during muscle development and regeneration. Defects in development that do not result in strong phenotypes are often revealed when regeneration is induced. The decreased fusion and myotube size seen in vitro could be translated into reduced myofiber size during regeneration model. To evaluate the regenerative capacity of knockout muscle, we induced regeneration of the tibialis anterior muscle by injection of the snake venom, cardiotoxin, which causes myofibers to degenerate. Myoblast progenitor cells are then activated for proliferation, differentiation, and fusion to reform muscle fibers within three weeks.[90,91] As had been seen in vitro, GPR56 mRNA expression in regenerating wildtype muscle is transiently increased and peaks at day 4 after cardiotoxin injection (Figure 3.5B), which is when early myofibers are being formed. We examined the muscle histology by H&E to determine whether there were any gross defects in the timing or extent of regeneration (Figure 3.5A). We found that morphologically, there was no gross defect when compared to wildtype muscle. To determine whether there was an initial defect in fusion during regeneration as had been seen in vitro, we quantified myofiber size

89

Figure 3.5. *Loss of GPR56 does not affect myofiber size after regeneration*

A. H&E staining of GPR56 WT and KO gastrocnemius muscle at days 4, 6, and 18 after cardiotoxin injury. KO morphology and timing does not look different from WT. **B**. mRNA expression of GPR56 by RT-qPCR shows transient upregulation of GPR56 during regeneration. **C**. Myofiber diameter in cardiotoxin-injured WT and GPR56 KO gastrocnemius muscle shows no difference in diameter between WT and KO. **D.** mRNA expression by RT-qPCR of various genes in WT (blue) and GPR56 KO (red) cardiotoxin-injured muscle. Many genes are delayed in expression in KO muscle. * p<0.05.
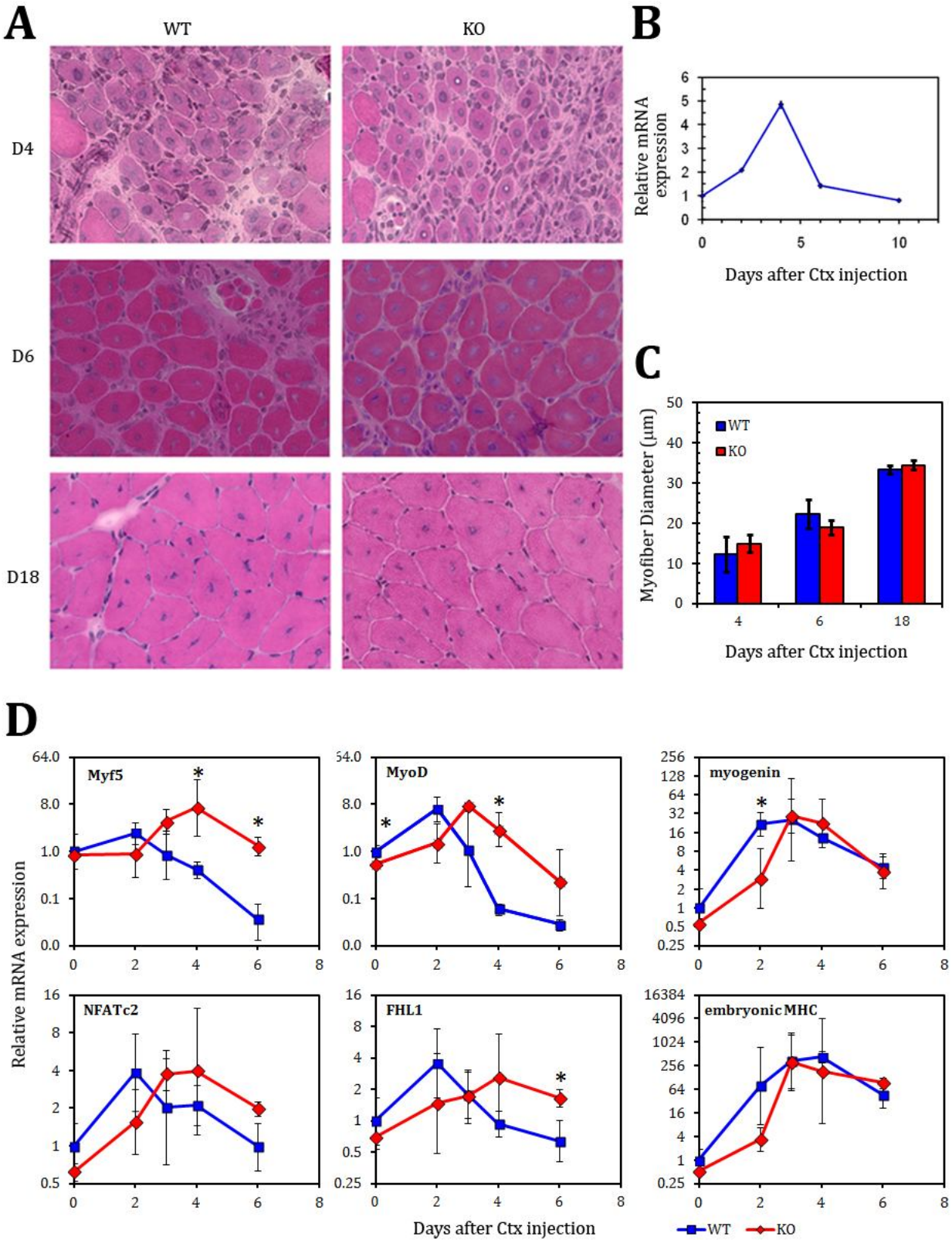
Figure 3.5 (Continued)

91

during regeneration. There was no difference in myofiber diameter during early myofiber formation four days after cardiotoxin injection between knockout and wildtype muscle tissue (Figure 3.5C). At six days, there was a trend towards smaller fibers in knockout mice that was not statistically significant, whereas again by eighteen days, there was no difference in myofiber diameter (Figure 3.5).

We then examined the expression of critical myogenic transcription factors in wildtype and knockout muscles undergoing regeneration. In wildtype mice, myoblast proliferation peaked two days after cardiotoxin injury, as seen by the peak in Myf5 and MyoD mRNA expression (Figure 3.5D). Early differentiation occurred at days 2 and 3, as seen by peaks in the expression of the differentiation transcription factors NFATc2, FHL1, and myogenin. Embryonic myosin heavy chain, which is transiently expressed in regenerating myofibers,[92,93] peaked at days 3 and 4. In contrast, myoblast proliferation in knockout mice, as marked by the peak in MyoD expression, occurred at day 3. Interestingly, Myf5 expression in knockout muscle was not only delayed, but its maximal expression level was much greater than in wildtype mouse muscle. Later phases of differentiation, as marked by FHL1, NFATc2, and myogenin expression, also were delayed. Early myofiber formation as indicated by the expression of embryonic myosin heavy chain, however, seems to match the timing in wildtype mice. Overall, although some of the molecular determinants of myoblast differentiation were slightly delayed, they may have been compensated for in expression by factors that overlap in their functions, such as Myf5. This compensation ultimately led to a largely normal regeneration phenotype in the knockout muscle.

GPR56 signaling induces transcription from SRE and NFAT elements

Several transcriptional pathways are involved in the early differentiation of myoblasts into myocytes and small myotubes in vitro. In particular, there is evidence that GPR56 signals to serum response element (SRE) and nuclear factor of activated T-cells response element (NFAT-RE).[94] The SRE DNA element is functionally equivalent to the CArG box in myogenic cells,[95] to which the serum response factor (SRF) binds. To confirm GPR56 signaling to the SRE and NFAT-RE, we created vectors expressing full-length GPR56 (mGPR56) and constitutively active, truncated C-terminal domain GPR56 (tGPR56)[61] and tested their ability to activate the SRE and NFAT-RE luciferase reporters. The use of constitutively active GPR56 was necessary to ensure that lack of signal was not due to the absence of ligand in the tested cells. Truncated GPR56 strongly activated the SRE reporter while mildly activating the NFAT reporter (Figure 3.6). As expected from previous reports showing constitutive activity of GPR56 when only the C-terminal domain is expressed, the truncated form of GPR56 constitutively activated both SRE and NFAT reporters. Interestingly, in HEK293 cells, increasing amounts of transfected full-length GPR56 were able to reach levels of SRE luciferase activation equal to GPR56-CTD, whereas this was not the case for NFAT-RE luciferase activation.

Targets of SRE transcription are downregulated in GPR56 knockout muscle

MyoD is one transcriptional target of SRE signaling during myoblast commitment and differentiation,.[22–24] During myogenic differentiation, knockout myoblasts exhibited a decrease in MyoD protein (Figure 3.3C). By the time muscle has fully formed in GPR56 knockout mice, MyoD mRNA expression has become decreased, as shown by decreased

Figure 3.6. *GPR56 signals through SRF and NFAT pathways*

A. Schematic showing full-length and truncated GPR56. GPS = G proteolytic site. Rectangles = transmembrane domains. **B.** Luciferase reporter assays in HEK293 cells of full-length (mGPR56, blue line) or truncated (tGPR56, green line) GPR56 with luciferase reporter constructs driven by SRE response elements (SRE) or NFAT response elements (NFAT-RE). GPR56 induces signaling from both SRE and NFAT-RE. * $p<0.05$. *** $p<0.001$. n=3. **C.** mRNA expression in WT and KO gastrocnemius muscle. Expression of FHL1, NFATc2, and NFATc3 are decreased in KO muscle. * $p<0.05$.
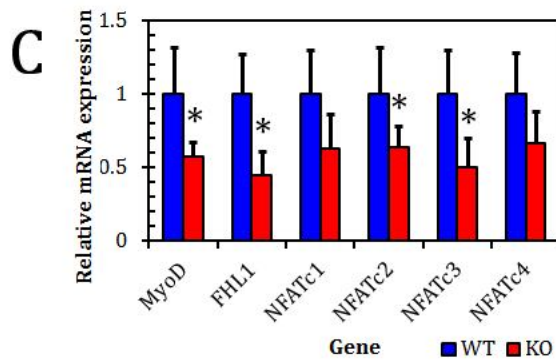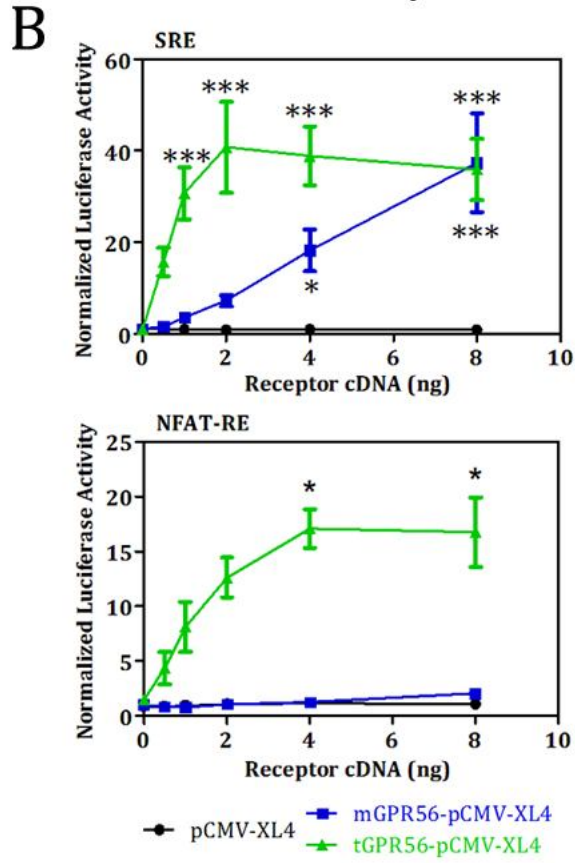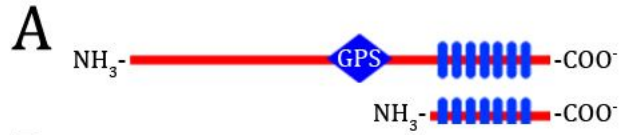
Figure 3.6 (Continued)

mRNA expression in knockout muscle compared to wildtype muscle (Figure 3.6B).

Similarly, the expression of NFAT family members that are involved in commitment and

early myoblast fusion are also affected in GPR56 knockout mice. NFATc3 activity supports

MyoD-directed myogenesis,[96,97] whereas NFATc2 is activated in early myotubes.[34] The

mRNA expression of both NFATc2 and NFATc3 were significantly downregulated in GPR56

knockout muscle (Figure 3.6B). In addition, FHL1, a co-factor of NFATc2 during early

differentiation[35] whose transcription is under the control of SRE,[98] also exhibited

decreased expression in knockout mouse muscle (Figure 3.6B).

Defects in SRE and NFAT signaling do not affect hypertrophy or fiber type differentiation

The SRE and NFAT signaling pathways activated during myoblast commitment and

differentiation are later re-used during myofiber maturation to regulate myofiber

hypertrophy[29,30] and fiber type differentiation,[37,38] respectively. Because the loss of GPR56

in knockout mice affected these pathways during muscle cell differentiation, we examined

the effects of loss of GPR56 on myofiber hypertrophy and fiber type differentiation. As we

had previously established in our initial investigation of GPR56 knockout muscle and the

regeneration study, the myofiber diameter in one-month-old GPR56 knockout mice was

not significantly different than the diameter in wildtype littermates under conditions of

normal development (Figure 3.1B) or regeneration (Figure 3.5).

We then examined whether signaling of GPR56 that influenced the NFAT pathway

during differentiation also had effects on the NFAT-directed process of fiber type

specification. Using antibodies specific to myosin heavy chains type (MHC) I, IIA, and IIB,

we examined MHC expression in wildtype and GPR56 knockout gastrocnemius muscle at

various ages by Western blotting (Figure 3.7B). There was no statistically significant difference in the amount of MHC expression for any of the MHCs examined. Because the differentiation defect seen in GPR56 knockout mice was subtle, we also used a more sensitive immunohistochemical assay to ensure that the lack of differences in MHC expression detected were not due to an inability to detect slight changes in expression by Western analysis. Gastrocnemius muscle was isolated from one-month-old littermates, and stained with antibodies against MHC I, IIA, or IIB with anti-laminin to outline the myofibers. The proportion of positive myofibers for each MHC type was quantified, and the ratio of positive myofibers in GPR56 knockout mice versus wildtype littermates was determined. Using this method, we also found no difference in the proportion of fiber types (Figure 3.7A, C). We concluded that although GPR56 affects the differentiation of myoblasts through the SRE and NFAT pathway, it does not affect the later SRE- and NFAT-directed processes in myofiber growth or fiber type specification. These findings are in agreement with the transient nature of GPR56 expression only during myoblast differentiation.

Discussion

The loss of GPR56 in humans results in the disease bilateral frontoparietal polymicrogyria.[75,76,99] Clinically, the similarity in brain phenotype and mechanism of disease development in BFPP with dystroglycanopathies has resulted in their classification as similar diseases.[77,80] However, despite a dystrophic phenotype in the dystroglycanopathies, the existence of a clear muscle phenotype in BFPP patients has not yet been established. The delays in the motor development of BFPP patients have been attributed to defects in the cerebellum that affect motor control,[79] and patients have shown

Figure 3.7. *Decreased NFAT signaling does not result in changes in fiber type proportion*

A. Sample immunostaining of gastrocnemius tissue for Myosin Heavy Chains I, IIA, or IIB (green) and laminin (red). **B**. Quantification of the % of positive MHCI, IIA, or IIB fiber types in knockout versus wildtype fibers (% pos fibers KO/% pos fibers WT), based on immunofluorescence staining in 3 littermate pairs. **C**. Quantification of the amount of MHC I, IIA, or IIB protein expression by Western blot in WT and KO gastrocnemius muscle in mice of various ages shows no difference in the amount of MHC isoforms between WT and KO.
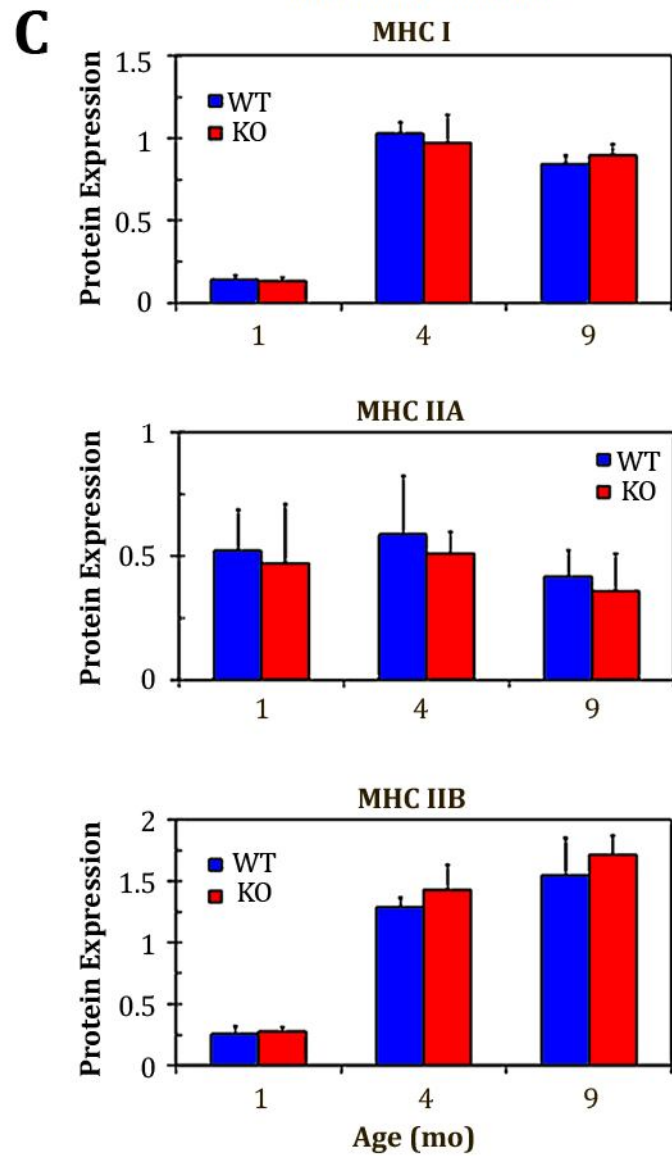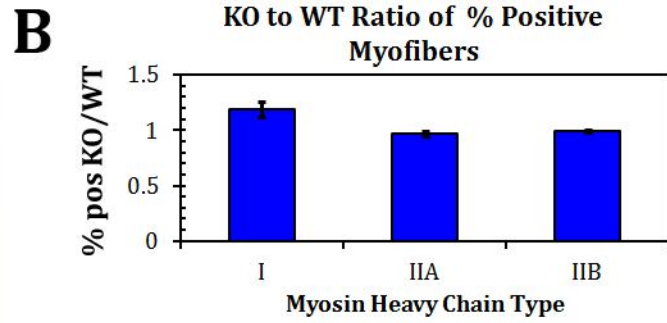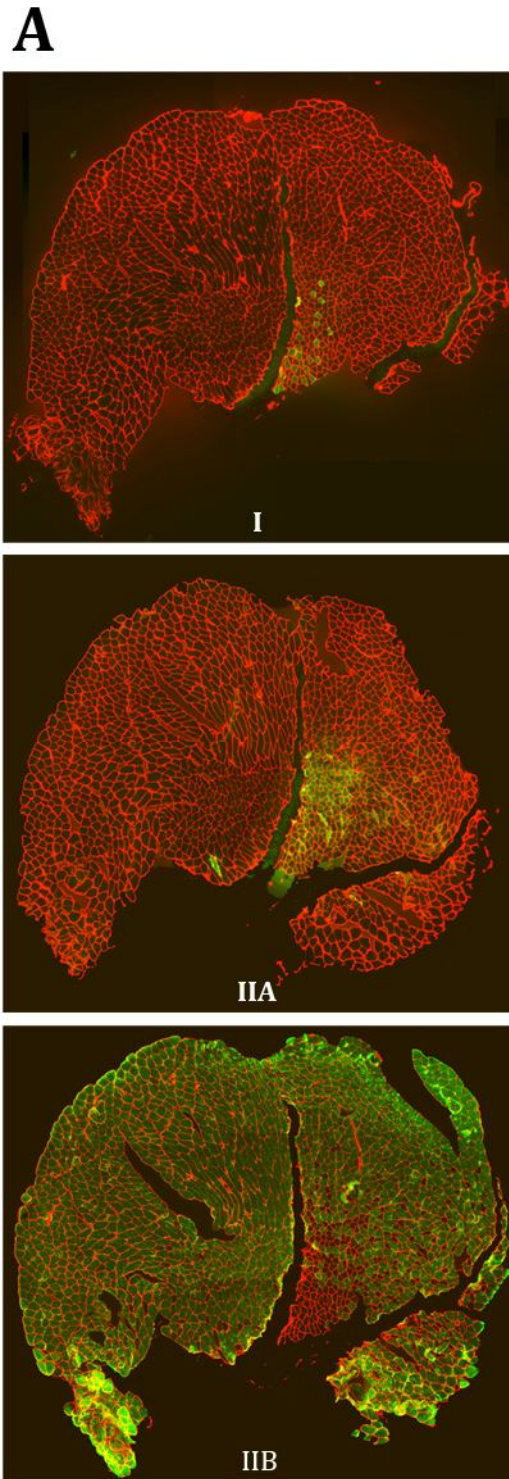
Figure 3.7 (Continued)

99

normal muscle biopsies and serum creatine kinase levels.[80] Independently, however, we had previously found that GPR56 was upregulated in differentiating human fetal muscle cells,[52] suggesting that its loss would result in a muscle phenotype. Besides the similarities in brain phenotype in the diseases caused by α-dystroglycan and GPR56 loss, the two genes also shared possible similarities in function. Both proteins bind the extracellular matrix; α-dystroglycan to laminin[100,101] and GPR56 to collagen III.[102] Thus, we investigated GPR56's role in the muscle. We used the GPR56 knockout mouse in conjunction with other cell-based assays to study GPR56's role.

In our initial examination of GPR56 knockout muscle histology, we found no gross changes in muscle histology or fiber size. We did, however, find a small but statistically significant increase in the serum CK levels, which can be an indication for the presence of muscular dystrophy.[103,104] However, in the case of GPR56 knockout mice, the degree of increase was much smaller than what is seen in *mdx* mice, which are a mouse model for DMD.[105] That the increase was slight, albeit significant, is in agreement with other studies that did not detect raised serum CK levels in BFPP patients.[80] Therefore, the loss of GPR56 in muscle did not lead to a clinically significant defect in muscle development.

We next studied the role of GPR56 during muscle cell differentiation in vitro. In myoblasts, the SRF transcription factor binds an SRE DNA element within the MyoD promoter to promote transcription of MyoD during proliferation and differentiation.[24,106,107] The activation of SRF transcriptional activity, in turn, is dependent on RhoA activity.[23] The upregulation of MyoD expression, in correlation with a switch in SRF phosphorylation,[26] induces proliferating myoblasts to exit the cell cycle.[17] MyoD then switches to a differentiation program to prepare the cells for fusion. This transcriptional

program is aided by many cofactors, including NFATc3. NFATc3 potentiates the ability of MyoD to both convert fibroblasts to myoblasts and to activate the myogenic differentiation program in C2C12 cells.[96] Mice lacking NFATc3 show diminished numbers of myofibers, which has been attributed to a decrease in myofiber number during primary myogenesis[97] and confirms that NFATc3 is indeed involved in promoting the early commitment of myoblasts. NFATc2 is then activated in the nascent myotubes to promote further fusion.[34] The complex interplay between the myogenic transcription factors makes it difficult to clearly define how GPR56 interacts with them. Our data suggests, nevertheless, that GPR56 promotes myoblast commitment and early differentiation through the activation of SRE and NFAT-RE signaling (Figure 3.8). First, GPR56 mRNA and protein expression patterns suggest that GPR56 acts in myocytes and in early differentiating myotubes. Secondly, GPR56 has been previously shown to activate both SRE and NFAT-RE directed signaling, with different human isoforms of GPR56 activating SRE-driven luciferase to varying degrees.[94] Our findings that GPR56 can activate luciferase driven by SRE and NFAT agree with these previous findings. The use of a truncated, constitutively active, GPR56 also ensured that any negative results from our assay were not due to a lack of agonist ligands in the culture. The data demonstrated that GPR56 more strongly activates SRE-driven rather than NFAT-RE driven transcriptional activity.

When viewed in the context of the changes observed following the loss of GPR56, these findings can be used to place GPR56 into a model of how differentiation is regulated. Our luciferase data links GPR56 expression with the activation of promoters containing the SRE DNA elements, while GPR56 localization data links its expression to myocytes and early differentiating myotubes. By combining these data with the previously published data
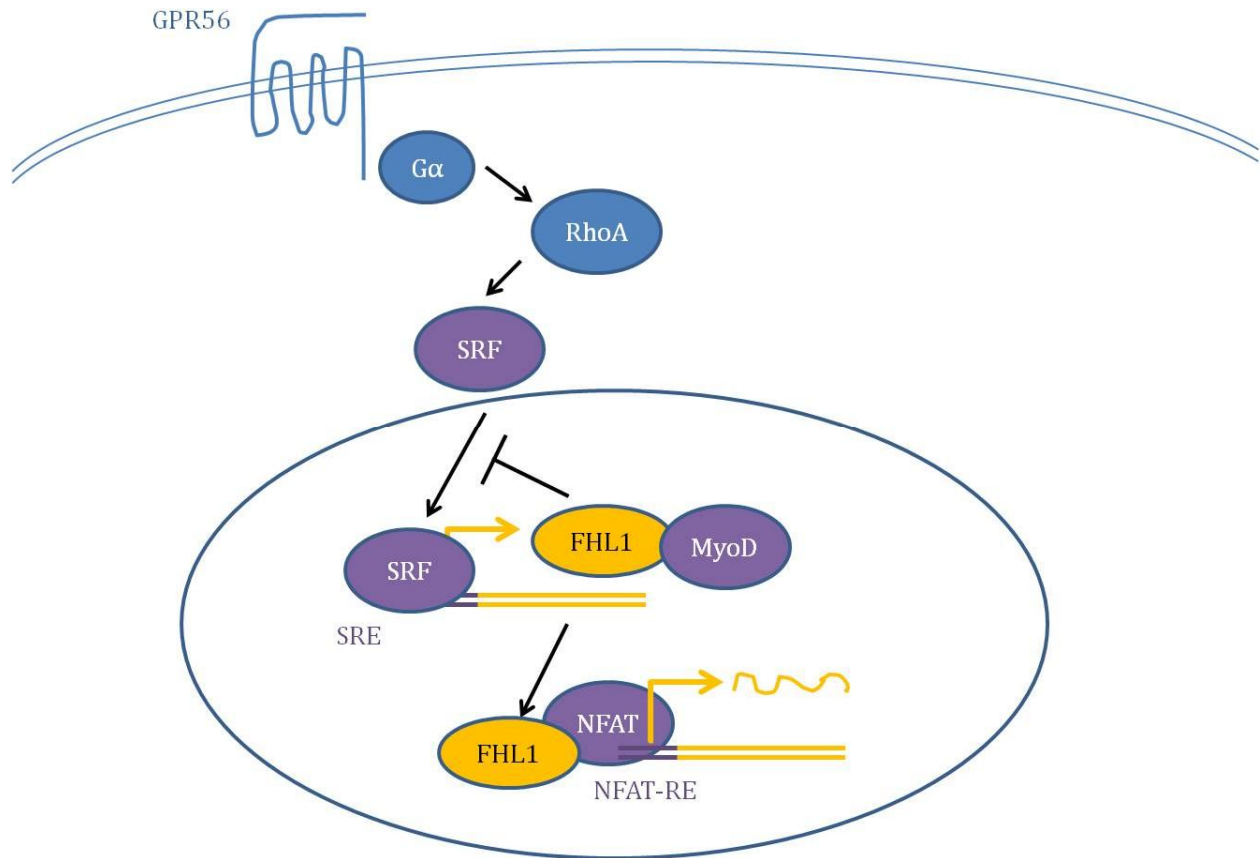
Figure 3.8

Figure 3.8. *Model of GPR56 Signaling Pathway*

GPR56 signals through RhoA to activate SRF signaling during myoblast differentiation

demonstrating that GPR56 activates RhoA,[61,68,102] we can draw a pathway for GPR56 at the

cell surface to activate RhoA signaling and subsequently activate the SRF-mediated

transcription of MyoD in the nuclei of myoblasts committed to differentiation.

The inhibition of SRF expression or activity has been shown to lead to decreased

MyoD[23] and myogenin expression.[108] In support of this model, we saw a decrease in MyoD

expression in knockout muscle, as well as decreases in MyoD and myogenin expression in

differentiating GPR56 knockout and GPR56 silenced myoblasts, respectively. Satellite cells

lacking MyoD, continue to proliferate and inefficiently express myogenin when induced to differentiate.[109] In our studies, GPR56 knockout myoblasts showed increased proliferation rates compared to wildtype myoblasts and increased Myf5 expression was also seen in regenerating muscle following cardiotoxin injury. Additionally, GPR56-silenced C2C12 cells induced to differentiate show increased Pax7 expression, which is normally expressed in undifferentiated satellite cells.[110]

During late myogenic differentiation, the inactivation of RhoA is necessary for differentiation to proceed.[111] Similarly, GPR56 expression sharply decreases following a peak in expression during myoblast commitment, possibly contributing to the decrease in RhoA activation at the later differentiation stage. This decrease matches well with the need for RhoA to be inactivated for the fusion of cells to proceed.[111]

In our luciferase assays, constitutively active GPR56 stimulated NFAT transcription to a lesser degree than it stimulated SRE transcription. There are some plausible reasons for the differential levels of activation. One possibility is that GPR56 can equally activate NFAT-RE and SRE-driven transcription, but truncated GPR56 is locked in a conformation that preferentially signals to SRE. Multiple conformational states that differentially activate downstream signaling pathways has been described for other GPCRs.[112,113] This explanation is less likely as full-length GPR56 also activated NFAT to a lesser degree than SRE; and would thus not be locked in to a particular conformational state. Another possibility is that GPR56 does not directly activate NFAT, but NFAT activation occurs downstream of proteins that are transcribed under SRE activation. One of the genes transcriptionally activated by the SRF is FHL1.[98,114] FHL1 is a co-activator of NFAT transcription in the muscle.[35] It is possible that GPR56 activation of NFAT-RE was not

direct, but instead through the induction of FHL1 transcription following activation of the SRF. Increased FHL1 expression was seen in GPR56 knockout myoblasts, but not in GPR56 silenced C2C12 cells, and this inconsistency may also be explained by this relationship.

Our findings not only tie GPR56 to the transcriptional regulation of myoblast differentiation, but possibly also to cell-surface drivers of myoblast differentiation. Previously published data showed that GPR56 associates with the tetraspanins CD9 and CD81.[72] These cell-surface molecules are involved in the early differentiation and fusion phases of myoblast differentiation.[51] The CD9 expression pattern peaks at day one of differentiation in C2C12 cells,[51] similar to GPR56. In muscle cells, loss of CD9 or CD81 delays C2C12 differentiation but does not affect the expression of myosin heavy chain during later differentiation.[51] This phenotype is similar to the phenotypes seen in our study of decreased fusion during early differentiation of both C2C12s and primary mouse myoblasts lacking GPR56. We also saw that during regeneration, MyoD and myogenin expression were delayed, but embryonic myosin heavy chain expression was not. These similarities in the phenotypes of molecular changes, along with the previous demonstration of interactions between GPR56, CD9, and CD81,[72] suggest that GPR56 in myoblasts may act in a signaling complex with CD9 and CD81 during early myoblast differentiation.

Although we did not directly test for the activity of ligands on GPR56, our studies can shed some light on ligand activation of GPR56. Our luciferase assays suggest that different ligands might activate GPR56 for downstream signaling to different pathways. Increasing amounts of transfected, full-length GPR56 receptor fully saturated SRE signaling, as seen by the ability of it to match the maximal levels of activity achieved by constitutively active GPR56. The same amounts of full-length GPR56 receptor, however,

were unable to activate NFAT-RE signaling. The difference in the ability of full-length

GPR56 to activate SRE and NFAT-RE suggests that in the case of NFAT-RE, the full

activation of GPR56 was not achieved. We had earlier suggested that NFAT transcriptional

activity could be downstream of SRE activity, thus explaining its overall decrease in

luciferase activation. However, this explanation does not fully explain why increasing

amounts of full-length GPR56 would not be able to eventually saturate NFAT signaling. One

explanation, which does not exclude our previous hypothesis, is a single ligand does not

activate GPR56 for downstream signaling to both pathways. In our model system, the

putative ligand for NFAT signaling may have been present in lesser amounts, or may have

had to compete with the ligand for SRE signaling. This duality in ligand activation may have

implications for the function and mechanism of action of GPR56. Although SRE and NFAT-

RE activation overlap during differentiation, the phases of commitment to differentiation

and early differentiation that lead to fusion require distinct sets of proteins. The timing and

control of these different sets of proteins that are activated by GPR56 signaling may be

controlled by distinct activators. Regardless of the mechanism, NFATc2 and NFATc3

expression were significantly reduced in GPR56 knockout muscle, supporting the

conclusion that the NFAT pathway is likely a downstream target of GPR56 signaling.

There is some evidence for GPR56 having multiple ligands. Previous reports have

identified two GPR56 ligands, tissue transglutaminase 2 (TG2)[66] and collagen III.[102] TG2 is a

singular protein that switches between functioning as a transglutaminase or a GTPase.[115]

Its role in muscle has not been well studied, although it has been localized in motor

endplates in the diaphragm.[116] Increases in its expression have also been found in the

idiopathic myopathies.[117] These studies show TG2 in adult muscle rather than developing

muscle or differentiating myoblasts, which is when GPR56 is expressed. Thus, TG2 expression in these cases is less likely to be related to GPR56 function. Nevertheless, TG2 has been shown to transamidate RhoA, allowing it to bind to another GPCR, serotonin.[118] As RhoA has been repeatedly shown to be activated by GPR56,[61,68,102] it is possible that transamidation of RhoA by TG2 is also a mechanism for increasing GPR56 activation of RhoA. Whether TG2 can also modify RhoA-GPR56 interactions or act as a ligand to activate GPR56 signaling in muscle remains to be determined.

On the other hand, collagen III activation of GPR56 and its subsequent signaling have a greater possibility for relevance as a mechanism of activation in the muscle. Collagen III binding to GPR56 leads to activation of RhoA in neural cells,[102] and the activation of RhoA by GPR56 has also been established in other studies of neural progenitor cells[68] and HEK cells.[61] During the in vitro differentiation of avian myoblasts, collagen III expression increases in differentiating myocytes[119] in a pattern which is similar to that of GPR56 expression. Collagen III expression was also found to increase in human fetal muscle cells undergoing differentiation.[52] Although we did not identify the ligand for GPR56 signaling in the muscle, collagen III is a likely candidate. Our data demonstrating different saturation levels of SRE and NFAT-RE signaling also suggest that during the phases of differentiation, distinct ligands might be able to activate GPR56 signaling, resulting in the activation of different downstream cytoplasmic and nuclear proteins.

Clearly, the in vitro loss of GPR56 negatively affected the ability of myoblasts to efficiently differentiate and fuse. However, the effects of GPR56 loss did not strongly affect the development of mouse muscle. The regeneration of GPR56 knockout muscle was not significantly altered when using the morphology of the tissue as a benchmark, although the

gene expression of Myf5, MyoD, and NFATc2 were delayed. The overall mild phenotype in vivo suggests that GPR56 could be one of many factors that promote commitment and differentiation and that the redundancy in function with other genes can compensate for its loss. Myf5 is known to be able to compensate for loss of MyoD,[106,107,120] and the delayed but emphatic increase during regeneration may act as a compensatory mechanism for the less efficient expression of MyoD expression. This hypothesis is supported by our findings that despite a significantly decreased ability of the GPR56 knockout myoblasts to fuse at early time points, the cultures were able to catch up in myotube size by later time points (D6). In addition, the inability to fuse was more obvious in the GPR56-silenced C2C12 cells, as opposed to the GPR56 knockout myoblasts. Because the knockout myoblasts develop in a GPR56-null environment and were isolated from postnatal muscle, it is possible that they developed mechanisms to compensate for the loss of GPR56. For example, increased Myf5 expression could contribute to the increased proliferative capacity of knockout myoblasts compared to wildtype ones, as Myf5 expression is associated with myoblast proliferation in vitro and in vivo.[15,121] These compensatory mechanisms, such as the upregulation of proteins that served a similar function to GPR56, would not have had time to develop in GPR56-silenced of C2C12 cells, and this hypothesis could be one reason for why the phenotype of silenced cells was more severe than in the knockout cells. Overall, GPR56 promotes commitment to differentiation and early fusion, but it is one of many factors that have this function and its loss does not lead to major muscle developmental defects.

The SRF and NFAT family member transcription factors promote myofiber hypertrophy during the late phases of myofiber development. Despite seeing decreased myotube size in GPR56 knockout myoblast cultures, we did not see an effect on myofiber

size in either uninjured or regenerating GPR56 knockout muscle. A noted decrease in MyoD expression could be indicative of decreased SRF signaling.[22] We also found decreased NFATc2 and NFATc3 levels in the GPR56 knockout mouse muscle, which are involved in fiber type specification. In skeletal muscle, there are four major fiber types that can be classified by their metabolic status and myosin heavy chain contractile abilities.[39] Type I fibers have slow myosin heavy chains and use oxidative metabolism. Types IIA, IIX, and IIB have fast myosin heavy chains; IIA uses oxidative metabolism while IIX and IIB use glycolytic metabolism. Various intrinsic and extrinsic factors lead to the specification of, maintenance of, and switching to a particular fiber type.[40] In vivo RNA silencing of different NFATs shows that fiber type specification is influenced and dictated by different combinations of four isoforms of NFAT (c1 through c4).[38] All four NFAT isoforms studied play roles in maintaining the Type I fiber type, whereas only NFATc2 through NFATc4 are required for Type IIA and Type IIX fibers, and only NFATc4 for Type IIB fibers. In our study, despite decreases in NFATc2 and NFATc3 expression in GPR56 knockout mice, we did not see effects in GPR56 knockout mouse fiber type specification. These findings are not entirely surprising, as knockouts of various isoforms of NFAT seem to have slight to no effect on fiber type specification.[34,97] Thus, GPR56 signaling through SRE and NFAT is likely to be important only during the early stages of fusion.

Overall, despite a clear role for GPR56 in myoblast commitment and differentiation, there are several reasons for why its loss may not severely impact muscle function in BFPP patients. GPR56 expression is very tightly regulated and restricted to early differentiation in both myoblasts in culture and regenerating muscle in vivo. It has been suggested that cell-surface molecules that have roles in myoblast differentiation have less severe

phenotypes when knocked out in mice, compared to the loss of cytoplasmic factors that may integrate signaling from several cell surface molecules, due to redundancy in their functions.[47] In addition, although the functions of α-dystroglycan and GPR56 seem similar, the relative importance of their ligands may differ in the brain versus the muscle. A clear role for the importance of α-dystroglycan binding to laminin has been established in both tissues.[122–124] Loss of GPR56, as well as loss of its ligand collagen III, has been shown to result in the neuropathies BFPP and Ehlers-Danlos Syndrome, respectively.[76,125] The similarity in cortical malformations and pial membrane breaks seen in these diseases[77–79,125] show that both laminin and collagen III are crucial extracellular matrix components necessary for neural adhesion and migration during development. While laminin is a major component of the muscle basal lamina,[126] collagen III is expressed only transiently.[119] Additionally, α-dystroglycan is a crucial membrane component of the dystrophin-associated protein complex that is expressed in both developing and mature muscle, whereas GPR56 is expressed transiently. It is likely that while in the brain, α-dystroglycan and GPR56 serve similar functions, they represent completely different pathways that are used separately in the muscle. Thus, while we see a role for GPR56 during muscle development, its loss does not result in the same muscular dystrophy phenotype as results from the loss of α-dystroglycan glycosylation.

References

1.   Moore, C. J. & Hewitt, J. E. Dystroglycan glycosylation and muscular dystrophy. *Glycoconj J* **26**, 349–57 (2009).

2.   Nance, J. R., Dowling, J. J., Gibbs, E. M. & Bönnemann, C. G. Congenital myopathies: an update. *Curr Neurol Neurosci Rep* **12**, 165–74 (2012).

3.   Kelly, A. M. & Zacks, S. I. The histogenesis of rat intercostal muscle. *J Cell Biol* **42**, 135–53 (1969).

4.   Rubinstein, N. A. & Kelly, A. M. Development of Muscle Fiber Specialization in the Rat Hindlimb. *Journal of Cell Biology* **90**, 50–52 (1981).

5.   Fredette, B. & Landmesser, L. Relationship of primary and secondary myogenesis to fiber type development in embryonic chick muscle. *Dev Biol* **18**, 1–18 (1991).

6.   Buckingham, M. *et al.* The formation of skeletal muscle: from somite to limb. *J Anat* **202**, 59–68 (2003).

7.   Abmayr, S. M. & Pavlath, G. K. Myoblast fusion: lessons from flies and mice. *Development* **139**, 641–56 (2012).

8.   Yaffe, D. Developmental Changes Preceding Cell Fusion During Muscle Differentiation In Vitro. *Experimental Cell Research* **66**, 33–48 (1971).

9.   Davis, R. L., Weintraub, H. & Lassar, A. B. Expression of a single transfected cDNA converts fibroblasts to myoblasts. *Cell* **51**, 987–1000 (1987).

10.   Tapscott, S. *et al.* MyoD1: a nuclear phosphoprotein requiring a Myc homology region to convert fibroblasts to myoblasts. *Science (80-)* **242**, 405–11 (1988).

11.   Braun, T., Buschhausen-Denker, G., Bober, E., Tannich, E. & Arnold, H. A novel human muscle factor related to but distinct from MyoD1 induces myogenic conversion in 10T1/2 fibroblasts. *EMBO J* **8**, 701–9 (1989).

12.   Edmondson, D. G. & Olson, E. N. A gene with homology to the myc similarity region of MyoD1 is expressed during myogenesis and is sufficient to activate the muscle differentiation program. *Genes & Development* **3**, 628–640 (1989).

13.   Lassar, A., Skapek, S. & Novitch, B. Regulatory mechanisms that coordinate skeletal muscle differentiation and cell cycle withdrawal. *Curr Opin Cell Biol* **6**, 788–94 (1994).

14.   Ott, M. O., Bober, E., Lyons, G., Arnold, H. & Buckingham, M. Early expression of the myogenic regulatory gene, myf-5, in precursor cells of skeletal muscle in the mouse embryo. *Development* **111**, 1097–107 (1991).

15.   Ustanina, S., Carvajal, J., Rigby, P. & Braun, T. The myogenic factor Myf5 supports efficient skeletal muscle regeneration by enabling transient myoblast amplification. *Stem Cells* **25**, 2006–16 (2007).

16.   Cooper, R. N. *et al.* In vivo satellite cell activation via Myf5 and MyoD in regenerating mouse skeletal muscle. *J Cell Sci* **112 (Pt 1**, 2895–901 (1999).

17. Halevy, O. *et al.* Correlation of terminal cell cycle arrest of skeletal muscle with induction of p21 by MyoD. *Science (80-)* **267**, 1018–1021 (1995).

18. Wright, W., Sassoon, D. & Lin, V. Myogenin, a factor regulating myogenesis, has a domain homologous to MyoD. *Cell* **56**, 607–17 (1989).

19. Rhodes, S. J. & Konieczny, S. F. Identification of MRF4: a new member of the muscle regulatory factor gene family. *Genes & Development* **3**, 2050–2061 (1989).

20. Hinterberger, T. J., Sassoon, D. A., Rhodes, S. J. & Konieczny, S. F. Expression of the muscle regulatory factor MRF4 during somite and skeletal myofiber development. *Developmental Biology* **147**, 144–156 (1991).

21. Montarras, D. *et al.* Developmental patterns in the expression of Myf5, MyoD, myogenin, and MRF4 during myogenesis. *New Biol* **3**, 592–600 (1991).

22. Gauthier-Rouviere, C. *et al.* Expression and activity of serum response factor is required for expression of the muscle-determining factor MyoD in both dividing and differentiating mouse C2C12 myoblasts. *Mol Biol Cell* **7**, 719–29 (1996).

23. Carnac, G. *et al.* RhoA GTPase and serum response factor control selectively the expression of MyoD without affecting Myf5 in mouse myoblasts. *Mol Biol Cell* **9**, 1891–902 (1998).

24. L'honore, A. *et al.* MyoD distal regulatory region contains an SRF binding CArG element required for MyoD expression in skeletal myoblasts and during muscle regeneration. *Mol Biol Cell* **14**, 2151–62 (2003).

25. Soulez, M. & Rouviere, C. Growth and differentiation of C2 myogenic cells are dependent on serum response factor. *Mol Cell Biol* **16**, 6065–74 (1996).

26. Iyer, D. *et al.* Serum response factor MADS box serine-162 phosphorylation switches proliferation and myogenic gene programs. *Proc Natl Acad Sci U S A* **103**, 4516–21 (2006).

27. Wei, L. *et al.* RhoA signaling via serum response factor plays an obligatory role in myogenic differentiation. *J Biol Chem* **273**, 30287–94 (1998).

28. Charrasse, S. *et al.* RhoA GTPase regulates M-cadherin activity and myoblast fusion. *Mol Biol Cell* **17**, 749–59 (2006).

29. Charvet, C. *et al.* New role for serum response factor in postnatal skeletal muscle growth and regeneration via the interleukin 4 and insulin-like growth factor 1 pathways. *Mol Cell Biol* **26**, 6664–74 (2006).

30.   Guerci, A. *et al.* Srf-dependent paracrine signals produced by myofibers control satellite cell-mediated skeletal muscle hypertrophy. *Cell Metab* **15**, 25–37 (2012).

31.   Schulz, R. a & Yutzey, K. E. Calcineurin signaling and NFAT activation in cardiovascular and skeletal muscle development. *Developmental Biology* **266**, 1–16 (2004).

32.   Abbott, K., Friday, B., Thaloor, D., Murphy, T. & Pavlath, G. Activation and cellular localization of the cyclosporine A-sensitive transcription factor NF-AT in skeletal muscle cells. *Mol Biol Cell* **9**, 2905–16 (1998).

33.   Armand, A.-S. *et al.* Cooperative synergy between NFAT and MyoD regulates myogenin expression and myogenesis. *J Biol Chem* **283**, 29004–10 (2008).

34.   Horsley, V. *et al.* Regulation of the growth of multinucleated muscle cells by an NFATC2-dependent pathway. *J Cell Biol* **153**, 329–38 (2001).

35.   Cowling, B. S. *et al.* Identification of FHL1 as a regulator of skeletal muscle mass: implications for human myopathy. *J Cell Biol* **183**, 1033–48 (2008).

36.   Friday, B. B. & Pavlath, G. K. A calcineurin- and NFAT-dependent pathway regulates Myf5 gene expression in skeletal muscle reserve cells. *J Cell Sci* **114**, 303–10 (2001).

37.   McCullagh, K. J. *et al.* NFAT is a nerve activity sensor in skeletal muscle and controls activity-dependent myosin switching. *Proc Natl Acad Sci U S A* **101**, 10590–5 (2004).

38.   Calabria, E. *et al.* NFAT isoforms control activity-dependent muscle fiber type specification. *Proc Natl Acad Sci U S A* **106**, 13335–40 (2009).

39.   Schiaffino, S. & Reggiani, C. Myosin isoforms in mammalian skeletal muscle. *Journal of Applied Physiology* **77**, 493–501 (1994).

40.   Wigmore, P. M. & Dunglison, G. F. The generation of fiber diversity during myogenesis. *Int J Dev Biol* **42**, 117–25 (1998).

41.   Schiaffino, S. & Serrano, A. Calcineurin signaling and neural control of skeletal muscle fiber type and size. *Trends in Pharmacological Sciences* **23**, 569–575 (2002).

42.   Moore, C. A., Parkin, C. A., Bidet, Y. & Ingham, P. W. A role for the Myoblast city homologues Dock1 and Dock5 and the adaptor proteins Crk and Crk-like in zebrafish myoblast fusion. *Development* **134**, 3145–53 (2007).

43.   Srinivas, B. P., Woo, J., Leong, W. Y. & Roy, S. A conserved molecular pathway mediates myoblast fusion in insects and vertebrates. *Nat Genet* **39**, 781–6 (2007).

44. Sohn, R. L. *et al.* A role for nephrin, a renal protein, in vertebrate skeletal muscle cell fusion. *Proc Natl Acad Sci U S A* **106**, 9274–9 (2009).

45. Vasyutina, E., Martarelli, B., Brakebusch, C., Wende, H. & Birchmeier, C. The small G-proteins Rac1 and Cdc42 are essential for myoblast fusion in the mouse. *Proc Natl Acad Sci U S A* **106**, 8935–40 (2009).

46. Nowak, S. J., Nahirney, P. C., Hadjantonakis, A.-K. & Baylies, M. K. Nap1-mediated actin remodeling is essential for mammalian myoblast fusion. *J Cell Sci* **122**, 3282–93 (2009).

47. Krauss, R. S. Regulation of promyogenic signal transduction by cell-cell contact and adhesion. *Exp Cell Res* **316**, 3042–9 (2010).

48. Prives, J. & Shinitzky, M. Increased membrane fluidity precedes fusion of muscle cells. *Nature* **268**, 761–763 (1977).

49. Van den Eijnde, S. M. *et al.* Transient expression of phosphatidylserine at cell-cell contact areas is required for myotube formation. *J Cell Sci* **114**, 3631–42 (2001).

50. Pavlath, G. K. Spatial and functional restriction of regulatory molecules during mammalian myoblast fusion. *Exp Cell Res* **316**, 3067–72 (2010).

51. Tachibana, I. & Hemler, M. Role of transmembrane 4 superfamily (TM4SF) proteins CD9 and CD81 in muscle cell fusion and myotube maintenance. *J Cell Biol* **146**, 893–904 (1999).

52. Cerletti, M. *et al.* Melanoma cell adhesion molecule is a novel marker for human fetal myogenic cells and affects myoblast fusion. *J Cell Sci* **119**, 3117–27 (2006).

53. Lapan, A. D., Rozkalne, A. & Gussoni, E. Human fetal skeletal muscle contains a myogenic side population that expresses the melanoma cell-adhesion molecule. *Hum Mol Genet* **21**, 3668–80 (2012).

54. Yoon, S., Molloy, M. J., Wu, M. P., Cowan, D. B. & Gussoni, E. C6ORF32 is upregulated during muscle cell differentiation and induces the formation of cellular filopodia. *Dev Biol* **301**, 70–81 (2007).

55. Jacoby, E., Bouhelal, R., Gerspacher, M. & Seuwen, K. The 7 TM G-protein-coupled receptor target family. *ChemMedChem* **1**, 761–82 (2006).

56. Lagerström, M. C. & Schiöth, H. B. Structural diversity of G protein-coupled receptors and significance for drug discovery. *Nat Rev Drug Discov* **7**, 339–57 (2008).

57. Lin, H., Stacey, M., Yona, S. & Chang, G. GPS proteolytic cleavage of adhesion-GPCRs. *Adhesion-GPCRs: Structure to Function* 49–58 (2010).

58.   Araç, D. *et al.* A novel evolutionarily conserved domain of cell-adhesion GPCRs mediates autoproteolysis. *EMBO J* **31**, 1364–78 (2012).

59.   Krasnoperov, V. G. *et al.* alpha-Latrotoxin stimulates exocytosis by the interaction with a neuronal G-protein-coupled receptor. *Neuron* **18**, 925–37 (1997).

60.   Nechiporuk, T., Urness, L. & Keating, M. ETL, a novel seven-transmembrane receptor that is developmentally regulated in the heart. ETL is a member of the secretin family and belongs to the epidermal growth factor-seven-transmembrane subfamily. *J Biol Chem* **276**, 4150–7 (2001).

61.   Paavola, K. J., Stephenson, J. R., Ritter, S. L., Alter, S. P. & Hall, R. The N terminus of the adhesion G protein-coupled receptor GPR56 controls receptor signaling activity. *J Biol Chem* **286**, 28914–21 (2011).

62.   Paavola, K. J. & Hall, R. A. Adhesion g protein-coupled receptors: signaling, pharmacology, and mechanisms of activation. *Mol Pharmacol* **82**, 777–83 (2012).

63.   Okajima, D., Kudo, G. & Yokota, H. Brain-specific angiogenesis inhibitor 2 (BAI2) may be activated by proteolytic processing. *J Recept Signal Transduct Res* **30**, 143–53 (2010).

64.   Silva, J.-P., Lelianova, V., Hopkins, C., Volynski, K. E. & Ushkaryov, Y. Functional cross-interaction of the fragments produced by the cleavage of distinct adhesion G-protein-coupled receptors. *J Biol Chem* **284**, 6495–506 (2009).

65.   Prömel, S. *et al.* The GPS motif is a molecular switch for bimodal activities of adhesion class G protein-coupled receptors. *Cell reports* **2**, 321–31 (2012).

66.   Xu, L., Begum, S., Hearn, J. D. & Hynes, R. O. GPR56, an atypical G protein-coupled receptor, binds tissue transglutaminase, TG2, and inhibits melanoma tumor growth and metastasis. *Proc Natl Acad Sci U S A* **103**, 9023–8 (2006).

67.   Huang, Y., Fan, J., Yang, J. & Zhu, G.-Z. Characterization of GPR56 protein and its suppressed expression in human pancreatic cancer cells. *Mol Cell Biochem* **308**, 133–9 (2008).

68.   Iguchi, T. *et al.* Orphan G protein-coupled receptor GPR56 regulates neural progenitor cell migration via a G alpha 12/13 and Rho pathway. *J Biol Chem* **283**, 14469–78 (2008).

69.   Chen, G., Yang, L., Begum, S. & Xu, L. GPR56 is essential for testis development and male fertility in mice. *Developmental Dynamics* **239**, 3358–3367 (2010).

70.   Shashidhar, S. *et al.* GPR56 is a GPCR that is overexpressed in gliomas and functions in tumor cell adhesion. *Oncogene* **24**, 1673–82 (2005).

71. Park, I.-H. & Chen, J. Mammalian target of rapamycin (mTOR) signaling is required for a late-stage fusion process during skeletal myotube maturation. *J Biol Chem* **280**, 32009–17 (2005).

72. Little, K. D., Hemler, M. E. & Stipp, C. S. Dynamic regulation of a GPCR-tetraspanin-G protein complex on intact cells: central role of CD81 in facilitating GPR56-Galpha q/11 association. *Mol Biol Cell* **15**, 2375–87 (2004).

73. Xu, L. *et al.* GPR56 plays varying roles in endogenous cancer progression. *Clinical and Experimental Metastasis* **27**, 241–249 (2010).

74. Ke, N. *et al.* Orphan G protein-coupled receptor GPR56 plays a role in cell transformation and tumorigenesis involving the cell adhesion pathway. *Mol Cancer Ther* **6**, 1840–50 (2007).

75. Piao, X. *et al.* G protein-coupled receptor-dependent development of human frontal cortex. *Science* **303**, 2033–6 (2004).

76. Piao, X. *et al.* Genotype-phenotype analysis of human frontoparietal polymicrogyria syndromes. *Ann Neurol* **58**, 680–7 (2005).

77. Barkovich, Aj., Millen, K. J. & Dobyns, W. B. A developmental and genetic classification for midbrain-hindbrain malformations. *Brain* **132**, 3199–230 (2009).

78. Li, S., Jin, Z., Koirala, S. & Bu, L. GPR56 regulates pial basement membrane integrity and cortical lamination. *J Neurosci* **28**, 5817–5826 (2008).

79. Koirala, S., Jin, Z., Piao, X. & Corfas, G. GPR56-regulated granule cell adhesion is essential for rostral cerebellar development. *J Neurosci* **29**, 7439–49 (2009).

80. Bahi-Buisson, N. *et al.* GPR56-related bilateral frontoparietal polymicrogyria: further evidence for an overlap with the cobblestone complex. *Brain* **133**, 3194–209 (2010).

81. Quattrocchi, C. C. *et al.* Conventional magnetic resonance imaging and diffusion tensor imaging studies in children with novel GPR56 mutations: further delineation of a cobblestone-like phenotype. *Neurogenetics* **ePub ahead**, (2012).

82. Lawlor, M. W. *et al.* Myotubularin-deficient myoblasts display increased apoptosis, delayed proliferation, and poor cell engraftment. *The American Journal of Pathology* **181**, 961–8 (2012).

83. Springer, M. L. & Blau, H. M. High-efficiency retroviral infection of primary myoblasts. *Somat Cell Mol Genet* **23**, 203–9 (1997).

84. Livak, K. J. & Schmittgen, T. D. Analysis of relative gene expression data using real-time quantitative PCR and the 2(-Delta Delta C(T)) Method. *Methods* **25**, 402–8 (2001).

85. Nolan, T., Hands, R. E. & Bustin, S. a Quantification of mRNA using real-time RT-PCR. *Nat Protoc* **1**, 1559–82 (2006).

86. Agbulut, O. & Destombes, J. Age-related appearance of tubular aggregates in the skeletal muscle of almost all male inbred mice. *Histochemistry and cell …* **114**, 477–481 (2000).

87. Pearce, J., RJ, P. & JN, W. Serum enzyme studies in muscle disease: Part II Serum creatine kinase activity in muscular dystrophy and in other myopathic and neuropathic disorders. *Journal of Neurology, Neurosurgery, and Psychiatry* **27**, 96–99 (1964).

88. Volonte, D., Liu, Y. & Galbiati, F. The modulation of caveolin-1 expression controls satellite cell activation during muscle repair. *FASEB journal : official publication of the Federation of American Societies for Experimental Biology* **19**, 237–9 (2005).

89. Sakuma, K. *et al.* Calcineurin is a potent regulator for skeletal muscle regeneration by association with NFATc1 and GATA-2. *Acta Neuropathol* **105**, 271–80 (2003).

90. Le Gros Clark, W. E. An experimental study of the regeneration of mammalian striped muscle. *J Anat* **80**, 24–36 (1946).

91. Bischoff, R. Regeneration of single skeletal muscle fibers in vitro. *Anat Rec* **182**, 215–35 (1975).

92. Gorza, L., Sartore, S., Triban, C. & Schiaffino, S. Embryonic-like myosin heavy chains in regenerating chicken muscle. *Exp Cell Res* **143**, 395–403 (1983).

93. Carraro, U., Dalla Libera, L. & Catani, C. Myosin light and heavy chains in muscle regenerating in absence of the nerve: Transient appearance of the embryonic light chain. *Experimental Neurology* **79**, 106–117 (1983).

94. Kim, J.-E. *et al.* Splicing variants of the orphan G-protein-coupled receptor GPR56 regulate the activity of transcription factors associated with tumorigenesis. *J Cancer Res Clin Oncol* **136**, 47–53 (2010).

95. Taylor, M., Treisman, R., Garrett, N. & Mohun, T. Muscle-specific (CArG) and serum-responsive (SRE) promoter elements are functionally interchangeable in Xenopus embryos and mouse fibroblasts. *Development* **106**, 67–78 (1989).

96. Delling, U. *et al.* A Calcineurin-NFATc3-Dependent Pathway Regulates Skeletal Muscle Differentiation and Slow Myosin Heavy-Chain Expression A Calcineurin-

NFATc3-Dependent Pathway Regulates Skeletal Muscle Differentiation and Slow Myosin Heavy-Chain Expression. *Mol Cell Biol* **20**, 6600–11 (2000).

97.   Kegley, K. M., Gephart, J., Warren, G. L. & Pavlath, G. K. Altered primary myogenesis in NFATC3(-/-) mice leads to decreased muscle size in the adult. *Dev Biol* **232**, 115–26 (2001).

98.   Miano, J. M., Long, X. & Fujiwara, K. Serum response factor: master regulator of the actin cytoskeleton and contractile apparatus. *Am J Physiol Cell Physiol* **292**, C70–81 (2007).

99.   Parrini, E., Ferrari, A. R., Dorn, T., Walsh, C. A. & Guerrini, R. Bilateral frontoparietal polymicrogyria, Lennox-Gastaut syndrome, and GPR56 gene mutations. *Epilepsia* **50**, 1344–53 (2009).

100. Talts, J. F., Andac, Z., Göhring, W., Brancaccio, A. & Timpl, R. Binding of the G domains of laminin alpha1 and alpha2 chains and perlecan to heparin, sulfatides, alpha-dystroglycan and several extracellular matrix proteins. *EMBO J* **18**, 863–70 (1999).

101. Saito, F. *et al.* Aberrant glycosylation of alpha-dystroglycan causes defective binding of laminin in the muscle of chicken muscular dystrophy. *FEBS Lett* **579**, 2359–63 (2005).

102. Luo, R. *et al.* G protein-coupled receptor 56 and collagen III, a receptor-ligand pair, regulates cortical development and lamination. *Proc Natl Acad Sci U S A* **108**, 12925–30 (2011).

103. Nichol, C. Serum creatine phosphokinase measurements in muscular dystrophy studies. *Clinica Chimica Acta* **11**, 404–407 (1965).

104. Pearce, J., Pennington, R. & Walton, J. Serum enzyme studies in muscle disease: Part III Serum creatine kinase activity in relatives of patients with the Duchenne type of muscular dystrophy. *Journal of Neurology, Neurosurgery, and Psychiatry* **27**, 181–5 (1964).

105. Wu, M. P. & Gussoni, E. Carbamylated erythropoietin does not alleviate signs of dystrophy in mdx mice. *Muscle Nerve* **43**, 88–93 (2011).

106. Rudnicki, M. *et al.* MyoD or Myf-5 is required for the formation of skeletal muscle. *Cell* **75**, 1351–9 (1993).

107. Braun, T. & Arnold, H. Myf-5 and myoD genes are activated in distinct mesenchymal stem cells and determine different skeletal muscle cell lineages. *EMBO J* **15**, 310–318 (1996).

108. Vandromme, M., Gauthier-Rouvière, C., Carnac, G., Lamb, N. & Fernandez, a Serum response factor p67SRF is expressed and required during myogenic differentiation of both mouse C2 and rat L6 muscle cell lines. *J Cell Biol* **118**, 1489–500 (1992).

109. Yablonka-Reuveni, Z. *et al.* The transition from proliferation to differentiation is delayed in satellite cells from mice lacking MyoD. *Dev Biol* **210**, 440–55 (1999).

110. Seale, P. *et al.* Pax7 Is Required for the Specification of Myogenic Satellite Cells. *Cell* **102**, 777–786 (2000).

111. Meriane, M., Roux, P., Primig, M., Fort, P. & Gauthier-Rouvière, C. Critical activities of Rac1 and Cdc42Hs in skeletal myogenesis: antagonistic effects of JNK and p38 pathways. *Mol Biol Cell* **11**, 2513–28 (2000).

112. Ghanouni, P. *et al.* Functionally different agonists induce distinct conformations in the G protein coupling domain of the beta 2 adrenergic receptor. *J Biol Chem* **276**, 24433–6 (2001).

113. Deupi, X. & Kobilka, B. Activation of G protein-coupled receptors. *Adv Protein Chem* **74**, 137–66 (2007).

114. Zhang, X. *et al.* Identification of New SRF Binding Sites in Genes Modulated by SRF Over-Expression in Mouse Hearts. *Gene regulation and systems biology* **5**, 41–59 (2011).

115. Mhaouty-Kodja, S. Ghalpha/tissue transglutaminase 2: an emerging G protein in signal transduction. *Biol Cell* **96**, 363–7 (2004).

116. Hand, D., Campoy, F. J., Clark, S., Fisher, a & Haynes, L. W. Activity and distribution of tissue transglutaminase in association with nerve-muscle synapses. *J Neurochem* **61**, 1064–72 (1993).

117. Choi, Y.-C., Kim, T.-S. & Kim, S.-Y. Increase in transglutaminase 2 in idiopathic inflammatory myopathies. *Eur Neurol* **51**, 10–4 (2004).

118. Guilluy, C. *et al.* Transglutaminase-dependent RhoA activation and depletion by serotonin in vascular smooth muscle cells. *J Biol Chem* **282**, 2918–28 (2007).

119. Sasse, J., Von der Mark, H., Kühl, U., Dessau, W. & Von der Mark, K. Origin of collagen types I, III, and V in cultures of avian skeletal muscle. *Dev Biol* **83**, 79–89 (1981).

120. Rudnicki, M., Braun, T., Hinuma, S. & Jaenisch, R. Inactivation of MyoD in mice leads to up-regulation of the myogenic HLH gene Myf-5 and results in apparently normal muscle development. *Cell* **71**, 383–90 (1992).

121. Lindon, C., Montarras, D. & Pinset, C. Cell cycle-regulated expression of the muscle determination factor Myf5 in proliferating myoblasts. *J Cell Biol* **140**, 111–8 (1998).

122. Sanes, J. R. Laminin, fibronectin, and collagen in synaptic and extrasynaptic portions of muscle fiber basement membrane. *The Journal of Cell Biology* **93**, 442–451 (1982).

123. Hunter, D. D., Llinas, R., Ard, M., Merlie, J. P. & Sanes, J. R. Expression of s-laminin and laminin in the developing rat central nervous system. *J Comp Neurol* **323**, 238–51 (1992).

124. Liesi, P. Do neurons in the vertebrate CNS migrate on laminin? *EMBO J* **4**, 1163–70 (1985).

125. Jeong, S.-J., Li, S., Luo, R., Strokes, N. & Piao, X. Loss of Col3a1, the gene for Ehlers-Danlos syndrome type IV, results in neocortical dyslamination. *PLoS One* **7**, e29767 (2012).

126. Sanes, J. R. The basement membrane/basal lamina of skeletal muscle. *J Biol Chem* **278**, 12601–4 (2003).

Chapter 4

Summary of Accomplishments and Significance of Findings

In this work, we sought to better understand how to enhance the process of myoblast fusion in an effort to improve therapies for the muscular dystrophies. In the first part of our work, we studied the effect of carbamylated erythropoietin (C-EPO), a drug that showed promise in promoting satellite cell proliferation and fusion, on the treatment of a mouse model of Duchenne muscular dystrophy (DMD), the mdx mouse. In the second part, we examined the role of the G-protein coupled receptor (GPCR) 56 (GPR56) in muscle cell differentiation and fusion and the development of a muscle phenotype in bilateral frontoparietal polymicrogyria (BFPP).

Advances in Our Understanding of Myoblast Differentiation and Fusion

In our study of C-EPO, we found that the administration of C-EPO to mdx mice has histological benefits in the short term, but not in the long term. As we found, compounds or biologics that show promise in inducing fusion in vitro may not work in in vivo settings. C-EPO had been shown to help in the healing of many different types of diseases involving the development of an inflammatory and fibrotic response, but did not show an effect in the case of DMD. Clearly the use of C-EPO as a therapy is highly dependent on the disease for which it is being used, and the failure of it to be clinically significant in the case of DMD highlights the need to test drugs in individual disease models. The possibilities of further clinical uses of C-EPO are discussed in the next section.

Our study of GPR56 added to our understanding of the process of muscle cell differentiation and fusion by expanding our knowledge of cell-surface regulators that transmit signals through cytoplasmic proteins and nuclear transcription factors. Cell surface receptors are amenable to therapies that deliver drugs or protein ligands through

the bloodstream, thus making them good therapeutic targets. We demonstrated that GPR56 promoted myoblast differentiation and fusion. GPR56 signaling likely promotes the activity of SRF and NFAT factors during differentiation. However, its transient expression limits its action to differentiation and not the later phases of myofiber growth and myofiber type specification.

Implications of Our Studies on Developing Therapies For Clinical Use

Lessons From Testing the Administration of C-EPO in Mdx *Mice*

Our trial of C-EPO as a possible treatment for muscular dystrophy showed that for the dosages tested, C-EPO was not an effective therapeutic drug. A clear understanding of the causes of success and failure of our study can give insight into the usefulness and approach of using C-EPO as a therapy for muscle diseases. We hypothesize that the duration of drug administration plus lack of targeting of the drug specifically to skeletal muscle resulted in the early improvement that was later lost. The short-term improvement of muscle histology in our study indicated that the EPO pathway did have some capacity to promote myoblast fusion in skeletal muscle. In the long-term, systemic administration of C-EPO allowed it to interact with the hematopoietic system, leading to the possible development of anemia; thus, a possible reduction in oxygen delivery to the muscle could have reversed C-EPO's stimulatory effects on myoblast fusion. If we were able to target the stimulation of erythropoietin signaling to the muscle only, it may have allowed for the growth of the muscle in the long-term.

The indications of efficacy in the short term suggest that C-EPO may be used in other ways to aid in muscle repair. For example, outside of the muscular dystrophies, muscle

degeneration and necrosis also occurs in cases of traumatic muscle injury. Administration of C-EPO may aid in this case, where the need for muscle regeneration is acute. Indeed, another group has demonstrated that EPO promotes the recovery of rat muscle after crush-induced injury.[1,2] In these studies, a single intraperitoneal or intramuscular injection of EPO was administered directly after the muscle was crushed. Erythropoietin was detected in the blood for only one day after injection, demonstrating quick clearance. They noted increases in muscle strength with decreases in fibrosis marked by collagen deposition, as well as increased satellite cell proliferation and decreased apoptosis, compared to saline-treated mice. Thus, their work validates the short-term use of EPO or C-EPO as a drug that can increase satellite cell proliferation and decrease fibrosis in regenerating muscle. Clinically, the type of crush injury modeled in these rats parallels muscle injuries in patients that are due to acute trauma and may aid in muscle regeneration and healing in these cases.

Another short-term application of EPO stimulation of myoblast fusion could be in the case of myoblast transplantation. We had initially proposed that if C-EPO demonstrated efficacy for the alleviation of muscular dystrophy, then it could also be tested for use in stimulating the fusion of transplanted myoblasts. Several groups have taken this approach with promising results.[3-5] Two groups tested whether administration of EPO or C-EPO could improve the engraftment of myoblasts into the heart. In the first attempt, Chanséaume et al. induced myocardial infarction in the rat heart, then two weeks later administered a single bolus of EPO one day prior to the injection of skeletal myoblasts.[3] They found that EPO did not improve cell survival and engraftment. A following study by Robey et al. used a slightly different approach and found that EPO and C-EPO

administration did improve cell engraftment.[4] They tested the ability of C2C12 skeletal

myoblasts and human embryonic cell-derived cardiomyocytes to engraft in a rat model of

myocardial infarction. In their case, they found that C-EPO (and EPO) increased the

engraftment and proliferation of both cell types. They ascribed the differences in their

results from the previous study to several differences in their methodology. For one, the

injection of cells was done immediately after the creation of an infarct, rather than two

weeks afterward. A more important difference, though, was that they pre-treated the cells

by incubating them with C-EPO for thirty minutes, as well as administered one dose of C-

EPO to the rats prior to injection and another one day after the injection. They postulated

that the priming of the cells and animals with C-EPO prior to injection was crucial to the

improvement of cell survivability. Thus, their experiment supports the idea that a short-

term dose of C-EPO may improve the engraftment of myogenic cells.

These studies took advantage of EPO's proliferative and anti-apoptotic effects on

myoblasts while minimizing overstimulation of the hematopoietic system by using only

short-term administration of EPO. The negative effects of overstimulation of the

hematopoietic system can be avoided, however, by a strategy that specifically targets the

skeletal muscle. Jia et al. found a way to promote long-term stimulation of EPO signaling in

the skeletal muscle by transducing transplanted myoblasts with a mutant EPO receptor

(tmEpoR) that had enhanced activity.[5] In a model that is directly relevant for treatment of

muscular dystrophy, Jia et al. used an injection of EPO to stimulate the engraftment of

C2C12 cells into the muscle of wildtype and mdx mice.[5] They found that compared to the

administration of EPO to the mice, the forced expression of tmEpoR in the transplanted

myoblasts resulted in a greater engraftment. The combination of both approaches resulted

in the greatest engraftment. This study demonstrated that stimulating EPO pathways in myoblasts does contribute to increased cell survival of myoblasts transplanted into skeletal muscle.

The question also of whether a drug that increases the fusion of endogenous satellite cells would be beneficial to the treatment of DMD remains unanswered; the initial increase in satellite cell division may lead to premature exhaustion of the satellite cells in DMD patients. The use of C-EPO may be more beneficial in muscle diseases where exhaustion of satellite cells is not a problem. For example, many patients with myopathies suffer from hypotonia; growth of the muscle by the additional fusion of myoblasts may improve the condition of patients with these diseases. Indeed, induction of muscle hypertrophy is being tested as a therapy for some myopathies.[rev in 6] Additionally, C-EPO's promotion of proliferation and cell survival may aid in the treatment of myopathies for which satellite cell apoptosis is an issue..[7,8]

In sum, when developing a therapy, consideration of the dosing regimen, the organs affected, and the disease etiology are crucial to its success. Many factors have been identified that can promote the fusion of myoblasts. When considering their use in therapy, future efforts should take note of these considerations. In cases of systemically administered drugs or biologics, the off-target effects on other organs become increasingly important as time of use of the drug increases.

Lessons From Studying the Effects of Loss of GPR56 on Muscle Development

Bilateral frontoparietal polymicrogyria is a congenital disease with striking defects in brain development.[9–11] These defects include mental retardation, motor developmental

delay, seizures, and defects in the brainstem and cerebellum.[10] In the dystroglycanopathies

Walker-Warburg syndrome, Fukuyama congenital muscular dystrophy, and Muscle-Eye-

Brain disease, patients have a brain phenotype defined as "cobblestone-like." Several

studies have noted the striking similarities in phenotype between BFPP and the

cobblestone-like cortexes of patients with these dystroglycanopathies,[9,10,12] even noting

that in the cases of BFPP and Walker-Warburg or Muscle-Eye-Brain disease, differential

diagnosis based on neuroimaging is extremely difficult.[9] These similarities suggest that

these diseases have shared mechanisms of pathology.

We found that despite the shared phenotype in the brain, GPR56 and α-dystroglycan

have markedly different roles in the muscle. Although studies showing GPR56 binding to

collagen III suggest that like α-dystroglycan, GPR56 is an extracellular matrix binding

protein, the differences in their expression and function suggest that they are actually

involved in different pathways. GPR56 is transiently expressed during muscle

differentiation, while α-dystroglycan is integral to maintaining the integrity of the

sarcolemma in both developing and mature muscle. Additionally, the relative importance of

their ligands may differ. In both the brain and muscle, laminin is a major component of the

basal lamina.[13,14] During cerebellar and cortex development, collagen III greatly increases

in expression in the pial membrane[15] and its presence is important for the attachment of

radial glial endfeet.[16] In the muscle, collagen III is expressed mostly during development

and regeneration.[17,18] Hence, we believe that GPR56-collagen III and α-dystroglycan-

laminin have distinct functions in the muscle. Others have also expressed this belief.[16]

Ultimately, because the causes of the dystroglycanopathies and BFPP are in

separate biochemical pathways, a therapy that can aid one may not be able to aid the other.

This dichotomy between phenotype and genetic cause highlight the need to identify and study the genetic causes of different diseases, despite shared clinical phenotypes. Only after understanding the genetics can therapies for specific diseases be intelligently developed.

Future Directions

Developing Therapeutics for Muscular Dystrophies

Many groups are pursuing different strategies in the search for therapies to treat the muscular dystrophies. We found that one drug, C-EPO, was not well-matched for the treatment of DMD at the dosages we tested. However, we suggest that C-EPO may be beneficial in other applications for the therapy of muscular dystrophy, or in different muscle diseases or injury conditions. Many groups are already investigating these approaches.[1–4] In the case of DMD, a fundamental question remains of whether the stimulation of endogenous satellite cells would aid or exacerbate the disease by prematurely exhausting the satellite cells. Future studies using different methods of satellite cells stimulation of proliferation and fusion that do not affect other organ systems would aid in answering this question.

Understanding the Process of Muscle Cell Differentiation and Fusion

One of our goals in studying GPR56 was to find a cell-surface molecule that is sufficient to induce muscle cell fusion as a way to increase the efficacy of myoblast transplantation in DMD. However, most of our studies focused on the role of GPR56 as determined by its loss, rather than its overexpression. We found that GPR56 promotes differentiation and fusion, but we did not determine whether its overexpression would

127

increase fusion. We also found, as others had seen, that truncated GPR56 greatly activates downstream signaling compared to full-length GPR56. Early pilot experiments have suggested that the overexpression of GPR56 in myogenic cells could promote greater fusion of those cells; overexpression of truncated GPR56 may be able to do so to an even greater degree. On the other hand, as we have seen with the C-EPO study, too much expression of a promising agent may be detrimental. This may also be the case with the constitutive overexpression of GPR56 in myoblasts. GPR56 expression is normally very tightly controlled during myoblast differentiation, with it being upregulated during only a small window of time between myoblast commitment and early myoblast fusion; it is then quickly downregulated. Likewise, the activation and later inactivation of one of its downstream messengers, RhoA, are necessary for myoblast fusion to proceed.[19] It is likely that GPR56 would also require eventual downregulation for further growth of the myofibers. In the case of therapy, it may be useful to investigate whether the transient upregulation of GPR56, rather than its permanent overexpression, would improve the engraftment of myoblasts. Alternatively, the identification of a soluble ligand for GPR56 could improve the engraftment of myoblasts as has been seen with EPO.

Additionally, from our in vivo studies on GPR56 knockout animals, it is clear that other proteins can compensate for the function of GPR56. One strong possibility for compensatory proteins would be other GPCRs. As we had noted, there is evidence that the different domains of GPR56 can interact with other GPCRs.[20] In the microarray screen performed previously in our lab, other GPCRs were upregulated during early differentiation and continually expressed through late fusion.[21] By Western blotting, we had seen cross-reactivity of the mouse GPR56 antibody with another protein that was not

128

GPR56, thus, it could be similar to GPR56. This cross-reactive protein was seen in lysates of differentiating myogenic cells from wildtype, GPR56 knockout, and GPR56-silenced C2C12 myoblasts. Additionally, GPR56 was found to act in a complex with CD9 and CD81,[22] which are scaffold proteins that have been implicated in myoblast fusion[23] as well as the fusion of other cell types.[rev in 24] Tetraspanins have been proposed to be molecules that act as organizers of lipid microdomains,[25] so it is possible that knocking out the tetratspanins CD81 or CD9 in conjunction with the loss of GPR56 would remove other proteins that act together with GPR56 and support its function. Tetraspanins act in many different complexes defined by a combination of factors, however, so knockouts of one tetraspanin or another may also knock out other functional complexes not related to GPR56. Future studies can investigate these possibilities in discovering protein partners or compensatory partners for GPR56 function.

References

1.   Rotter, R. *et al.* Erythropoietin improves functional and histological recovery of traumatized skeletal muscle tissue. *J Orthop Res* **26**, 1618–26 (2008).

2.   Rotter, R. *et al.* Erythropoietin enhances the regeneration of traumatized tissue after combined muscle-nerve injury. *The journal of trauma and acute care surgery* **72**, 1567–75 (2012).

3.   Chanséaume, S. *et al.* Can erythropoietin improve skeletal myoblast engraftment in infarcted myocardium? *Interact Cardiovasc Thorac Surg* **6**, 293–7 (2007).

4.   Robey, T. E., Saiget, M. K., Reinecke, H. & Murry, C. E. Systems approaches to preventing transplanted cell death in cardiac repair. *J Mol Cell Cardiol* **45**, 567–81 (2008).

5.   Jia, Y., Warin, R., Yu, X., Epstein, R. & Noguchi, C. T. Erythropoietin signaling promotes transplanted progenitor cell survival. *FASEB* **23**, 3089–99 (2009).

6.   Nance, J. R., Dowling, J. J., Gibbs, E. M. & Bönnemann, C. G. Congenital myopathies: an update. *Curr Neurol Neurosci Rep* **12**, 165–74 (2012).

7.   Lawlor, M. W. *et al.* Myotubularin-deficient myoblasts display increased apoptosis, delayed proliferation, and poor cell engraftment. *The American Journal of Pathology* **181**, 961–8 (2012).

8.   Girgenrath, M., Dominov, J. A., Kostek, C. A. & Miller, J. B. Inhibition of apoptosis improves outcome in a model of congenital muscular dystrophy. *J Clin Invest* **114**, 1635–9 (2004).

9.   Quattrocchi, C. C. *et al.* Conventional magnetic resonance imaging and diffusion tensor imaging studies in children with novel GPR56 mutations: further delineation of a cobblestone-like phenotype. *Neurogenetics* **ePub ahead**, (2012).

10.   Piao, X. *et al.* Genotype-phenotype analysis of human frontoparietal polymicrogyria syndromes. *Ann Neurol* **58**, 680–7 (2005).

11.   Li, S., Jin, Z., Koirala, S. & Bu, L. GPR56 regulates pial basement membrane integrity and cortical lamination. *J Neurosci* **28**, 5817–5826 (2008).

12.   Bahi-Buisson, N. *et al.* GPR56-related bilateral frontoparietal polymicrogyria: further evidence for an overlap with the cobblestone complex. *Brain* **133**, 3194–209 (2010).

13.   Sanes, J. R. Laminin, fibronectin, and collagen in synaptic and extrasynaptic portions of muscle fiber basement membrane. *The Journal of Cell Biology* **93**, 442–451 (1982).

14.   Liesi, P. Do neurons in the vertebrate CNS migrate on laminin? *EMBO J* **4**, 1163–70 (1985).

15.   Sievers, J., Pehlemann, F. W., Gude, S. & Berry, M. Meningeal cells organize the superficial glia limitans of the cerebellum and produce components of both the interstitial matrix and the basement membrane. *Journal of Neurocytology* **23**, 135–149 (1994).

16.   Jeong, S.-J., Li, S., Luo, R., Strokes, N. & Piao, X. Loss of Col3a1, the gene for Ehlers-Danlos syndrome type IV, results in neocortical dyslamination. *PLoS One* **7**, e29767 (2012).

17.   Sasse, J., Von der Mark, H., Kühl, U., Dessau, W. & Von der Mark, K. Origin of collagen types I, III, and V in cultures of avian skeletal muscle. *Dev Biol* **83**, 79–89 (1981).

18.   Luo, R. *et al.* G protein-coupled receptor 56 and collagen III, a receptor-ligand pair, regulates cortical development and lamination. *Proc Natl Acad Sci U S A* **108**, 12925–30 (2011).

19.   Meriane, M., Roux, P., Primig, M., Fort, P. & Gauthier-Rouvière, C. Critical activities of Rac1 and Cdc42Hs in skeletal myogenesis: antagonistic effects of JNK and p38 pathways. *Mol Biol Cell* **11**, 2513–28 (2000).

20.   Silva, J.-P., Lelianova, V., Hopkins, C., Volynski, K. E. & Ushkaryov, Y. Functional cross-interaction of the fragments produced by the cleavage of distinct adhesion G-protein-coupled receptors. *J Biol Chem* **284**, 6495–506 (2009).

21.   Cerletti, M. *et al.* Melanoma cell adhesion molecule is a novel marker for human fetal myogenic cells and affects myoblast fusion. *J Cell Sci* **119**, 3117–27 (2006).

22. Little, K. D., Hemler, M. E. & Stipp, C. S. Dynamic regulation of a GPCR-tetraspanin-G protein complex on intact cells: central role of CD81 in facilitating GPR56-Galpha q/11 association. *Mol Biol Cell* **15**, 2375–87 (2004).

23. Tachibana, I. & Hemler, M. Role of transmembrane 4 superfamily (TM4SF) proteins CD9 and CD81 in muscle cell fusion and myotube maintenance. *J Cell Biol* **146**, 893–904 (1999).

24. Chen, E. H. & Olson, E. N. Unveiling the mechanisms of cell-cell fusion. *Science* **308**, 369–73 (2005).

25. Hemler, M. E. Tetraspanin functions and associated microdomains. *Nat Rev Mol Cell Biol* **6**, 801–11 (2005).

Appendix I

Investigation of the Appearance of Tubular Aggregates in GPR56 knockout mouse tissue

Attribution of Collaborator Contributions

Introduction

Skeletal muscle can suffer from many signs of distress or disease, including atrophy, necrosis, degeneration, and inflammation. One rare sign that has been found in a wide variety of muscle conditions and for which a distinct mechanism for its development has not been determined is the tubular aggregate. Tubular aggregates were first described in detail by Engel et al. in 1970.[1] After examining 1500 biopsies from various patients, he found 24 male patients that presented with double-walled tubules in the cytoplasm of their skeletal muscle fibers. The patients with the most aggregates had hypo- or hyperkalemic periodic paralysis; of the other patients, one had porphyria cutanea tarda, and the rest were heavy drug users. Two other groups performed similar surveys of muscle biopsies from their clinics, and one group found patients with tubular aggregates with hypo- or hyperkalemic periodic paralyses, myotonia, myopathies, and undiagnosed muscle pain/cramps.[2] The other group found a predominance in patients with myalgia and associated diseases.[3]

Tubular aggregates have been found in many other human diseases or conditions. These include the gyrate atrophy of the choroids and retina and hyperornithinemia,[4] Fukuyama type congenital muscular disease,[5] non-diagnosed, apparently inherited neuromuscular diseases[6-8], and undiagnosed muscle weakness, stiffness, and or pain[9-11]. They have been predominately found in male patients, although occasionally in females as well. They are also almost exclusively found in Type II fibers (one case reported findings in Type I fibers).[12] Table A1.1 shows a summary of some of the literature reporting tubular aggregates in humans. The diseases in which tubular aggregates are most commonly found include the periodic paralyses and inherited myopathies (both autosomal dominant and

Table A1.1. *Reports of tubular aggregates in humans*

Disease/ condition	Sex	Age (yr)	Muscle	Tubular Aggregate description and related phenotypes found	Ref
hypo/hyperkalemic periodic paralysis, porphyria cutanea tarda, chronic drug users	M	?		Double walled in Type II fibers, 24 of >1500 biopsies	1
Hypo/hyperkalemic PP, myotonia congenital, inflammatory myopathies, muscle pain/cramps	M	?	?	15 of 1500 biopsies	2
Myalgia, Myalgia+ALS, Myalgia+neuropathy. ALS, congenital myopathy, muscle weakness	M, F	?	biceps or quad	Double walled 19 of 3000 biopsies	3
Gyrate atrophy or the choroids and retina and hyperornithinemia	M, F	?	?	Double walled in Type II fibers	4
Fukuyama type congenital muscular dystrophy	M, F	.75 - ~2	Biceps	Honeycomb	5
Dominant neuromuscular disease with mild progressive proximal weakness	M, F	10- 59	biceps or quad	Double walled in Type I and Type II fibers Positive for Fast SR Ca-pump protein, calsequestrin (weak)	6, 12
Dominant myopathy (late onset, muscle pain, cramps, stiffness)	M	86, ~60's?		Three types of tubules?	7
Three generations with elevated CK, myopathy	M	19, 42, 71	vastus lateralis, vastus lateralis, deltoid	Double walled	8
'myasthenic myopathy,'aka limb-girdle myopathy	M	31		Double walled in Type II fibers	9
Myopathy: pain and stiffness in legs induced by exertion	M	42	vastus lateralis	Double walled Positive for HSP72, tubulin, Negative for desmin, ubiquitin	10
Case study: depression, complaints of leg pain, weakness and numbness on the left side	M	42	Quad	Single walled Also has cylindrical spirals	11
Various patients (mostly PP, one myalgia)	M, F	2.5 - 30	Various	Positive for SERCA-2, GRP78, GRP94, dysferlin, gamma-sarcoglycan	13

Table A1.1 (Continued).

Disease/ condition	Sex	Age (yr)	Muscle	Tubular Aggregate description and related phenotypes found	Ref
Patients with myasthenic features, autosomal dominant (3), autosomal recessive (1), sporadic (2)	M, F	40s - 50s	Deltoid	Type I and Type II, Positive for SERCA1, SERCA2, Calsequestrin, Sarcalumenin, Triadin, RyR1/2, DHPR, emerin, no COX-2 or COX-7	14
Not stated	?	?	Quad	Positive for some, but not all mitochondrial proteins	17
Alcoholics + chronic liver disease	M, F	47, 52	Rectus femoris	Double walled in Type II fibers	24
Acute alcoholic intoxication		34		48 hours after hospitalization: yes 7 days later: no	25

autosomal recessive), so it is believed that their formation does include a genetic component.

Because of the diversity of diseases and conditions in which tubular aggregates are found, and the rarity with which they are found, there is controversy as to their pathology. Based on their morphology, Engel et al. proposed that tubular aggregates were outgrowths of the lateral sacs of the sarcoplasmic reticulum.[1] Many of the diseases and conditions feature disrupted metabolism; therefore the overproliferation of the sarcoplasmic reticulum (SR) as a compensatory mechanism has been proposed as one hypothesis for their development. This hypothesis has been supported by the finding that tubular aggregates sequester increased levels of Ca^{2+}.[12] However, the inner tubules seen in the aggregates are not a normal feature of the SR. Due to the detection of mitochondrial proteins in tubular aggregates, some believe that there is a mitochondrial component. Screening for proteins found in mouse and human tubular aggregates has revealed presence of endoplasmic/sarcoplasmic reticulum proteins (SERCA ATPases,[13-16] ryanodine

receptor,[14] calsequestrin,[6,14] glucose response proteins GRP78 and GPR94,[13] sarcalumenin[14]), mitochondrial proteins (bcl1[16], NADH, succinate dehydrogenase),[17] sarcolemmal proteins (dysferlin and γ-sarcoglycan),[13] and cytoplasmic/nuclear proteins(HSP72, tubulin, emerin).[10] Most, if not all, of the studies that have looked for the presence of sarcoplasmic reticular proteins have found them.

Studies in mice and rats have shed some light on the molecular basis of development of tubular aggregates (Table A1.2). Their development is age-related in mice[18,19,14,15] (although the same does not seem to be true for humans), and they can occur in inbred, wildtype strains, but were not detected in outbred strains.[15] In mice, the development of tubular aggregates is limited to males and type IIB fibers. The predominance of tubular aggregates in males is likely attributable to the balance of testosterone and other sex hormones. Castration of male rats that normally develop tubular aggregates eliminates the development of aggregates.[19,20] Administration of testosterone to castrated males and females results in development of tubular aggregates.[20] Knockouts of three genes, caveolin-2,[21] myostatin,[22] and creatine kinase,[23] have been attributed to development of tubular aggregates.

In our investigation of GPR56 knockout mice, we found that GPR56 knockout mice, and heterozygote male mice to a much lesser extent, had tubular aggregates, while females and wildtypes did not. However, investigations of our colony two years later (which was founded by three mice) showed tubular aggregates in both wildtype and GPR56 knockout mice. As the phenotype of tubular aggregates occurred in both wildtype and GPR56 knockout muscle at this later time point, we were unable to equivocally attribute the presence of tubular aggregates to the loss of GPR56 expression.

Table A1.2. *Reports of tubular aggregates in rats and mice*

Genotype/ disease/ condition	Sex	Age	Muscle	Tubular Aggregates and related phenotypes	Ref
MRL +/+ (autoimmune)	M	1 mo – 2 years	GA	Up to 70%, Mostly Type II, some double walled, at outer perimeter	19
MRL +/+	M	1 mo – 2 years	Soleus	Very rare	19
MRL +/+, castrated at 1 mo	M	6 mo	GA	very rare	19
MRL +/+	F	1 mo – 2 years	GA, Soleus	No	19
MRL +/-, MRL lpr/lpr, BXSB/MpJ, C3H HEJ	M/ F	1 mo – 2 years	GA, soleus	No	19
BALB/c, SJL/J, A/J	M	1 mo – 2 years	GA, soleus		19
C57BL/6	M	5 mo and on	GA, plantaris, TA, Quad, sternomastoid	10% at 5 months, 50% at 10 months SERCA1 ATPase+ Single walled	15
DBA2, Balb/c, 129 SV, 129O1a (inbred strains)	M	?	?	Yes SERCA1 ATPase+ Single walled	15
OF1, NMRI, ICR (outbred strains)	M	?	?	No	15
C57BL6/L, NMRI	M	2 mo – 19 mo	TA (EM), GA (IHC)	Muller Ic (single walled) Type IIB, IIX Express SERCA 1, RyR1, calsequestrin, sarcalumenin	14
SAMP8	M	6 mo (not at 2 mo)	Quad	Yes. By EM did not look to be very frequent Higher plasma testosterone, possibly higher CK	18
129 ReJ dy+/- (hets), but not wt or ko	M	1-3 mo	GA, soleus, quad	5% of fibers Type II Single walled	26
Isolated muscle incubated in anoxic conditions	?	?	EDL, soleus	Double-walled Yes in EDL, not in soleus	27

Table A1.2 (Continued).

Genotype/ disease/ condition	Sex	Age	Muscle	Tubular Aggregates and related phenotypes	Ref
Cav-1-/-, Cav-2 -/-	M	3 mo	GA	Yes. Also see mitochondrial abnormalities, and delayed regeneration	21
Cav-3 -/-	M	3 mo	GA	No	21
Mstn -/-	M			Yes, also increase in Type IIB fibers	22
CK-/- (mitochondrial and cytosolic)	M	?	GA-soleus-psoas	Yes. Concurrent changes in metabolic enzymes.	23, 28
CK-/- *WT were not examined	M	3-5 mo	GA	Express bc1 (mitochondrial), SERCA1 by immunogold in EM, note that TAs were not very distinct	16
Transgenic dominant α-tropomyosin$_{slow}$	M	1 – 12 mo	Superficial GA	Yes. Concurrent with other signs of nemaline myopathy: rod formation	29

Methods

Sample preparation for electron microscopy

GPR56 wildtype, heterozygote, and knockout (B6N.129S5-*Gpr56^{tm1Lex}*/Mmcd) gastrocnemius and soleus muscle were dissected and minced into approximately 1 mm x 1 mm pieces. The pieces were fixed in 2% formaldehyde, 2.5% glutaraldehyde in 0.1 M sodium cacodylate buffer, pH 7.4, overnight at 4°C. Sample preparation after fixation, Epon embedding, copper staining, and ultrathin sectioning of the tissue were performed by Maria Ericsson, Louise Trakimas, and Elizabeth Benecchi at the Harvard Medical School EM Facility according to standard methods. Sections were imaged on a Tecnai G^2 Spirit BioTWIN electron microscope by Dr. Michael Lawlor.

H&E staining

Ten micron sections of muscle tissue were sectioned onto charged glass slides.

Tissue sections were fixed for 3 min in 70% ethanol, 3% formalin, 5% glacial acetic acid,

and then rinsed in water. Slides were then dipped in hematoxylin (Harleco #638) for at

least 5 min, rinsed in tap water, and differentiated in acid alcohol (0.3% HCl, 70% ethanol).

Hematoxylin was then allowed to blue in Scott's Tap Water (0.2% $NaHCO_3$ w/v, 2%

$MgSO_4 \cdot 7H_2O$ w/v) for 1 hr to overnight and rinsed in tap water. Slides were then stained in

Eosin Y alcoholic (Sigma #HT110116) for 2 minutes, dehydrated in an ethanol series (50%,

70%, 80%, 90%, 100%, 100%), cleared in Histoclear-II (Electron Microscopy Sciences

#64111-01), and mounted in Cytoseal. (Richard-Allan #8310-16). Tissue was imaged using

a Nikon E1000 microscope with a SPOT Insight Color 3.2.0 camera using SPOT 4.5.9.9

software (Diagnostic Instruments).

Toluidine blue staining

Ultrathin or 10 μm sections were fixed in 100% methanol for 3 min, and then dried

on a hot plate set to low temperature. Toluidine blue solution (1% toluidine blue in 1%

sodium borate for ultrathin sections, 0.01% toluidine blue in 0.01% sodium borate for 10

μm sections) was dropped onto the slide and stained for 30 sec on the hot plate. The stain

was rinsed off with water, the slides dried, and sections were mounted in Cytoseal.

Myosin heavy chain staining

Ten micron tissue sections were fixed with 4% PFA in phosphate buffered saline

(PBS) for 15 min and permeabilized with 1% Triton X-100. After washing with PBS,

sections were blocked with blocking buffer (10% FBS/0.1% Triton X-100 in PBS) for 1 hour at RT. Sections were then incubated with anti-myosin heavy chain type IIB (1:50, BF-F3 DSHB developed by S. Schiaffino) in blocking buffer overnight at 4°C. After washing 3 times with PBS, slides were incubated with secondary antibody (Dylight 488 or Dylight 594, Jackson Immunoresearch) in blocking buffer for 1 hour at RT. After incubation, slides were washed 3 times with PBS, and mounted with DAPI Vectashield (Vector Labs #H-1200). Slides were imaged on a Nikon E1000 using an Orca-ER camera (#C4742-95-12ER) and Openlab 5.5.0 software (Improvision).

Results

We found by H&E staining that knockout mice have acidic inclusions within the muscle fibers that increase and aggregate with age (Figure A1.1). To determine whether these inclusions were real or artifact, we first confirmed through H&E that older (5 month old) knockout mice, but not heterozygote mice (which were have been used as controls in other studies) had the inclusions (Table A1.3). We found that toluidine blue stained the inclusions more clearly (Figure A1.1), giving credence to the fact that these inclusions were real and not due to freezing or fixation artifacts. Using the older mice, we investigated the inclusions by electron microscopy and found that these inclusions were tubular aggregates (Figure A1.2). In agreement with previous studies, these appearance of aggregates were limited to males and type II fibers (Table A1.3, Figure A1.3). The incidence of tubular aggregates seemed to increase with age, where young knockout (3 mo) mice had no tubular aggregates, 5 month old mice had some, and 7 month old mice had aggregates in nearly all
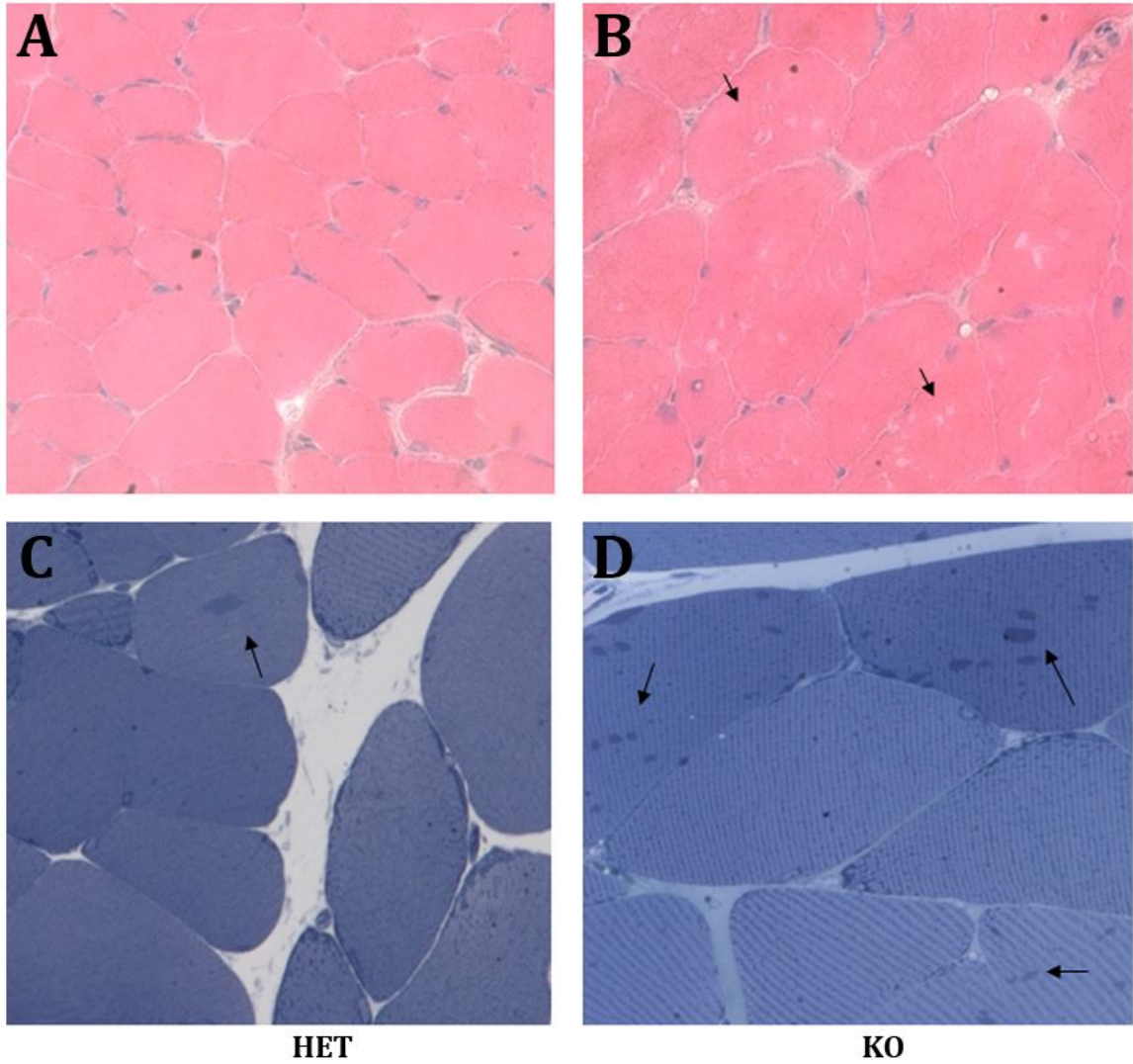
Figure A1.1

Figure A1.1. *Tubular aggregates in male heterozygote and knockout GPR56 mice*

A, B: H&E Stain. **C,D**: Toluidine blue. Toluidine blue stains the tubular aggregates (arrows).

the fibers. The incidence seemed to increase as well in heterozygote mice, although they

were not first detected until 7 months of age by H&E.

Table A1.3: *Mouse muscle samples, early investigations*

Sex	Muscle	Genotype	Age (mo)	ID	Tubular Aggregates Detected		
					H&E	**Toluidine Blue**	**EM**
M	GA	WT	5	218	-	-	No
		Het	8	OH	No	-	-
			7	F	No	Yes, fewer	~12 total, some amorphous
				G	-	Yes, fewer	Low, amorphous
			5	37	No	-	-
			3	YH	No		
		Ko	12	OK	Yes	-	-
			7	E	Yes	Yes	High
				H	-	Yes	Low
				I	-	Yes	High
			5	36	Yes	-	-
				214	-	-	High
			3	YK	No	-	-
	Sol	Het	7	F	-	-	No
				G	-	-	No
		KO	7	E	-	-	No
				H	-	-	No
				I	-	-	No
F	GA	WT	5	237	-	-	No
		Het	5	235	-	-	No
		KO	5	216	-	-	No

M: Male, F: Female, GA: Gastrocnemius, Sol: Soleus, -: Not surveyed

Two years after our initial investigations, we wanted to quantify the number of tubular aggregates found in each genotype (rather than use the original qualitative assessments in number). By this time the colony had grown significantly from the initial 3 founder mice. We examined 10 µM sections from the gastrocnemius muscle of wildtype and knockout mice of 3 months of age by toluidine blue staining. We found that tubular
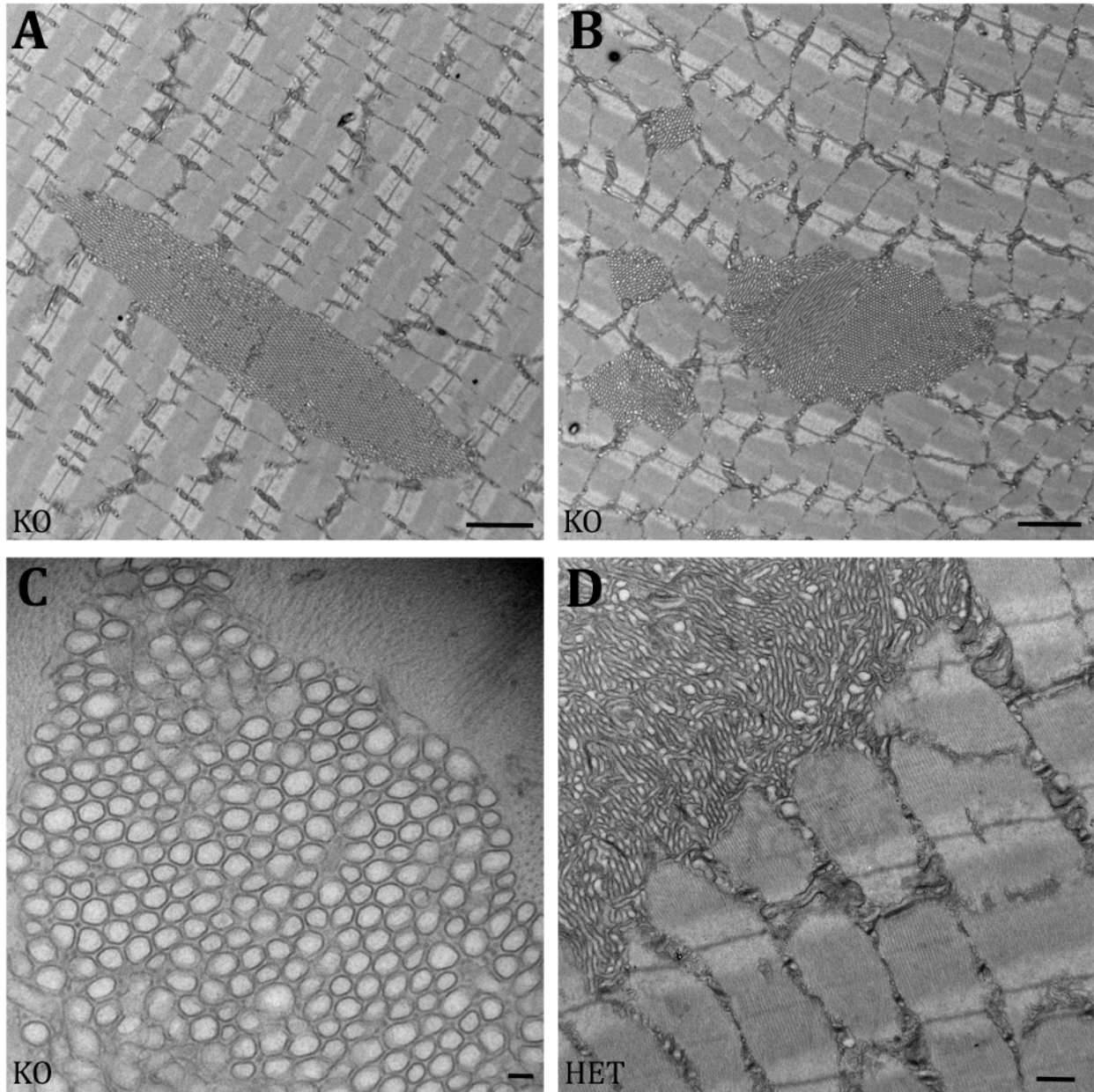
Figure A1.2

Figure A1.2. *Inclusions in the muscle are shown to be tubular aggregates by EM*

A,B. KO gastrocnemius muscle, 7-month-old, with tubular aggregate. Scale bar = 2 μm. **C.**

KO gastrocnemius muscle, 7-month-old, with showing cross-section of tubular aggregate.

Scale bar = 100 nm. **D.** HET gastrocnemius muscle, 5-month-old, with amorphous tubular

aggregate. Scale bar = 500 nm.

Figure A1.3.*Tubular aggregates occur in Type IIB fibers*

A-C. H&E staining of myofibers showing inclusions. **D-F.** Toluidine Blue staining of myofibers showing aggregates in dark blue. **G.** MHC Type I staining (green), sequential to A and D. **H,I**. MHC Type IIB staining (red), sequential to B, E and C,F. Arrows point to MHC Type I positive fibers. Asterisks mark the same myofiber for a point of reference.
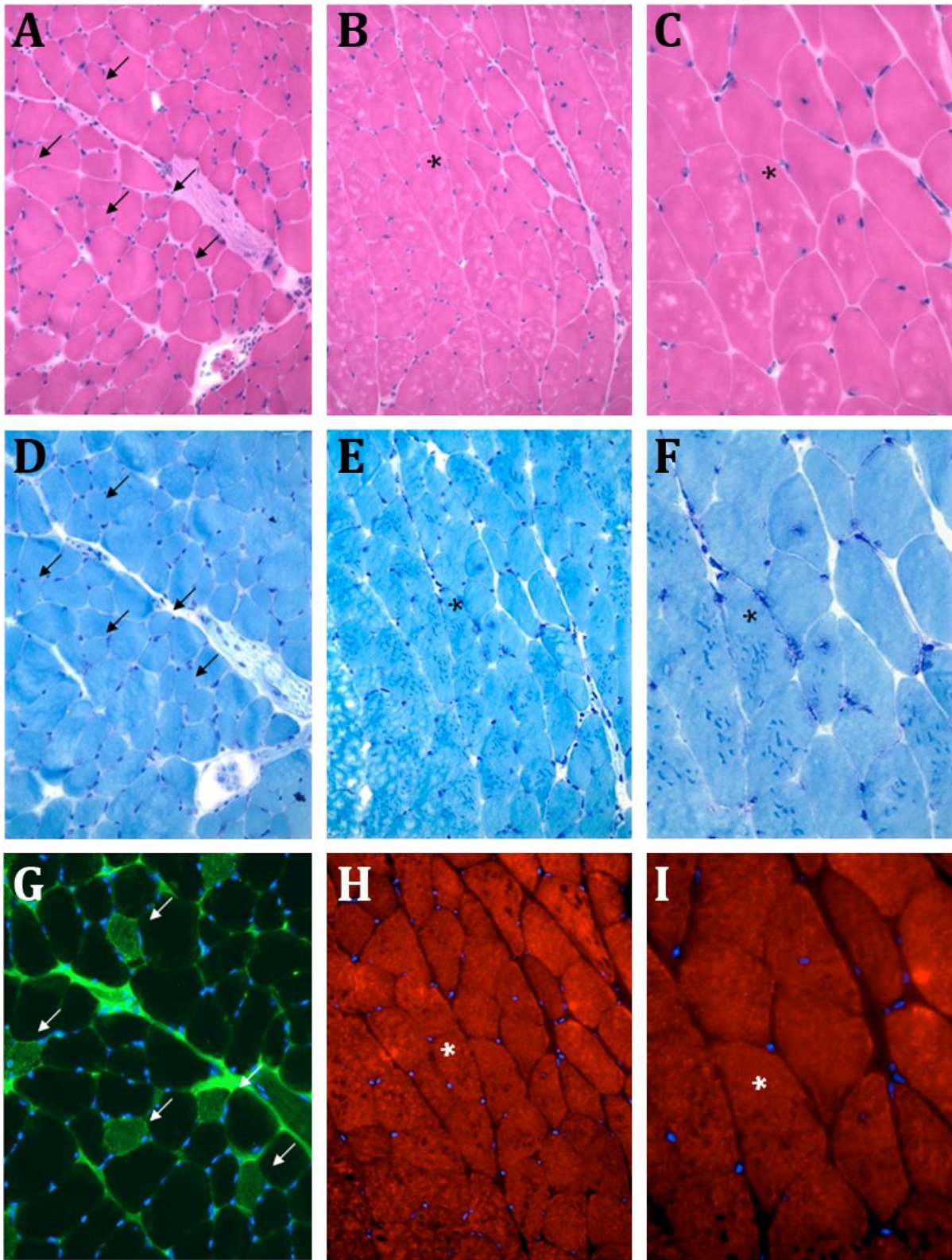
Figure A1.3 (Continued)

Table A1.4: *Mouse muscle samples, after two years, toluidine blue staining*

Sex	Muscle	Genotype	Age (mo)	ID	Tubular Aggregates Detected
M	GA	WT	3	1761	No
				1763	Yes
				1768	No
				1769	Yes
		KO	3	1760	No
				1762	Yes
				1773	NO

aggregates now existed in both wildtype and knockout mice, and no difference in the
numbers of aggregates were noted between the genotypes (Table A1.4).

Discussion

Our initial discovery of tubular aggregates presented an interesting phenotype.
Tubular aggregates are a rare phenotype found in a wide variety of muscle conditions, and
their composition and mechanism of development are still unknown. To date, only four
genes, caveolin-2, myostatin, creatine kinase, and α-tropomyosin$_{slow}$ have been associated
with the development of tubular aggregates. Finding more genetic models for the
development of tubular aggregates would be important for being able to study both the
development and the impact of tubular aggregates on muscle.

Our initial findings of tubular aggregates were consistent with other findings of
tubular aggregates in muscle. They were confined to only male mice, and existed in only
type IIB myofibers. It is not surprising that we detected no tubular aggregates in GPR56
knockout soleus muscle, as it is made up of mostly Type I and Type IIA muscle fibers.
However, as our colony grew in age, the tubular aggregates were detected at earlier ages (3

months) and also in both wildtype and knockout muscle, although not consistently. As tubular aggregates have also been found in the muscle of inbred colonies,[15] we believe that inbreeding within our colony led to the eventual development of tubular aggregates in both wildtype and knockout muscle. This finding obscured the possible contribution that loss of GPR56 may have had in contributing to their development.

Due to the non-specific nature of the tubular aggregates and the dearth of knowledge on the significance of their development, we decided not to continue the investigations of their development in GPR56 knockout mice.

References

1.   Engel WK, Bishop DW, Cunningham GG. Tubular aggregates in type II muscle fibers: ultrastructural and histochemical correlation. *J Ultrastruct Res* **31**, 507-525 (1970).

2.   Rosenberg NL, Neville HE, Ringel SP. Tubular aggregates. Their association with neuromuscular diseases, including the syndrome of myalgias/cramps. *Arch Neurol* **42,** 973-976 (1985).

3.   Niakan E, Harati Y, Danon MJ. Tubular aggregates: their association with myalgia. *J Neurol Neurosurg Psychiatry* **48,** 882-886 (1985).

4.   Sipila I, Simell O, Rapola J, Sainio K, Tuuteri L. Gyrate atrophy of the choroid and retina with hyperornithinemia: Tubular aggregates and type 2 fiber atrophy in muscle. *Neurology* **29**, 996-1005 (1979).

5.   Miike T, Ohtani Y, Tamari H, Ishitsu T, Nonaka I. An electron microscopical study of the T-system in biopsied muscles from Fukuyama type congenital muscular dystrophy. *Muscle & Nerve* **7**, 629-635 (1984).

6.   Pierobon-Bormioli Sandra, Armani M, Ringel SP, Angelini C, Vergani L, Betto R, Salviati G. Familial neuromuscular disease with tubular aggregates. Muscle & Nerve **8**, 291-298 (1985).

7.   Müller H, Vielhaber S, Brunn A, Schröder M. Dominantly inherited myopathy with novel tubular aggregates containing 1-21 tubulofilamentous structures. *Acta Neuropathologica* **102**, 27-35 (2001).

8.   Martin J-J, Ceuterick C, Van Goethem G. On a dominantly inherited myopathy with tubular aggregates. *Neuromuscular Disorders* **7**, 512-520 (1997).

9.   Morgan-Hughes JA, Lecky BR, Landon DN, Murray NM. Alterations in the number and affinity of junctional acetylcholine receptors in a myopathy with tubular aggregates. A newly recognized receptor defect. *Brain* **104**, 279-295 (1981).

10.   Martin Joanne E, Mather K, Swash M. Expression of heat shock protein epitopes in tubular aggregates. *Muscle & Nerve* **14**, 219-225 (1991).

11.   Danon Moris J, Carpenter S, Harati Y. Muscle pain associated with tubular aggregates and structures resembling cylindrical spirals. *Muscle & Nerve* **12**, 265-272 (1989).

12.   Salviati G SP-B, Romeo Betto, Ernesto Damiani, Corrado Angelini Steven P. Ringel, Sergio Salvatori, Alfredo Margreth. Tubular aggregates: Sarcoplasmic reticulum origin, calcium storage ability, and functional implications. *Muscle & Nerve* **8**, 299-306 (1985).

13.   Ikezoe K, Furuya H, Ohyagi Y, Osoegawa M, Nishino I, Nonaka I, et al. Dysferlin expression in tubular aggregates: their possible relationship to endoplasmic reticulum stress. *Acta Neuropathologica* **105,** 603-609 (2003).

14.   Chevessier F, Marty I, Paturneau-Jouas M, HantaÔ D, VerdiËre-SahuquÈ M. Tubular aggregates are from whole sarcoplasmic reticulum origin: alterations in calcium binding protein expression in mouse skeletal muscle during aging. *Neuromuscular Disorders* **14,** 208-216 (2004).

15.   Agbulut O, Destombes J, Thiesson D, Butler-Browne G. Age-related appearance of tubular aggregates in the skeletal muscle of almost all male inbred mice. *Histochemistry and Cell Biology* **114**, 477-481 (2000).

16.   Novotova, M, Zahradnik I, Brochier G, Pavloviova, M, et al. Joint participation of mitochondria and sarcoplasmic reticulum in the formation of tubular aggregates in gastrocnemius muscle of CK-/- mice. *European Journal of Cell Biology* **81**, 101-106 (2002).

17.   Meijer AE. Histochemical features of tubular aggregates in diseased human skeletal muscle fibres. *J Neurol Sci* **86**, 73-82 (1988).

18.   Nishikawa T, Takahashi JA, Matsushita T, Ohnishi K, Higuchi K, Hashimoto N, et al. Tubular aggregates in the skeletal muscle of the senescence-accelerated mouse; SAM. *Mech Ageing Dev* **114**, 89-99 (2000).

19.   Kuncl RW, Pestronk A, Lane J, Alexander E. The MRL +/+ mouse: a new model of tubular aggregates which are gender- and age-related. *Acta Neuropathologica* **78**, 615-620 (1989).

20. Yoshitoshi M, Ishihara T, Yoshimura Y, Tsugane T, Shinohara Y. [The effect of sex hormones on tubular aggregates in normal mouse skeletal muscles]. *Rinsho Shinkeigaku* **31**, 974-980 (1991).

21. Schubert W, Sotgia F, Cohen AW, Capozza F, Bonuccelli G, Bruno C, et al. Caveolin-1(-/-)- and Caveolin-2(-/-)-Deficient Mice Both Display Numerous Skeletal Muscle Abnormalities, with Tubular Aggregate Formation. *Am J Pathol* **170**, 316-333 (2007).

22. Amthor H, Macharia R, Navarrete R, Schuelke M, Brown SC, Otto A, et al. Lack of myostatin results in excessive muscle growth but impaired force generation. *Proc Natl Acad Sci U S A* **104**, 1835-1840 (2007).

23. Steeghs K, Oerlemans F, de Haan A, Heerschap A, Verdoodt L, de Bie M, et al. Cytoarchitectural and metabolic adaptations in muscles with mitochondrial and cytosolic creatine kinase deficiencies. *Molecular and Cellular Biochemistry* **184**, 183-194 (1998).

24. del Villar Negro A, Angulo JM, Rivera Pomar JM, Errasti A. Tubular aggregates in skeletal muscle of chronic alcoholic patients. *Acta Neuropathol* **56,** 250-254 (1982).

25. Chui LA, Neustein H, Munsat TL. Tubular aggregates in subclinical alcoholic myopathy. *Neurology* **25,** 405 (1975).

26. Craig ID, Allen IV. Tubular aggregates in murine dystrophy heterozygotes. *Muscle Nerve* **3,** 134-140 (1980).

27. Schiaffino S, Severin E, Cantini M, Sartore S. Tubular aggregates induced by anoxia in isolated rat skeletal muscle. *Lab Invest* **37**, 223-228 (1977).

28. Steeghs K, Benders A, Oerlemans F, de Haan A, Heerschap A, et al. Altered Ca^{2+} responses in muscles with combined mitochondrial and cytosolic creatine kinase deficiencies. *Cell* **89**, 93-103 (1997).

29. Corbett M, Robinson C, Dunglison G, Yang N, Joya J, et al. A mutation in α-tropomyosin$_{slow}$ affects muscle strength, maturation and hypertrophy in a mouse model for nemaline myopathy. *Hum Mol Gen* **10**, 317-328 (2006).

Appendix II

Supplementary Figures

% of Myofibers Counted by Automation
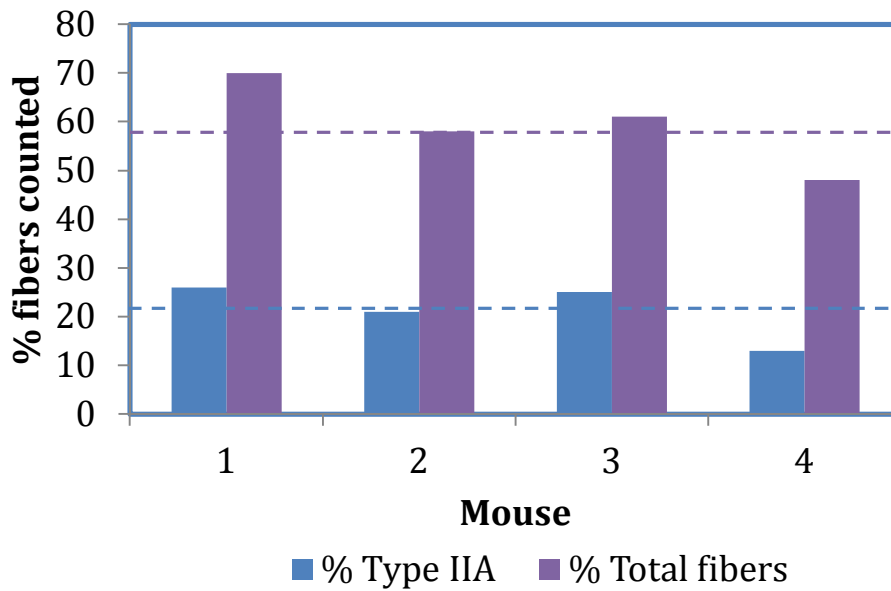
Figure A2.1

Figure A2.1. *Verification of the precision of counting positively staining myofibers by automated technique*

Positively stained myofibers were counted through an automated technique. Sample sections were counted manually, and the counts compared by dividing the automatically counted fibers by the manual counts. Verification shows that in total, approximately 59% of the total fibers were counted, and 21% of Type IIA fibers were counted. However ,the overall proportion of fiber types remained the same. Therefore, the automated counts undercounted but maintained the same proportion of myofibers.